CONTINUOUS AND DISCRETE PROPERTIES OF STOCHASTIC PROCESSES

Wai Ha Lee, MMath

Thesis submitted to the University of Nottingham for the degree of

Doctor of Philosophy

July 2009

Abstract

This thesis considers the interplay between the continuous and discrete properties of random stochastic processes. It is shown that the special cases of the one-sided Lévy-stable distributions can be connected to the class of discrete-stable distributions through a doubly-stochastic Poisson transform. This facilitates the creation of a one-sided stable process for which the *N*-fold statistics can be factorised explicitly. The evolution of the probability density functions is found through a Fokker-Planck style equation which is of the integro-differential type and contains non-local effects which are different for those postulated for a symmetric-stable process, or indeed the Gaussian process. Using the same Poisson transform interrelationship, an exact method for generating discrete-stable variates is found. It has already been shown that discrete-stable distributions occur in the crossing statistics of continuous processes whose autocorrelation exhibits fractal properties. The statistical properties of a nonlinear filter analogue of a phase-screen model are calculated, and the level crossings of the intensity analysed. It is found that rather than being Poisson, the distribution of the number of crossings over a long integration time is either binomial or negative binomial, depending solely on the Fano factor. The asymptotic properties of the inter-event density of the process are found to be accurately approximated by a function of the Fano factor and the mean of the crossings alone.

Acknowledgements

This thesis would not have been possible without my supervisors Keith Hopcraft and Eric Jakeman. Their support has been unwavering, and my conversations with them have always proven invaluable in guiding me through the entire PhD process, and for that, I owe them my eternal gratitude. It has been a pleasure to work with them.

This research has been funded both by the EPSRC and a scholarship from the school of Mathematics at the University of Nottingham. I would also like to thank all the support staff at the University, who have always been more than willing to take time out of their very busy schedules to answer my niggling questions.

Many thanks go to Oliver French, Jason Smith and Jonathan Matthews for enlightening discussions which have not only been tremendously helpful, but have helped to shape this thesis.

I am deeply indebted to my parents for always being there for me, and in particular for supporting me to finish my studies. Not to mention the countless fantastic meals that they have either cooked or taken me out to over all these years.

Without my friends, I would certainly not be the person that I am today, and would probably not be writing this thesis. They've made me laugh, made me cry, and above all else, they have always been there for me when I've needed them. I thank them for

all the good times that we've had over the years. I really could not have asked for better friends.

I would also like to thank all the people from ice skating, who have helped me to become the (increasingly less) inept skater that I am today. Without them, my Saturdays would not be anywhere near as interesting, and I would not have stuck with skating long enough to experience the satisfaction of finally learning how to do backwards '3' turns, crossrolls, or '3'-jumps.

Finally, I would like to express my deepest gratitude to my beautiful girlfriend Amber. She has kept me sane all of these years, and has put up with hearing almost nothing but maths from me for the last several months. My life has certainly been enriched since meeting her, and I can only hope that one day I can make her as happy as she makes me.

A mathematician is a device for turning coffee into theorems.

– Paul Erdős

Table of Contents

1. Introduction

1.1 Background

Power-law phenomena and $1/f$ noise are ubiquitous [e.g. 1] in physical systems, and are characterised by distributions which have power-law tails. These systems are often little understood, with distributions which have undefined moments and exhibit self-similarity. Following the discovery of power-law tails in physical systems, interest in 'stable distributions' has increased. The stable distributions arise when considering the limiting sums of N independent, identically distributed (i.i.d.) variables as N tends to infinity, and can be used as models of power-law distributions. Commonly encountered *continuous*-stable distributions include the Gaussian and Cauchy distributions. A class of *discrete*-stable distributions exists and share many of the properties of their continuous counterparts – the Poisson being one such distribution. It is logical to question the connection between the two classes of distribution – for instance, is there some deeper connection between them, or are they entirely separate mathematical entities?

A mathematical approach to gain an understanding of a process is to create a model which fits the available information – investigation of the model will ultimately aid understanding of the process. For instance, population processes governed by very simple laws have been used [e.g. 2, 3, 4] to analyse complex physical systems. Discrete-stable processes have been found and analysed [e.g. 2, 5, 6], however a non-

Gaussian continuous-stable process has never been found, despite the burgeoning evidence of continuous-stable distributions in nature. It would be enormously advantageous to find such a process. Conversely, algorithms which permit the generation of uncorrelated continuous-stable *variates* exist, but there are no such algorithms for *discrete*-stable variates. The discovery of such an algorithm would aid, for instance, Monte Carlo simulation of processes which have discrete-stable distributions.

Power-law tails also arise when considering the zero and level crossings of continuous processes for which the correlation function has fractal properties. It has been shown that over asymptotically long integration times, the distribution of zero crossings of *Gaussian* processes falls into either the class of binomial, negative binomial or, exceptionally, Poisson distributions. It would be informative to examine the level crossing distributions of *non*-Gaussian processes and to investigate the distribution of *intervals* between crossings, as they are the properties which are often of the most interest in physical systems.

1.2 Literature Review

The research literature which has an effect on this thesis has evolved from two disparate paths – whilst there has obviously been some interplay between the two, results have tended to be incremental, eliciting a two-part literature review. Figure 1.1 gives an outline of the branches of research which will be followed, and shows the

connections between the avenues of research. Note that this diagram is a very brief sketch rather than being an exhaustive illustration of the research.

The first section details the work of Lévy and Mandelbrot with their importance to power-law distributed phenomena. The importance and versatility of stable distributions and population models will then be illustrated, largely from an analytical perspective. The second section starts from the studies of Brown and Einstein, which will be followed along a random walk and signal processing perspective, eventually leading to level crossing statistics of Gaussian processes, and the significance of the K distributions.

1.2.1 Power-Law distributions

In 1963, Benoît Mandelbrot [7] studied the fluctuations of cotton prices and noticed that the fluctuations in price viewed over a certain time scale (e.g. one month) looked statistically similar to those viewed at another time-scale (e.g. one year). He found that the distribution of the fluctuations in prices was governed by a power-law such that $P(f) \sim 1/f^{\gamma}$ for large values of the fluctuation in price f, and γ the power-law index. Such behaviour is often termed $1/f$ noise or flicker noise [8], and the associated distributions are termed 'scale free' due to their self-similarity. Mandelbrot called systems with self-similarity and power-law behaviour "fractal" from the Latin "fractus". Fractal behaviour has subsequently been found in countless other situations, and brought the studies of such systems out of the realms of pathologies.

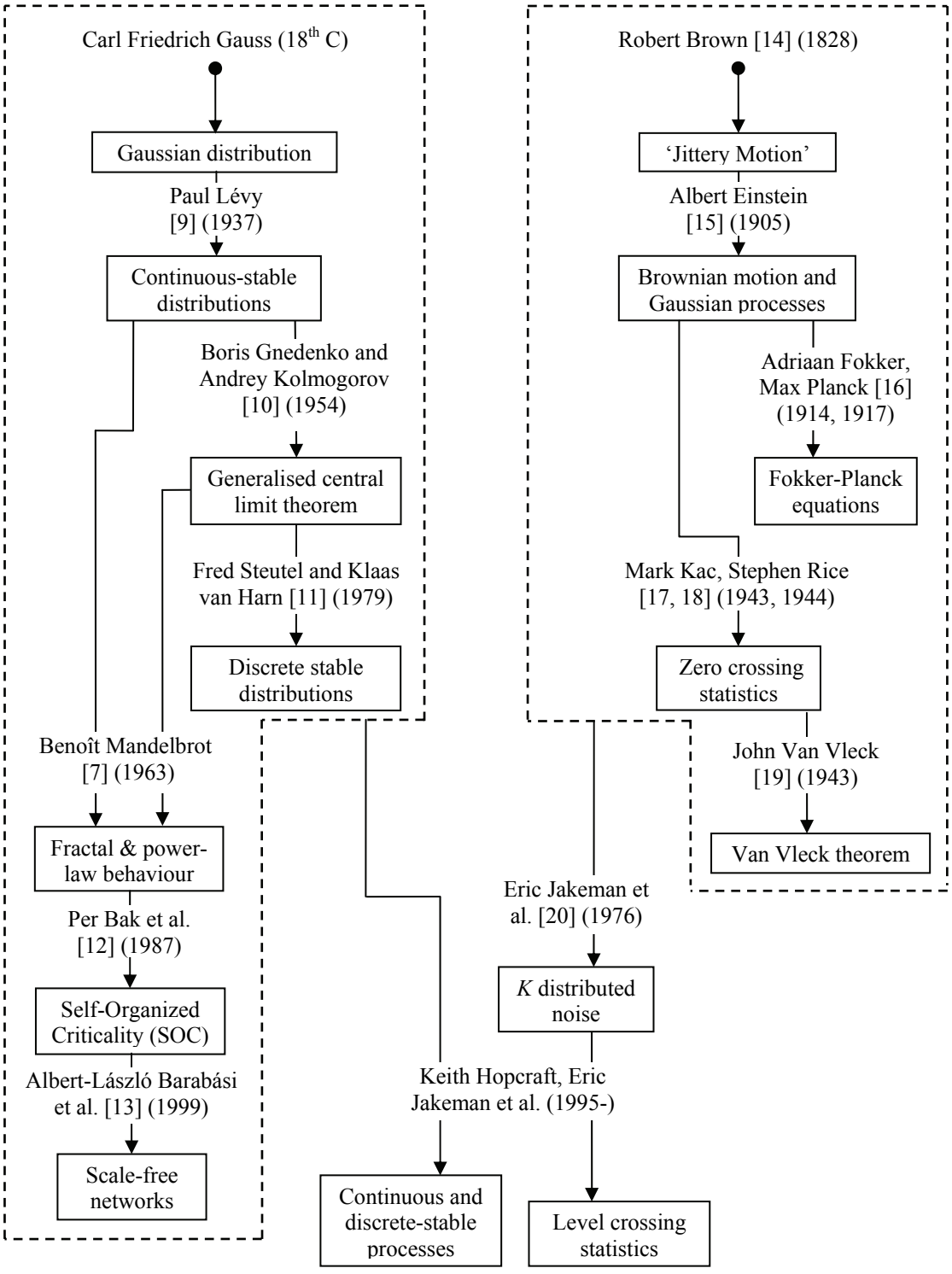

Figure 1.1

Showing the avenues of research outlined below. The arrows show the development of one theory by the named author(s), a reference to, and the date of their first publication on the development.

After Mandelbrot's initial work, self-similarity and fractals were studied mostly by condensed-matter physicists, as they noted power-law behaviour occurring at critical points of phase transitions. This changed in 1987 when, in an attempt to explain the ubiquity of $1/f$ noise, Bak et al. [12, 21] introduced the notion of the sandpile. A sandpile is a system where grains of sand are modelled as falling onto a 'pile'. Once the steepness of the pile becomes too great, the pile will collapse in an avalanche until the pile is again stable; the addition of further grains of sand may disturb this stability, causing more avalanches. Bak et al. found that various measures gauging the size and frequency of avalanches followed power-law distributions, and they subsequently introduced the concept of Self-Organised Criticality (SOC), where systems evolve naturally to their critical points. Deviations from the critical state exhibit scale-free behaviour, which are characterised by power-law tails in the distributions of the associated measurable quantities.

Since then, there has been significant interest in fractals; they have been found in and applied to art [22, 23], image compression [24], fracture mechanics [25], river networks and ecology [26], and economics [27]. Similarly, there has been a great deal of study into fractals and SOC, as they can be used to model many physical systems [28, 29, 30, 31]. It is for this reason that interest in continuous-stable distributions received a revival in the late 1980s.

Continuous power-law behaviour has been observed in a diverse range of places [1, 32], from the population sizes of cities, diameters of craters on the moon, the net

economic worth of individuals [33], duration of wake-periods during the night [34] to the distribution of sizes of earthquakes [35, 36]. Even rainfall exhibits power-law behaviour [37] – with periods of flooding caused by exceptionally high levels of rain being inevitable, and indeed necessary if governed by SOC.

Whilst the processes which drive $1/f$ noise and scale-free behaviour have been studied extensively, the full range of their behaviour is not understood. For instance, despite many efforts, there is still no analytical result [e.g. 38] for the power-law index of a given system with set conditions, even for the sandpile, for which the governing rules are remarkably simple. With numerous new examples of power-law behaviour being found, gaining a better understanding of such processes is becoming increasingly important in order to infer properties of the underlying governing physical processes themselves.

Paul Lévy, a major influence on the young Mandelbrot, discovered the continuous-stable distributions [9, 39] in the 1930s when he investigated a class of distributions which were invariant under convolution, such that if two (or more) independent variables drawn from a stable distribution are added, the distribution of the resultant is also stable. Until then, the only known continuous-stable distributions were the Gaussian (whose mean and all higher moments exist) and the Cauchy distributions. The continuous-stable distributions (with the exception of the Gaussian distribution, which is a special case) all have infinite variance and power-law tails such that $P(x) \sim |x|^{-\nu-1}$ for large x with $0 < \nu < 2$. Furthermore, they are defined through their

characteristic function since there is no general closed-form expression for the entire class of distributions. A subset of the continuous-stable distributions are one-sided [40], where again $P(x) \sim |x|^{-\nu-1}$ for large x, and (depending on the choice of parameters) $P(x) = 0$ for $\mathrm{sgn}(x) = \pm 1$, with the range of the power-law index reduced to $0 < \nu < 1$.

The central limit theorem of probability theory (e.g. [9, 10]) states that the sum of N i.i.d. variables with finite variance tends to the Gaussian distribution as the number of variables N tends to infinity. Gnedenko and Kolmogorov [10] generalised this in 1954 to: the sums of N i.i.d. variables with *any* variance (finite or otherwise) tend to the class of stable distributions as $N \to \infty$. Hence, systems which exhibit fluctuations with power-law tails and infinite variance will have distributions which will tend to stable distributions. A student under Kolmogorov, Vladimir Zolotarev studied the continuous-stable distributions, and his results were summarised in 1986 as a monograph [40] which continues to be a core text on stable distributions to this day.

The concept of infinite divisibility [9, 10, 41, 42, 43, 44] of probability distributions states that: if a distribution D is infinitely divisible, then for any positive integer n and any random variable X with distribution D, there are always n i.i.d. random variables $X_1, \ldots, X_i, \ldots, X_n$ whose sum is equal in distribution to X. For example, the gamma distributions [e.g. 41] can be constructed from sums of exponentially distributed variables, which themselves are a member of the gamma class of

distributions. By definition, all the continuous-stable distributions are infinitely divisible – indeed this is a defining characteristic of the stable distributions.

Examples of *discrete*, infinitely divisible distributions are the Negative Binomial and Poisson distributions [e.g. 41]. When attempting to find self-decomposable discrete distributions, Steutel and Van Harn [11] discovered the discrete-stable distributions, which were *all* expressible by their simple moment-generating function $Q(s) = \exp(-as^{\nu})$. As with the continuous-stable distributions, there are no known closed-form expressions for the entire class of distributions – only a handful are known. With the exception of the Poisson, all the discrete-stable distributions have power-law tails such that $P(N) \sim N^{-\nu-1}$, where $0 < \nu < 1$ (note that the range of ν is equal to that of the one-sided continuous-stable distributions). The Poisson distribution can be thought of as the discrete analogue of the continuous Gaussian distribution, as they are both the limiting distributions for sums of i.i.d. variables *without* power-law tails, and they are the only stable distributions for which *all* moments exist.

The Central Limit Theorem for *discrete* variables states that the limiting distribution of the sums of i.i.d. discrete variables with finite mean is Poisson. However, if the mean of the distribution does not exist, the limiting sum belongs to the class of discrete-stable distributions. Building upon Steutel and Van Harn's work, Hopcraft et al. formulated a series of limit theorems [45] for discrete scale-free distributions. It was found that for distributions with power-law tails, the rate of convergence to the

discrete-stable attractor slows considerably when the index ν tends to unity, when the distribution approaches the boundary between scale-free behaviours and Poisson.

More recently, researchers have been looking into *discrete* power-law distributions in networks, where the term *network* may refer to any interconnected system of objects, such as the internet, social networks, or even semantics [46]. To borrow a term from graph theory, the order distribution of a network gives the *discrete* distribution of the number of links that each node has to other nodes. Power-law behaviour has been noted in an extraordinarily varied range of order distributions in physical systems. Examples range from the distribution of links between actors [47] (where co-starring in a production together signifies a link), the number of citations to a given paper catalogued by the Institute for Scientific Information [48], to the distribution of connections between sites in the human brain [49]. A fuller review of instances of discrete power-law distributions in nature can be found in (for example) [13 or 50].

An understanding of power-law behaviour in networks can be used, for instance, to control the spread of viruses or to prevent disease [51] by preferentially inoculating nodes with a large degree of connectivity which would otherwise spread the disease to a large number of nodes. Conversely, this knowledge may be used for malicious purposes – one example of this is the attacks [52] in 2002 against the thirteen major Domain Name Servers of the internet which are relied on by every connected computer.

The broadening evidence of discrete power-law behaviour prompted the development of stochastic models which would produce power-law distributions as their stationary state. One such model is the Death-Multiple Immigration (DMI) process [53], which describes a population for which deaths occur in proportion to its size N. Multiple immigrants enter the population, with immigrants entering the population independent of its instantaneous size, with single immigrants and groups of two, three $\ldots m$ entering the population at rates α_m. The distribution of immigrants α_m and the rate of death μ jointly determine the 'stationary state' that the population reaches in the limit as time tends to infinity once the deaths and the multiple-immigrations equilibrate. Hopcraft et al. [5] were able to formulate a discrete-stable DMI process which produces a discrete-stable stationary state. The addition of *births* to the DMI process, while altering the dynamics of the process, also permits a discrete-stable distributed stationary state.

It is often impossible to study a system directly without disrupting it. It is instead preferable to use an indirect method of monitoring which retains the characteristics of the system. A suitable method, applied to the DMI model, takes a proportion of the deaths in the population and counts them over a specified monitoring time; once a death has occurred, the individual does not affect the dynamics of the system. The deaths, or 'emigrants' of the internal population form a point process [54], which itself generates a train of events in time that may be analysed. The distribution of the number of emigrants, together with the time-series characteristics (such as inter-event times, correlations, etc.) reveal information about the dynamics of the system being

monitored without disrupting the system itself. This technique was used by Hopcraft et al. to distinguish between a population being driven by the DMI process [53], and another by the BDMI process, which both had the same stationary state through examination of the correlation functions of the counting statistics.

The Poisson process [55, 56, 57] is a memoryless stochastic process which is completely characterised by a rate λ, which denotes the expected number of occurrences of an event in a unit time. The *doubly stochastic* Poisson process (or the Cox process) is a Poisson process where the mean itself is a (continuous) stochastic variable. The Poisson *transform* was originally developed by Cox [58], who modelled the number of breakdowns of looms in a textile mill as being dependent on a continuous parameter: the quality of the material used. Applications of the doubly stochastic Poisson process since have been diverse, for instance, Mandel and Wolf [59] describe a photon counting process from a quantum-mechanical standpoint, using the Poisson transform as the core of their result. In the broadest and most general sense, the Poisson transform is of great importance in that it provides a direct link between continuous and discrete distributions without resorting to mean-field approximations (which do not necessarily always work for discrete phenomena).

A useful statistic when considering discrete distributions is the Fano factor [60], which is given by $F = \left(< N^2 > - < N >^2\right) / < N >$, and can be used as a measure of how Poissonian a distribution is. For $F = 1$, the distribution is Poisson, whereas for $F < 1$ and $F > 1$ the distribution is closer to being Binomial (i.e. narrower) and

Negative Binomial (i.e. broader), respectively. The Binomial distribution arises when considering the number of successes from a given number of independent Bernoulli trials (e.g. coin tosses). *Negative* binomial distributions arise when considering the number of failures before a given number of successes in an independent Bernoulli trial. The distribution of a binomial is narrower than a Poisson of the same mean, whereas a negative binomial is broader than a Poisson distribution of the same mean. Jakeman et al. state [61] that the *entire* class of discrete distributions with Fano factor $F < 1$, and many for which $F > 1$, cannot be generated through a doubly stochastic Poisson process. They considered a model whereby the immigrations into a DMI process enter only in pairs, and found that under certain circumstances, only even numbers of individuals will be observed in the population.

1.2.2 The Brownian path

In 1828 Robert Brown [14] studied pollen particles suspended in water, and found that the particles executed 'jittery' motions instead of following a smooth path, but was unable to provide an explanation for this movement. It was nearly eighty years before an explanation was found by Einstein in 1905. Einstein found [15] that the particles' displacements in each 'jitter' followed a Gaussian distribution, and that the mean squared displacement of the particles from their initial position scales linearly with the monitoring time, such that $< x^2(t) > \sim ct$. Einstein called such behaviour "Brownian Motion", and his paper silenced those sceptical about the existence of atoms [e.g. 62].

The linearity in the mean squared displacement is characteristic of Brownian motion, and of 'normal' diffusion. Further to those processes which can be described as following Brownian motion, processes exist for which the mean squared displacement is nonlinear in time, following a power-law instead: $< x^2(t) > \sim ct^{\alpha}$. In processes for which $\alpha < 1$, the diffusion is *slower* than that of 'normal' diffusion, and they are 'sub-diffusive'. Similarly, those for which $\alpha > 1$ are 'super-diffusive' (the special case $\alpha = 2$ is termed 'ballistic diffusion'), as they are faster than normal diffusion [63]. These are all part of a wider class of diffusion called anomalous diffusion [e.g. 64, 65].

Brownian motion can be simulated through a process called a 'random walk'. In the simplest, one-dimensional case, this refers to a particle on a line, which at each time step can either travel one step to the left or one step to the right with equal probability. The root mean square of the displacement can be shown [e.g. 66] to scale with the square root of the number of steps N. Taking the limit $N \to \infty$, where N is fixed, and with appropriate rescaling of the distances, the distribution of the displacement is Gaussian, by the central limit theorem. However, if the number of steps is itself a random variable, then the rescaled distribution of the displacement is not necessarily Gaussian. In fact, Gaussian distributed displacements are the exception rather than the rule.

There are many cases when making the Gaussian assumption for processes is simply wrong, for instance when the recorded data makes strong departures from Gaussian,

or when the central limit theorem does not apply. Often, if the underlying physical processes are not well understood or are too complex to analyse mathematically, measurements of the processes can be made and properties inferred from them. This empirical approach will only lead to an understanding of the particular system at hand, so the study of non-Gaussian processes is equally as important as the study of Gaussian processes.

Allowing the displacement of each individual step in a random walk to alter also changes the asymptotic behaviour of a random walk process. A Lévy flight is an example of a super-diffusive process [67]; occurring when the displacement in each step has a power-law tail. According to the generalised Central Limit Theorem [10], as the number of steps $N \to \infty$ the resultant rescaled displacement itself is also a continuous-stable distribution. In this case, the *trace* of the particle in space exhibits extreme clustering, staying within small regions for extended periods of time, rarely undertaking large steps, and staying within the new region until the next large step. As asymptotic behaviour of the (non-Gaussian) continuous-stable distributions follows a power-law, large steps are far more likely in Lévy flights than in Brownian motion; in fact it is the large steps which characterise Lévy flights. This can be seen in Figure 1.2, which compares a normal one-dimensional random walk with a Lévy flight. Note that for a Lévy flight, the mean squared displacement is infinite. It is apparent that large jumps dominate the behaviour of the Lévy flight, but do not occur in Brownian motion.

A Lévy random walk [68] is essentially a generalised Lévy flight, but instead of the particle essentially jumping from point to point with a fixed jump interval, the length of the interval is permitted to vary; having its own (continuous) probability density function. This can, for instance, be used to give a process a finite mean squared displacement, i.e. $< x^2(t) > \sim ct^{\alpha}$. Lévy walks have been used to model numerous diffusive processes [69], memory retrieval [70], and even the foraging patterns of animals [71].

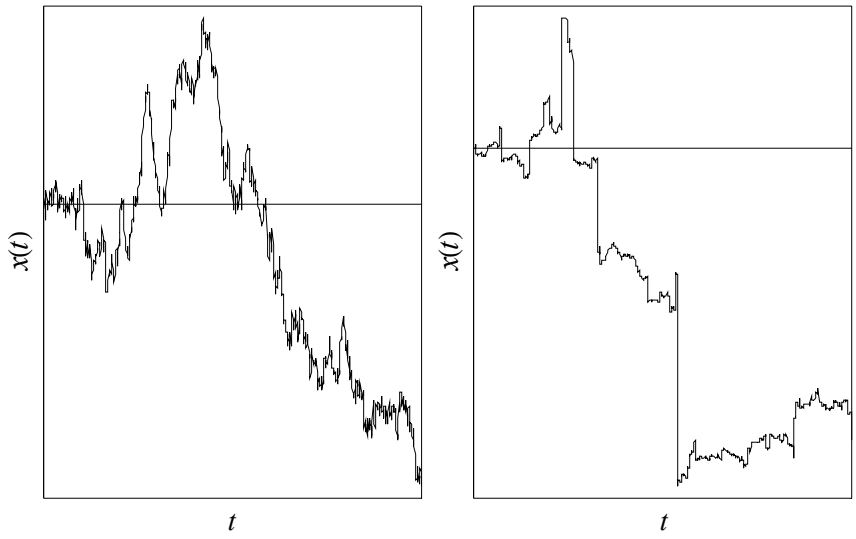

Figure 1.2

Showing the difference between Brownian motion and Lévy flights in one dimension. The Brownian motion is simulated by adding a Gaussian variable at each step in time; the Lévy flight adds a Cauchy variable at each time step. Note that since the motions are self-similar, the addition of scales on the axes is unnecessary.

In the context of radars and remote sensing, clutter, or 'sea echo', is the term given to unwanted returns from the sea surface which are *not* targets but which are detected. When designing a radar system, it is imperative to minimise the number of 'false alarms' which need to be appraised manually. This problem is made harder when considering radars for which the so-called 'grazing angle' (i.e. the angle between the sea surface and the area being investigated) is very small. In the 1970s, when trying to model sea echo, Jakeman and Pusey [20] proposed a model advocating the so-called K distributions, which fitted with much of the existing data on sea clutter. The proposed model regarded the surface of the sea illuminated by the radar as being a finite ensemble of individual scatterers, each returning the radar signal with random phase and fluctuating amplitude [72]. One interpretation of this is that the scattered field is an N step random walk where the value of N fluctuates, therefore the classical central limit theorem does not apply. The K distributed noise model has been widely regarded as an excellent model for non-Gaussian scattering; this has been justified both by empirical data and the comparison with analytically tractable scattering models.

The Fokker-Planck equation [3, 73] was developed in the 1910s by Fokker and Planck [16] when they attempted to establish a theory for the fluctuations in Brownian motion in a radiation field. The Fokker-Planck equation describes the time evolution of the Probability Density Function (PDF) of a process, and is a generalisation of the diffusion equation [15]. The Fokker-Planck equation and its

subsequent generalisations have themselves since been used for a myriad of applications [65, 66, 72, 74, 75].

It is frequently the case that real-world continuous stochastic processes [55] are too complex to measure and analyse in full. This may be because instrumentation with sufficiently high resolution does not exist, or because analysis of the resultant data would be prohibitive. Instead, it is often instructive simply to examine crossings of a process. This effectively reduces the continuous process under scrutiny to a point process [56], which is comprised entirely of a series of points in time. A basic example of crossing analysis is the deduction of the frequency of a sinusoidal signal as its amplitude passes through zero (i.e. the zero crossings). Likewise, studying share prices over a given time interval, one could predict the frequency that a given share will exceed some value, and thus make better-informed trading decisions. This is then studying the *level* crossings (see Figure 1.3) of the share's price. Results from analysis of zero and level crossings have countless applications, from studying rainfall levels to predict the next major flood, to monitoring the value of equities to estimate a suitable point in time to trade.

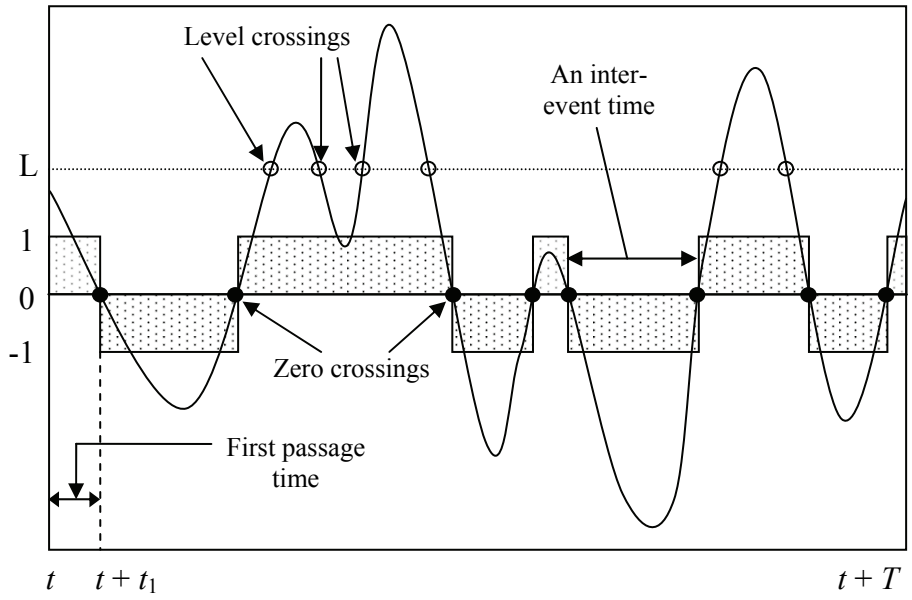

Figure 1.3

Illustrating the concept of zero (filled circles) and level (unfilled circles) crossings of a process over a time $[t, t + T]$. A clipped version of the zero crossing process is shown also (dotted boxes), where the value of the process is either +1 or -1, depending on the sign of the original. The first passage time (dashed line) and one inter-event time for the clipped process is shown.

A random process with a large number of i.i.d. increments of finite variance, will tend, by the central limit theorem, to have a Gaussian (or 'Normal') distribution. In the case of a Gaussian process, the increments themselves are *always* Gaussian, so the distribution of the process is *always* Gaussian. Many systems have been modelled (correctly or not) as Gaussian processes based on the assumption of a large number of increments, and due to their analytical tractability. For that reason, the largest proportion of studies on crossings pertains to Gaussian processes [e.g. 55, 76]. Also, through understanding the crossing statistics of Gaussian processes, it is possible to estimate the crossing statistics (and indeed other properties) of processes for which

Gaussian models are suitable. By studying the statistical properties of the level crossings, an understanding of the underlying processes which *drive* the fluctuations can be inferred.

Stephen Rice published his seminal papers "Mathematical Analysis of Random Noise" in the 1940s [17]. A groundbreaking result in these papers expanded on a result [18] of Kac's to derive the mean number $\overline{N}$ of zero crossings over a time T of a Gaussian process with autocorrelation function $\rho(\tau) =< x(t)x(t+\tau) >$. Rice showed that $\overline{N} = T(-\rho''(0)/\rho(0))^{1/2}/\pi$, indicating that the autocorrelation must be twice differentiable at the origin for the mean to exist. Conversely, if $\rho''(0)$ is undefined, then this implies that the mean number of zero crossings is infinite.

Rice's work was used by a team led by J. H. Van Vleck to explore the use of electronic noise as a radar countermeasure [77]. One source of electronic noise is clipping [78], which is when the amplitude of a signal is limited to a maximum value. In one form of clipping, the signal is replaced with a telegraph wave, which assumes the values ±1 depending on the sign of the original signal (see Figure 1.3), the motivation being to "spread the spectrum" [77] and thereby severely limit the information contained within the signal. This technique is called radar jamming [78]. A major discovery [19] of Van Vleck's was that even in this extreme case of nonlinear processing, if the original signal was a Gaussian process, then the correlation function of the original signal can still be recovered.

Further research was then conducted which found the variance [79] and higher-order moments [80] of zero crossings, all of which depend on the autocorrelation function being differentiable. The level crossings of Gaussian processes were also investigated; Rice showed that the mean number of crossings decayed exponentially with the square of the level L. The first-passage time provides the time taken between the initiation of a process and the first crossing (whether zero or level), and again has many applications [e.g. 81]. A statistic of note with regard to continuous processes is the inter-crossing time distribution, as it describes (for instance) how long the process will exceed a certain level, i.e. its persistence. Results regarding zero crossings and the information they convey from them are reviewed in [82]; a review of crossings of Gaussian processes in particular is given by Smith et al. in [83].

The current scope of research into zero and level crossings is demonstrated schematically in Figure 1.4; the remainder of this review will map out a path on the figure, illustrating the route from continuous, discrete and back to continuous phenomena.

Recently, Hopcraft et al. [84] were able to identify that if the zero crossings of a process had a discrete-stable (or asymptotically stable) distribution, the process itself has fractal characteristics. Such characteristics include ‘extreme clustering’, where cascades of crossings occur in clusters, each cluster comprised of infinitely many crossings. This cascade of crossings is analogous to fractal cascades of emigrations which occur in the discrete-stable DMI processes [84, 85].

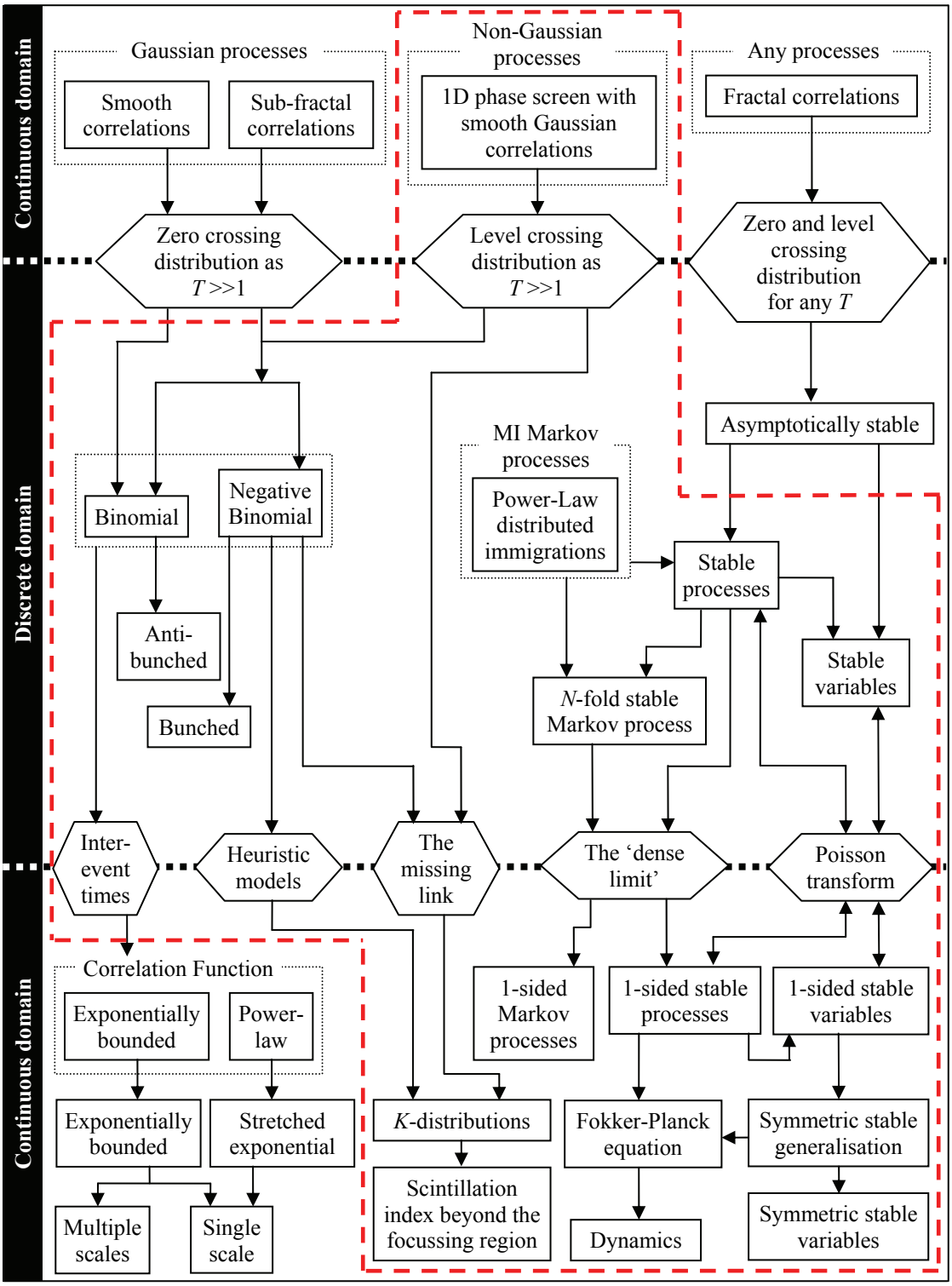

Figure 1.4

Showing the connection between the branches of research in crossing statistics. The hexagons represent the mechanism for transferring between continuous and discrete properties.

'Sub-fractal' processes are continuous everywhere, but have *derivatives* which show fractal properties. In this case of sub-fractal Gaussian processes, it was shown by Smith et al. [83] that the zero crossings are either bunched (attracted to each other) or anti-bunched (repelled by each other) depending on the structure of the correlation function. Additionally, the crossing distributions are shown to belong to the class of Poisson (exceptionally), or more generally, binomial or negative-binomial distributions.

1.3 Outline of thesis

A background of the key mathematical concepts used in this thesis is given in Chapter 2, which introduces the stable distributions and their parameterisation, as well as the multiple immigration models which can be used to form discrete-stable processes.

The concept of the Gaussian, Poisson and stable transforms are introduced in Chapter 3. It is shown that the symmetric-stable distributions can be linked by a hierarchy of transforms which reduce their power-law index by modifying the scale parameter. A Poisson transform interrelationship is found for the discrete-stable and one-sided stable distributions. The necessary scaling which occurs when undertaking this Poisson transform is found, and the limit as the power-law index $\nu \to 1$ (corresponding to the Poisson distribution) is examined.

Chapter 4 applies the Poisson transform to define a one-sided continuous-stable process, for which properties such as a Fokker-Planck style equation and the transient solution are found. Multiple-interval statistics are also examined; an n-fold generating function for a discrete-stable process is explicitly stated and used to find the n-fold generating function of a one-sided *continuous*-stable process.

In Chapter 5 the Poisson transform relationship is utilised to generate discrete variates from their continuous counterparts. The accuracy and speed of these simulations will be considered, both for known results (e.g. generating negative binomial variates from gamma-distributed variates), and later, for discrete-*stable* variates.

Chapter 6 considers a signal processing analogue of a phase screen model and finds properties such as the level crossing distribution and the inter-crossing times. In particular, the distribution of the number of level crossings over very long integration times are compared to the binomial, negative binomial and Poisson results of Smith et al [83]. Furthermore, a heuristic approximation is found for the asymptotic properties of the inter-event times.

Conclusions are drawn in Chapter 7, and suggestions are given for possible further avenues for research which could be undertaken.

2. Mathematical background

2.1 Introduction

The continuous-stable distributions, which were discovered by Paul Lévy in the 1930s, arise in the generalised central limit theorem which states that the sum of N independent, identically distributed (i.i.d.) variables will always tend to a continuous-stable distribution as N tends to infinity, subject to an appropriate change of scale and shift. If the distribution of the variables has a finite variance, the limiting distribution is Gaussian (or Normal). If the distribution has a power-law tail such that $p(x) \sim 1/|x|^{1+\nu}$ (and $0 < \nu < 2$), the variance is infinite and the limiting distribution is a non-Gaussian stable distribution. This has a wider currency as it means that the sums of *all* processes which have power-law tails have the potential to have asymptotically stable marginal distributions. For this reason alone, the continuous-stable distributions are worthy of further study. The abundance of examples where they occur in nature exemplifies this point [e.g. 1, 12, 13, 28, 30, 50]. Any stable distribution is invariant under convolution with itself; it is from this property that the epithet stable is derived. In this thesis, an understanding of these stable distributions will be necessary.

This chapter will firstly define the continuous-stable distributions and review some of their properties. Secondly, the discrete-stable distributions are introduced – their properties and behaviour are outlined. Known closed-form expressions for the

continuous and discrete-stable distributions are given. Finally, a Death-Multiple-Immigration (DMI) population process, which can be used to form a discrete-stable process is introduced.

2.2 The Continuous-stable distributions

2.2.1 Definition

The continuous-stable distributions are defined through their characteristic function – the Fourier transform of their probability density function [40]:

$$\begin{aligned} C(u,\nu,\beta,a) &= \int_{-\infty}^{\infty} p(x)\exp(iux)dx \\ &= \exp\left(-a|u|^{\nu}\left(1-i\beta\,\mathrm{sgn}(u)\Phi(u,\nu)\right)\right) \end{aligned} \tag{2.1}$$

$$\Phi(u,\nu) = \begin{cases} \tan\left(\dfrac{\pi\nu}{2}\right) & \nu \neq 1 \\ -\dfrac{2}{\pi}\log|u| & \nu = 1 \end{cases} \tag{2.2}$$

where $a > 0$ is a scale factor. The symmetry of the distribution is described by $-1 \leq \beta \leq 1$. In the case when $\beta = 1$ or $\beta = -1$ and $0 < \nu < 1$, the distributions are defined only when x is positive or negative, respectively – these distributions are termed 'one-sided'. When $\beta = 0$, the distribution is symmetric, and defined for all real values of x. The parameter $0 < \nu \leq 2$ describes the power-law behaviour for $|x| >> 1$, such that:

$$p(x,\nu,\beta,a) \sim \begin{cases} \dfrac{1}{|x|^{\nu+1}} & 0 < \nu < 2 \\ \exp\left(-x^2\right) & \nu = 2. \end{cases}$$

All the distributions for which closed-form expressions for the probability density functions (PDFs) exist are given in §2.4. In general, however, the densities are recovered upon inverse Fourier transforming the characteristic function (2.1):

$$p(x,\nu,\beta,a) = \frac{1}{2\pi}\int_{-\infty}^{\infty} \exp(-ixu)C(u,\nu,\beta,a)du. \tag{2.3}$$

Continuous-stable distributions for which $0 < \nu \leq 1$ have an infinite mean (all higher moments are also infinite), whereas when $1 < \nu < 2$ the mean is finite, but the variance is infinite. When $\nu = 2$, the symmetry parameter is arbitrary and immaterial (c.f. (2.2)), and the distribution is the familiar Gaussian (Normal) distribution of variance $2a$

$$p(x,2,\beta,a) = \frac{1}{2\sqrt{\pi a}}\exp\left(-\frac{x^2}{4a}\right).$$

Therefore, the *only* continuous-stable distribution whose variance is finite is the Gaussian.

The effect of the symmetry parameter is best demonstrated through a relation derived from the form of the characteristic function:

$$p(x,\nu,-\beta,a) = p(-x,\nu,\beta,a). \tag{2.4}$$

This elicits the fact that the range of behaviour given by varying β need only be investigated for $0 \leq \beta \leq 1$; negative values of β can be transformed accordingly.

Figure 2.1 plots the continuous-stable distributions for $\nu = 0.9$ and $\nu = 1.1$, and $a = 1$. Note that for $\nu > 1$, β shifts the mode in the opposite direction to when $\nu < 1$.

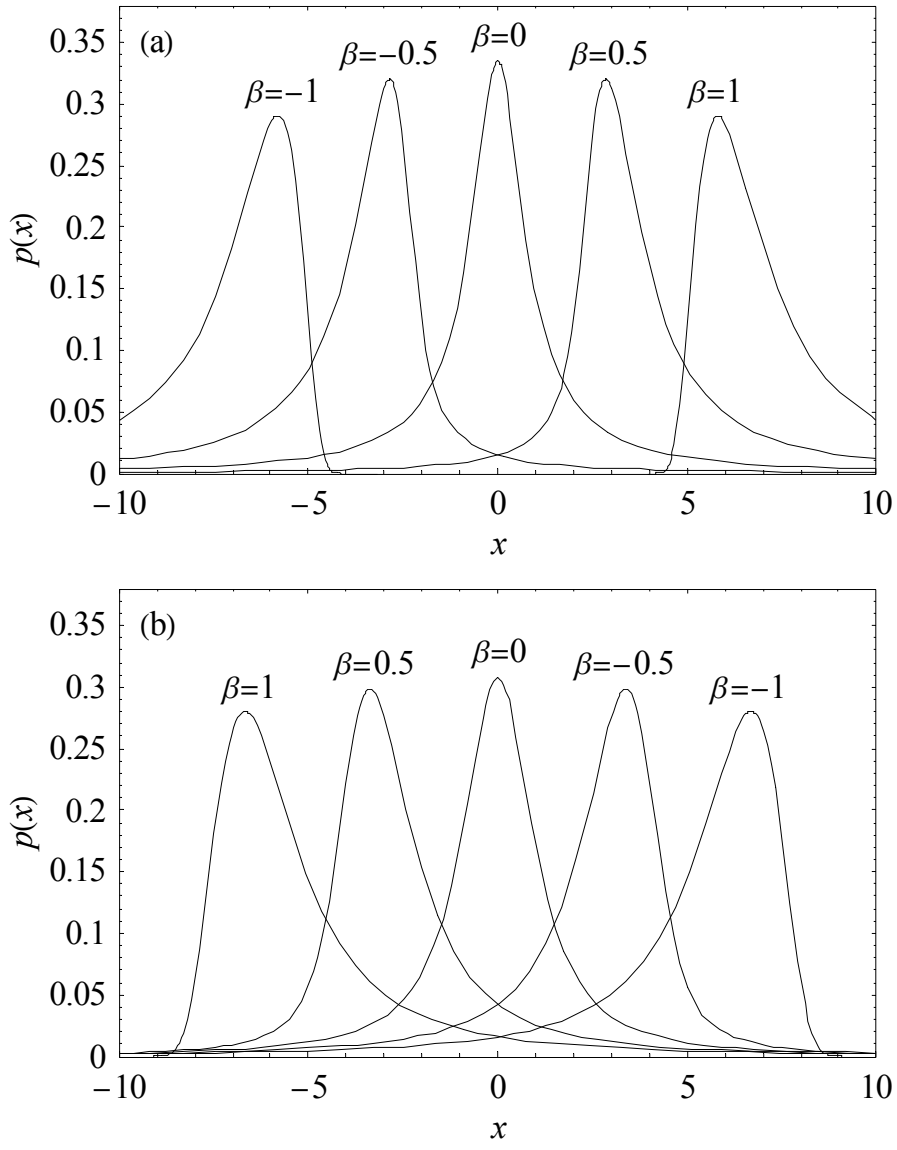

Figure 2.1

Illustrating the effect of varying β on the shape of the continuous-stable distributions, for (a) $\nu = 0.9$, $a = 1$, and (b) $\nu = 1.1$, $a = 1$.

It is instructive to examine the behaviour of the scale parameter on the distributions, since some authors simply give the densities with $a = 1$. From the characteristic function (2.1), it is easy to see the effect of a linear scale factor in a on a distribution with unit scale factor:

$$p(x,\nu,\beta,a) = \frac{1}{a^{1/\nu}}\, p\left(\frac{x}{a^{1/\nu}},\nu,\beta,1\right). \tag{2.5}$$

There is a great deal of confusion in the literature regarding the parameterisation of the stable distributions – for instance, some authors note that when $|\beta| = 1$ and $0 < \nu < 1$ the distributions are one-sided, but do not state that when $1 \le \nu \le 2$ the distributions are *always* two-sided. Other authors incorrectly change the sign of the imaginary term in $C(u)$ when $\nu = 1$, though the densities of this distribution are seldom actually calculated (except for the Cauchy case, when $C(u)$ is real). Many more have quoted the closed-form expressions of stable distributions from incorrect results. This confusion is compounded by the fact that there are at least five [86] different parameterisations for the distributions, each created for its own purpose. The characteristic function given above is the most commonly used, and will be the one used throughout this thesis.

Many properties of the distributions are not known, for instance, it was not until 1978 that it was shown by Yamazato [87] that the continuous-stable distributions were unimodal – the *location* of the mode of the continuous-stable distributions was found by Nolan [86] via yet another parameterisation. Only the properties which are

pertinent to this thesis are stated here – for a fuller review of stable distributions, key works include that of Lévy [9], Zolotarev [40], and Samorodnitsky and Taqqu [39].

2.2.2 Probability Density Functions

General closed-form expansions of the PDFs in terms of well-understood functions do not exist [e.g. 88]. For instance, Metzler and Klafter [64] transform the parameters and provide the stable densities in terms of Fox's H functions [89], whereas Hoffmann–Jørgensen [90] defines them (again through a different parameterisation) using incomplete hypergeometric functions. Bergström [91] proved that there is an infinite series representation for *all* the continuous-stable distributions in terms of elementary functions. Generally, the *symmetric*-stable distributions have received the most attention, as the form of their characteristic function is simpler than that of their asymmetric counterparts.

The case $v = \beta = 1$ is rather peculiar in that as the index v tends to unity from below, the distribution is one-sided with diverging mode. As the index tends to unity from above, the mode tends diverges to negative infinity – this behaviour clearly exemplifies the fact that the case $v = 1$ is a singular value with special properties. This effect is illustrated in Figure 2.2. Continuity in the modes of the distributions as v varies is allowed through a different parameterisation [86] in which a term is added to shift the distributions, such that $p(x) \to p\left(x + \beta \tan(\pi v/2)\right)$. This, however, destroys the one-sidedness in the PDF when $0 < v < 1$.

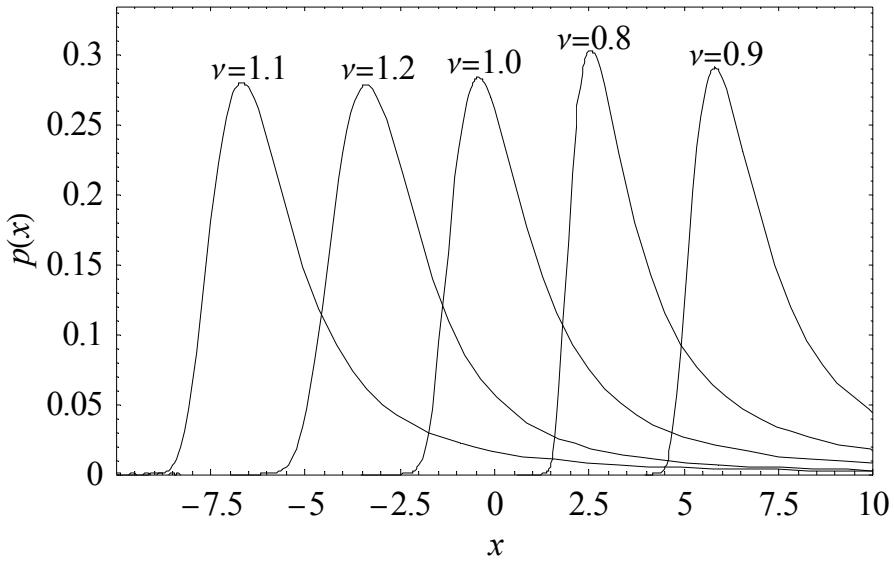

Figure 2.2

Showing the effect of altering the power-law index v on the location of the mode of the distribution. $a = \beta = 1$ for these plots.

The behaviour of the one-sided distributions in the limit as $v \to 1$ will be considered in more detail later in this thesis (Section 3.3.4).

The tail behaviour of the continuous-stable distributions can either be found through the use of a central-limit theorem type argument [41], or by stationary phase type methods [e.g. 92] to be:

$$p(x,\nu,\beta,a) \sim \begin{cases} \dfrac{1+\beta}{2\pi}\Gamma(\nu+1)\sin\left(\dfrac{\pi\nu}{2}\right)a^{\nu}x^{-\nu-1} & x >> 1 \\ \dfrac{1-\beta}{2\pi}\Gamma(\nu+1)\sin\left(\dfrac{\pi\nu}{2}\right)a^{\nu}x^{-\nu-1} & x << 1 \end{cases} \tag{2.6}$$

It can then be inferred from (2.6) that when $\beta = \pm 1$, (even in the regime $1 < \nu < 2$ when the stable distributions are *two*-sided), the tail for the $x\beta < 0$ end of the distribution decays faster than a power-law.

2.3 The Discrete-stable distributions

When attempting to create *discrete* analogues for the continuous-stable distributions, Steutel and Harn [11] discovered a class of distributions which also exhibited stability and therefore infinite divisibility. As with the continuous-stable distributions, they are defined through a transform – in this case, their moment generating function:

$$Q(s,\nu,A) = \sum_{N=0}^{\infty} (1-s)^N P(N,\nu,A) \tag{2.7}$$

$$= \exp(-As^{\nu}) \tag{2.8}$$

where A is a positive scale factor, and $0 < \nu \leq 1$ characterises the power-law behaviour: for $0 < \nu < 1$, the distributions follow

$$\lim_{N\to\infty} P(N,\nu,A) \sim \frac{1}{N^{\nu+1}}$$

(see Figure 2.3) and for $\nu = 1$, the distribution is Poisson with mean A:

$$P(N,\nu,A) = \frac{A^N}{N!}\exp(-A). \tag{2.9}$$

It is especially interesting to note that the range of the power-law index for the discrete-stable distributions is exactly that of the one-sided continuous-stable distributions. Also note that the form of the generating function is the same as the characteristic function of the symmetric-stable distributions, found by setting $\beta = 0$ in (2.1). This is due to the fact that convolutions of both generating functions and characteristic functions with themselves are manifested as products; the exponential form is the only one which permits both classes of distributions to be stable.

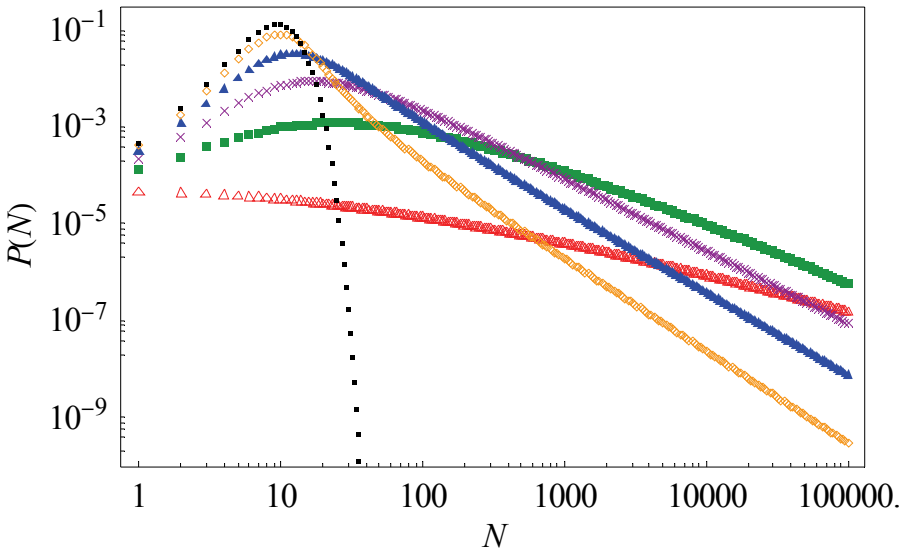

Figure 2.3

Showing the power-law behaviour of the discrete-stable distributions as the index v varies. For all the distributions shown, A = 10, whereas the values of v chosen are: 0.1 (unfilled triangles, red), 0.3 (filled squares, green), 0.5 (crosses, purple), 0.7 (filled triangles, blue), 0.9 (diamonds, yellow), and 1 (points, black). $P(1)$ increases with the index v.

The probabilities and moments of any discrete distribution can always be recovered through repeated differentiation of the generating function:

$$P(N) = \frac{(-1)^N}{N!} \frac{d^N Q(s)}{ds^N}\bigg|_{s=1} \tag{2.10}$$

$$\begin{aligned} < N(N-1)...(N-(r-1)) >= & \sum_{N=0}^{\infty} P(N) \cdot [N(N-1)...(N-(r-1))] \\ = & \left(-\frac{d}{ds}\right)^r Q(s)\bigg|_{s=0}. \end{aligned} \tag{2.11}$$

To date, there are only a few discrete-stable distributions for which there are closed-form expressions for the probabilities – these are given in §2.4. The probabilities for

any A and $0 < \nu \leq 1$ can always be found by substituting $Q(s,\nu,A)$ into (2.10), however for anything other than small values of N this becomes rather cumbersome. For instance, the first few probabilities of the discrete-stable distributions are:

$$P(0,\nu,A) = \exp(-A)$$
$$P(1,\nu,A) = A\nu\exp(-A)$$
$$P(2,\nu,A) = \frac{A\nu\exp(-A)}{2}(1-\nu+A\nu)$$

hence closed-form expressions are much more suitable for obtaining distributions. A more suitable method for obtaining the distributions is discussed in Section 5.7.

From (2.11) we can demonstrate that the mean, and hence all higher moments of the discrete-stable distributions are infinite. The mean of a discrete-stable distribution is:

$$< N >= -\frac{d}{ds}\exp\left(-As^{\nu}\right)\Big|_{s=0}$$
$$= \left(A\nu s^{\nu-1}\right)\Big|_{s=0}$$

which is undefined unless $\nu = 1$, in which case $< N >= A$, corresponding to the mean of the Poisson.

In the limit $v \to 1$, a discrete-stable distribution of scale parameter A and a Poisson distribution with mean A are almost indistinguishable for small values of N; the power-law behaviour is initiated for $N >> 1$. This behaviour is illustrated in Figure 2.4. As such, the discrete-stable distributions in this regime can be thought of as a heuristic model for Poisson distributed variables with outliers. Judicious choosing of

the index would then allow tailoring of the frequency of the outliers to correspond to the data at hand [e.g. 85].

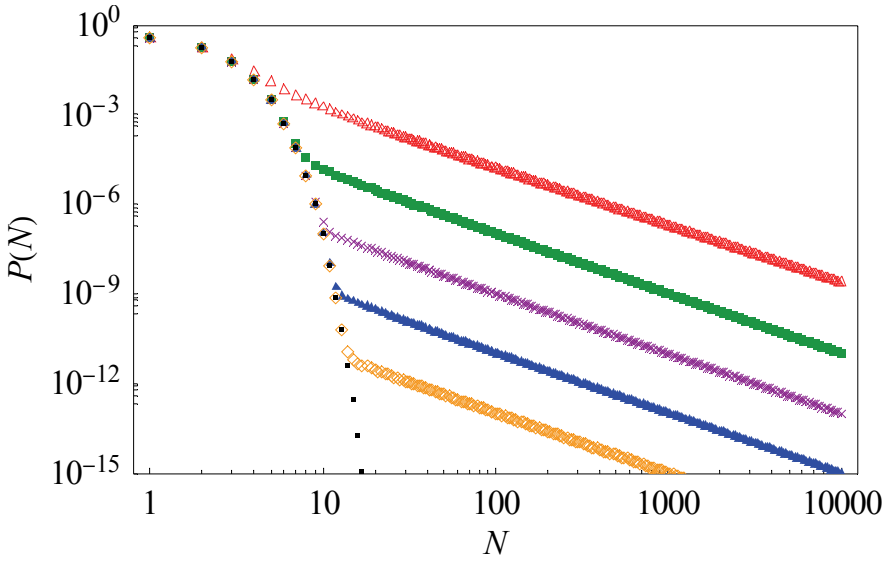

Figure 2.4

Illustrating the behaviour of the discrete-stable distributions for which the scale parameter A is unity and the index ν tends to unity. The values of the power-law index ν plotted are: 0.9 (unfilled triangles, red), 0.999 (squares, green), 0.99999 (crosses, purple), $1\text{-}10^{-7}$ (filled triangles, blue), $1\text{-}10^{-9}$ (diamonds, yellow), and $\nu = 1$ (the Poisson; dots, black).

The tail when $\nu = 1$, corresponding to the Poisson, which does not have a power-law tail can be calculated by applying Stirling's formula [e.g. 93] to the Poisson probability distribution (2.9):

$$\lim_{N\to\infty} P(N,1,A) = \lim_{N\to\infty} \frac{A^N}{N!}\exp(-A)$$
$$= \exp(-A)\lim_{N\to\infty} \frac{A^N}{N!}$$
$$= \frac{\exp(N-A)}{\sqrt{2\pi A}}\left(\frac{A}{N}\right)^{N+1/2}$$

which clearly decays at a faster-than power-law rate.

2.4 Closed-form expressions for stable distributions

The most general characteristic functions of the continuous-stable distributions are defined in a four-parameter space: the power-law index ν, the symmetry parameter β, a scale parameter a, and a location parameter δ. The location parameter can be removed entirely, as its only effect is a shift of the PDF; the scale parameter can be removed also, as (2.5) shows that *any* scale parameter can be catered for by an appropriate scaling of the PDF. The symmetry parameter β has its own symmetry relation (2.4), so we need only consider the range $0 \le \beta \le 1$. The only parameter whose range cannot be reduced (or removed) is ν, so the continuous-stable distributions can be defined in $0 \le \nu \le 2$, $0 \le \beta \le 1$. The closed-form expressions for the PDFs of the continuous-stable distributions are given for $a = 1$ and $\delta = 0$. The discrete-stable distributions, however, have no such scaling relation for different values of N due to their discrete nature, so are given with the value of A left free.

It is certainly not necessary to have closed-form expressions for continuous-stable distributions to obtain the densities – there are alternative parameterisations which

lend themselves to numerical integration of the inverse Fourier transform (2.3) of the characteristic function (2.1) [e.g. 40, 94]. Indeed there are packages which will evaluate densities for any values of ν, β, and a [e.g. 95]. As it is often the case that a numerical result lends itself to other problems, not least numerical errors, closed-form expressions continue to be sought. The parameters for the eleven known closed-form expressions for the continuous-stable distributions and the three expressions for the discrete-stable distributions can be shown in (ν, β) phase-space for clarity:

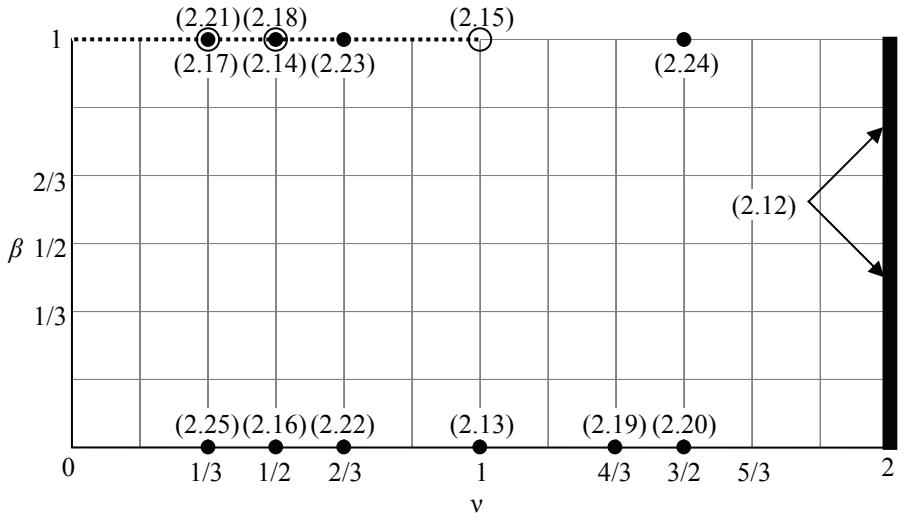

Figure 2.5

A phase space diagram representing the continuous-stable distributions (represented by dots) for which closed-form expansions are known. The full line at $v = 2$ represents the invariance of the Gaussian with respect to the β. The dotted line at $0 < v < 1$, $\beta = 1$ represents one-sided distributions. Circles on the dotted line represent *discrete*-stable distributions whose probabilities have closed-form expressions (references above).

Note that the scarcity of expressions for the continuous-stable distributions in the literature has led to some inconsistencies in the expressions given. This is partly due

to the fact that some expressions are given in terms of little-known special functions for which many numerical software packages cannot readily evaluate. In some cases, the results given have even been found to be entirely incorrect (e.g. see [96]). Those stated below have been verified by numerical methods. For the sake of simplicity, the distributions are categorised by the functions which appear in them.

2.4.1 In terms of elementary functions

The two most well-known continuous-stable distributions are the Gaussian ($\nu = 2$, β arbitrary, though usually considered to be zero):

$$p(x,2,0,1) = \frac{1}{2\sqrt{\pi}} \exp\left(-\frac{x^2}{4}\right);\ -\infty < x < \infty \tag{2.12}$$

and the Cauchy ($\nu = 1$, $\beta = 0$):

$$p(x,1,0,1) = \frac{1}{\pi}\frac{1}{x^2+1};\ -\infty < x < \infty. \tag{2.13}$$

A third stable distribution also often found in the literature is the so-called 'Lévy-Smirnov' distribution ($\nu = 1/2$, $\beta = 1$) [e.g. 40] , which is one-sided:

$$p\left(x,\frac{1}{2},1,1\right) = \frac{1}{\sqrt{2\pi}} x^{-3/2} \exp\left(-\frac{1}{2x}\right);\ 0 \le x < \infty. \tag{2.14}$$

The only *discrete*-stable distribution whose closed form is given in terms of elementary functions is the Poisson, for which $\nu = 1$:

$$P(N,1,A) = \frac{A^N}{N!}\exp(-A);\ 0 \le N < \infty \tag{2.15}$$

2.4.2 In terms of Fresnel integrals

The symmetric-stable distribution for which $\nu = 1/2$ is [97]:

$$p\left(x,\frac{1}{2},0,1\right) = \frac{|x|^{-3/2}}{\sqrt{2\pi}}\left(\sin\left(\frac{1}{4|x|}\right)\left[\frac{1}{2}-\mathrm{S}\left(\sqrt{\frac{1}{2\pi|x|}}\right)\right]+\cos\left(\frac{1}{4|x|}\right)\left[\frac{1}{2}-\mathrm{C}\left(\sqrt{\frac{1}{2\pi|x|}}\right)\right]\right)$$
$$-\infty < x < \infty \qquad (2.16)$$

where $C(z)$ and $Z(z)$ are Fresnel integrals [93]:

$$\mathrm{C}(z) = \int_0^z \cos\left(\frac{\pi t^2}{2}\right)dt\,,\ \mathrm{S}(z) = \int_0^z \sin\left(\frac{\pi t^2}{2}\right)dt\,.$$

2.4.3 In terms of modified Bessel functions

For $\nu = 1/3$ the one-sided continuous distribution is [97]:

$$p\left(x,\frac{1}{3},1,1\right) = \frac{1}{\pi}\frac{2^{3/2}}{3^{7/4}}x^{-3/2}K_{1/3}\left(\frac{2^{5/2}}{3^{9/4}}x^{-1/2}\right);\ 0 \le x < \infty \qquad (2.17)$$

where $K_\alpha(x)$ is a modified Bessel function of the second kind [93].

The discrete-stable distribution with $\nu = 1/2$ is [6]:

$$P\left(N,\frac{1}{2},A\right) = \frac{2}{\sqrt{\pi}N!}\left(\frac{A}{2}\right)^{N+1/2}K_{N-1/2}(A);\ 0 \le N < \infty\,. \qquad (2.18)$$

2.4.4 In terms of hypergeometric functions

An expression for the symmetric distribution with index $\nu = 4/3$ is given by Garoni and Frankel [96]:

$$p\left(x,\frac{4}{3},0,1\right)=\frac{3^{5/4}}{2^{5/2}\sqrt{\pi}}\frac{\Gamma(7/12)\Gamma(11/12)}{\Gamma(6/12)\Gamma(8/12)}{}_2F_2\left(\frac{7}{12},\frac{11}{12};\frac{6}{12},\frac{8}{12};\frac{3^3x^4}{2^8}\right)$$
$$-\frac{3^{11/4}|x|^3}{2^{13/2}\sqrt{\pi}}\frac{\Gamma(13/12)\Gamma(17/12)}{\Gamma(18/12)\Gamma(15/12)}{}_2F_2\left(\frac{13}{12},\frac{17}{12};\frac{18}{12},\frac{15}{12};\frac{3^3x^4}{2^8}\right)$$

$$-\infty<x<\infty. \tag{2.19}$$

The Holtsmark [40] distribution, which arises in astrophysics and is symmetric-stable with index $\nu=3/2$, is [96]:

$$p\left(x,\frac{3}{2},0,1\right)=\frac{1}{\pi}\Gamma(5/3){}_2F_3\left(\frac{5}{12},\frac{11}{12};\frac{1}{3},\frac{1}{2},\frac{5}{6};-\frac{2^2x^6}{3^6}\right)$$
$$-\frac{x^2}{3\pi}{}_3F_4\left(\frac{3}{4},1,\frac{5}{4};\frac{2}{3},\frac{5}{6},\frac{7}{6},\frac{4}{3};-\frac{2^2x^6}{3^6}\right)$$
$$+\frac{7x^4}{3^4\pi}\Gamma(4/3){}_2F_3\left(\frac{13}{12},\frac{19}{12};\frac{7}{6},\frac{3}{2},\frac{5}{3};-\frac{2^2x^6}{3^6}\right)$$

$$-\infty<x<\infty \tag{2.20}$$

The discrete-stable distribution with index $\nu=1/3$ is:

$$P\left(N,\frac{1}{3},A\right)=\frac{A^{3N}}{(3N)!}{}_0F_2\left(N+\frac{1}{3},N+\frac{2}{3};-\frac{A^3}{27}\right)$$
$$+\frac{A^2\Gamma(-1/3)\Gamma(N-2/3)}{6\sqrt{3}\pi N!}{}_0F_2\left(\frac{4}{3},\frac{5}{3}-N;-\frac{A^3}{27}\right)$$
$$-\frac{A\Gamma(-2/3)\Gamma(N-1/3)}{3\sqrt{3}\pi N!}{}_0F_2\left(\frac{2}{3},\frac{4}{3}-N;-\frac{A^3}{27}\right)$$

$$0\le N<\infty. \tag{2.21}$$

A derivation of this new result is given in §3.3.3.

2.4.5 In terms of Whittaker functions

The Whittaker functions [93, 98] which feature in the following expressions are defined as:

$$W_{\lambda,\mu}(z) = \frac{z^{\lambda}\exp(-z/2)}{\Gamma(\mu-\lambda+1/2)}\int_0^{\infty}\exp(-t)t^{\mu-\lambda-1/2}\left(1+\frac{t}{z}\right)^{\mu-\lambda-1/2}dt\,,$$

$$\Re(\mu-\lambda) > -1/2\,,\ |\arg(z)| < \pi\,.$$

The only known symmetric-stable distribution involving Whittaker functions is [99]:

$$p\left(x,\frac{2}{3},0,1\right) = \frac{1}{2\sqrt{3\pi}}|x|^{-1}\exp\left(\frac{2}{27}x^{-2}\right)\mathrm{W}_{-1/2,1/6}\left(\frac{4}{27}x^{-2}\right);\ -\infty < x < \infty\,. \quad (2.22)$$

A one-sided stable distribution for $\nu = 2/3$ is given in [100]:

$$p\left(x,\frac{2}{3},1,1\right) = \frac{\sqrt{3}}{\sqrt{\pi}}x^{-1}\exp\left(-\frac{16}{27}x^{-2}\right)\mathrm{W}_{1/2,1/6}\left(\frac{32}{27}x^{-2}\right);\ 0 \le x < \infty\,. \quad (2.23)$$

A closed-form expression for the continuous-stable distribution exists for $\beta = 1$ and $\nu = 3/2$, but is not one-sided [101] since $\nu > 1$:

$$p\left(x,\frac{3}{2},1,1\right) = \begin{cases} \dfrac{\sqrt{3}}{\sqrt{\pi}}|x|^{-1}\exp\left(\dfrac{1}{27}x^{3}\right)\mathrm{W}_{1/2,1/6}\left(-\dfrac{2}{27}x^{3}\right) & x < 0 \\ \dfrac{1}{2\sqrt{3\pi}}|x|^{-1}\exp\left(\dfrac{1}{27}x^{3}\right)\mathrm{W}_{-1/2,1/6}\left(\dfrac{2}{27}x^{3}\right) & x > 0 \end{cases} \quad (2.24)$$

This is the only continuous-stable distribution which is neither one-sided nor symmetric, and for which a closed-form expression for the density is available.

2.4.6 In terms of Lommel functions

Garoni and Frankel [96] provide the expression for the symmetric continuous-stable distribution of index $\nu = 1/3$ in terms of Lommel functions [102, 103]:

$$p\left(x, \frac{1}{3}, 0, 1\right) = \mathrm{Re}\left[\frac{2\exp(-i\pi/4)}{3\sqrt{3}\pi}|x|^{-3/2} S_{0,1/3}\left(\frac{2\exp(i\pi/4)}{3\sqrt{3}}|x|^{-1/2}\right)\right];$$

$$-\infty < x < \infty \tag{2.25}$$

Having now introduced the continuous and discrete-stable distributions, we shall now examine a process which can produce discrete-stable distributions as its stationary state.

2.5 The Death-Multiple-Immigration (DMI) process

2.5.1 Definition

The size of a population of individuals whose members die at a rate proportional to its size will decay exponentially, eventually reaching extinction. By allowing immigrants to enter in groups of 1,2,3…m from elsewhere at a rate which is independent to the size of the population, the population will equilibrate to a nonzero size.

In a slight alteration to the original work of Hopcraft et al. [5, 6], we denote the probability that there are exactly m immigrants entering the population as F_m such that F_m defines a valid discrete probability distribution function. Defining $P_N(t)$ to be the probability that the population has size N at time t, a simple model which has

only a death term (at a rate μN) and multiple immigrations (with rate ε and distribution F_m) has the transition diagram shown in Figure 2.6.

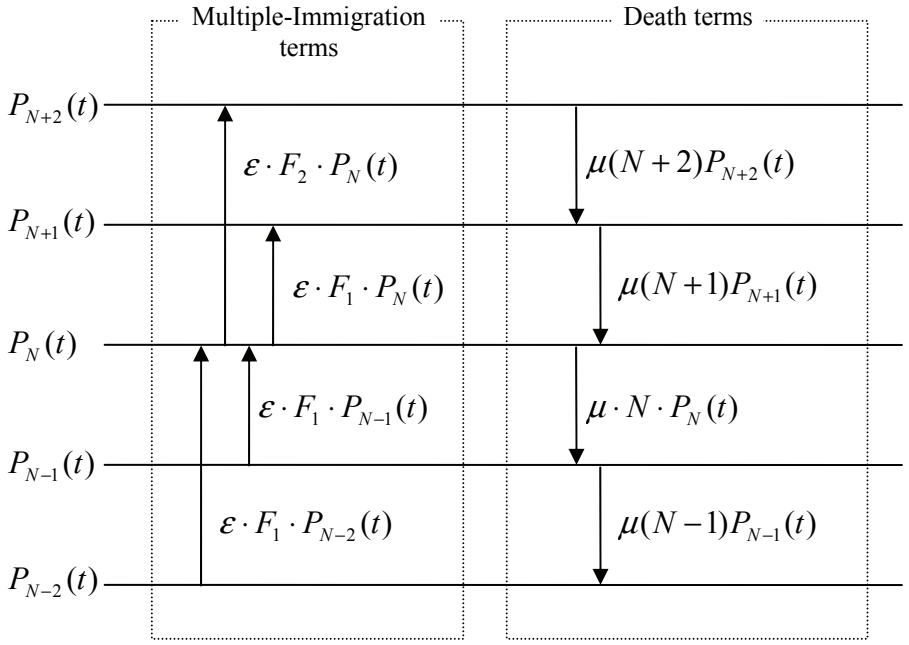

Figure 2.6

A transition diagram for the death-multiple immigration model.

The corresponding rate equation is:

$$\begin{aligned}\frac{dP_N(t)}{dt} &= \mu(N+1)P_{N+1}(t) - \mu N P_N(t) + \varepsilon\sum_{m=0}^{N} F_m P_{N-m}(t) - \varepsilon\sum_{m=0}^{\infty} F_m P_N(t) \\ &= \mu(N+1)P_{N+1}(t) - \mu N P_N(t) + \varepsilon\sum_{m=0}^{N} F_m P_{N-m}(t) - \varepsilon P_N(t)\end{aligned} \tag{2.26}$$

the second line resulting from the fact that F_m is itself a valid probability distribution and hence has unit sum.

Defining a generating function $Q(s,t)$ of $P_N(t)$, the above set of equations may be transformed into a single Partial Differential Equation (PDE) dependant on $Q_f(s)$, the generating function corresponding to the forcing terms F_m:

$$Q(s,t) = \sum_{N=0}^{\infty} (1-s)^N P_N(t) \tag{2.27}$$

$$Q_f(s) = \sum_{m=0}^{\infty} (1-s)^m F_m \tag{2.28}$$

$$\frac{\partial}{\partial t} Q(s,t) = -\mu s \frac{\partial}{\partial s} Q(s,t) + \varepsilon \cdot Q(s,t)\big(Q_f(s) - 1\big). \tag{2.29}$$

Through the use of Laplace transforms, the solution subject to the initial condition $Q(s,0) = Q_0(s)$ is obtained:

$$Q(s,t) = \frac{Q_{st}(s)}{Q_{st}\big(s\exp(-\mu t)\big)} Q_0\big(s\exp(-\mu t)\big); \tag{2.30}$$

$$Q_{st}(s) = \exp\left(\frac{\varepsilon}{\mu}\int_0^s \frac{Q_f(s')-1}{s'} ds'\right). \tag{2.31}$$

Here $Q_{st}(s)$ is the stationary state of the distribution – the limiting distribution to which the population will equilibrate in the large t limit.

The probability distribution of the stationary state is found using (2.10), i.e.

$$P_N = \frac{(-1)^N}{N!} \frac{d^N Q_{st}(s)}{ds^N}\bigg|_{s=1}.$$

Jakeman et al. [104] show that if the forcing distribution has the generating function:

$$Q_f(s) = 1 - s^\nu;\ 0 < \nu \le 1 \tag{2.32}$$

then the distribution of the immigrants is [2, 6]

$$F_m = \begin{cases} 0 & m = 0 \\ -\dfrac{\Gamma(m-\nu)}{\Gamma(m+1)\Gamma(-\nu)} & m > 0. \end{cases}$$

and the corresponding stationary state is stable:

$$Q_{st}(s) = \exp\left(-\frac{\varepsilon}{\mu\nu}s^\nu\right) = \exp(-As^\nu). \tag{2.33}$$

It then follows that the DMI process with forcing distribution (2.32) is a discrete-stable process, for which the PDE governing the generating function is:

$$\frac{\partial}{\partial t}Q(s,t) = -\mu s\frac{\partial}{\partial s}Q(s,t) - \varepsilon s^\nu Q(s,t). \tag{2.34}$$

Finally, the 'transient' generating function for the state of the discrete-stable process prior to it reaching equilibrium is:

$$Q(s,t) = \frac{\exp(-As^\nu)}{\exp(-A(s\exp(-\mu t))^\nu)}Q_0\left(s\exp(-\mu t)\right). \tag{2.35}$$

Setting $Q_0(s) = (1-s)^N$ is equivalent to setting the initial size of the population to N. The corresponding transient solution is then:

$$Q^{[N]}(s,t) = \frac{\exp(-As^\nu)}{\exp(-A(s\exp(-\mu t))^\nu)}\left(1 - s\exp(-\mu t)\right)^N. \tag{2.36}$$

Figure 2.7 plots the probability distribution of the size of a population subject to deaths and multiple immigrations as obtained from (2.34), and shows that the power-law tail on the distribution is established instantaneously.

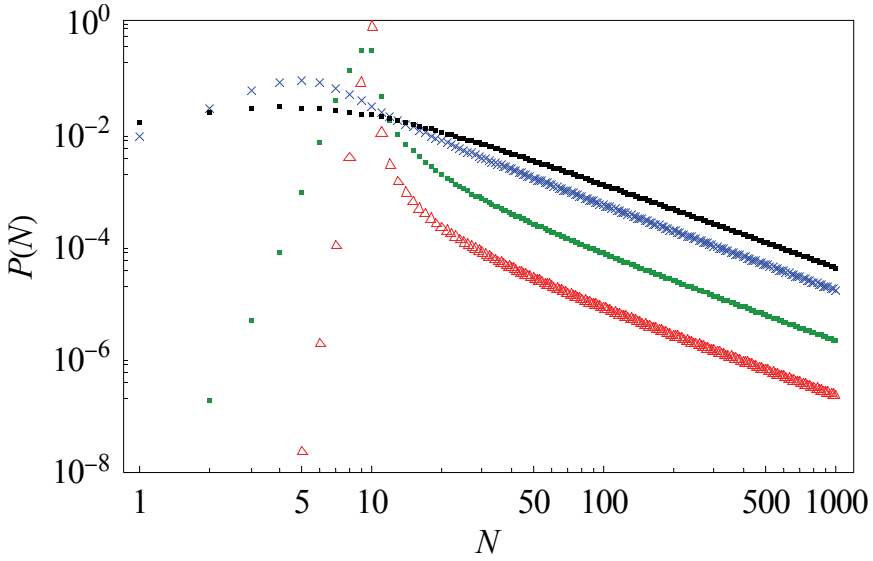

Figure 2.7

Illustrating the initialisation of the power-law even for very small values of time. The probability distribution of a Death, Multiple Immigration process with an initial condition of exactly ten individuals in the population, and for which $A = 5$, $\nu = 0.5$ is plotted. The values of μt are 0.001, 0.1, 1 (red triangles, green points and blue crosses respectively), and $\mu t = \infty$ (corresponding to the stationary solution, in black points).

2.5.2 Multiple-interval statistics

One may consider the question: what is the probability that a population has sizes N and N' following a separation time t? Given the Markovian nature of the DMI process, this result can be derived from the transient generating function (2.35) subject to the condition $Q_0(s) = (1-s)^N$, i.e. setting the initial size of the population

to N. We then denote the joint generating function corresponding to this joint probability:

$$\begin{aligned} Q(s,s';t) &= \left\langle (1-s)^N (1-s')^{N'} \right\rangle \\ &= \sum_{N=0}^{\infty} (1-s)^N P_N \sum_{N'=0}^{\infty} (1-s')^{N'} P(N'|\,N) \\ &= \sum_{N=0}^{\infty} (1-s)^N P_N Q^{[N]}(s';t) \end{aligned}$$

The joint generating function for the discrete-stable process is [6]:

$$= \exp\left(-\frac{a}{\nu\mu} \left\{ s'^{\nu} \left[1 - \exp(-\nu\mu t) \right] + \left[s + (1-s)s' \exp(\mu t) \right]^{\nu} \right\} \right) \qquad (2.37)$$

From a joint generating function, the correlation functions [e.g. 41] of a process can in principle be formed. However, as all the moments of the discrete-stable process are infinite, correlation functions are undefined. It will be shown in Chapter 4 that despite this, the joint generating function has a wider currency since it enables the generation of *continuous*-stable processes.

The use of the higher-order statistics of a process can be used to distinguish between population processes, even those for which the stationary states are identical. One such example of this is when two population processes with identical stationary states are distinguished by their third-order statistics in [53].

2.5.3 Monitoring and other population processes

Often it is difficult, if not impossible to measure a population directly without changing its dynamics. In such cases, one may monitor the *emigrants* of a population: if they are not to re-enter the population, then their being counted does not affect the dynamics. A method of monitoring emigrants of a population, which is also analytically tractable, is to model the emigrants as an additional death rate, and consider the joint distribution $P_{N,n}(T)$ of the population and the count of its emigrants. Now the variable n refers to the number of individuals which have emigrated and been counted, and T is the integration time over which the emigrants are counted. For the distribution of counts to have any sensible meaning, the internal population must already be at equilibrium before monitoring begins.

We then define the generating function of the population and its emigrants:

$$Q_c(s,z;T) = \sum_{N=0}^{\infty}(1-s)^N \sum_{n=0}^{\infty}(1-z)^n P_{N,n}(T) \tag{2.38}$$

where the variable z corresponds to the transform of the count variable n. By setting $s=0$ we obtain the generating function of the counts alone $Q_c(0,z;T)$ from which the distribution can be recovered using (2.10). Altering the rate equation (2.26) suitably, including a counting process, and using the generating function (2.38), the counting statistics of any discrete Markov population process can be deduced. Note, however, that if the stationary solution of the population has an infinite mean, then the distribution of the counts will have an infinite mean for any nonzero monitoring time T. In particular, the distribution of counts from monitoring the discrete-stable

process (2.34) with $0 < \nu \leq 1$ is *also* discrete stable [e.g. 5], the case $\nu = 1$ corresponding to a Poisson process, for which the distribution of the counts is also Poisson.

The Birth-Death-Immigration (BDI) process [e.g. 41] is a first-order Markov process in which deaths occur as in the DMI process, but immigrants enter singly and births occur at a rate proportional to the number of individuals present. When the death rate is greater than the birth rate, the stationary state of the population is negative binomial. When the births and deaths occur at the same rate, the stationary solution has a Bose-Einstein or geometric distribution – this particular process has been used for a model for thermal light, and characterises the photon statistics of lasers below threshold [105].

The Death, Multiple Immigration [e.g. 5] process is a generalisation of the death, *double* immigration process in which immigrants only ever enter in pairs. This 'pairs' process [61] was used to model the production of photon pairs in a non-linear crystal [106] – one of the first methods found to produce so-called 'non-classical' light. Through tailoring the rate of immigration in the process, it is possible to create strong odd-even effects which clearly cannot be represented through mean-field approximations.

2.6 Summary

This chapter has introduced the continuous and discrete stable distributions, and stated some of their properties and peculiarities. Despite the lack of general closed-form expressions for the distributions and the profusion of incorrect results, the stable distributions are ubiquitous in nature, and progress is still being made on understanding them.

A discrete-stable process was introduced as a special case of the Death, Multiple-Immigration (DMI) process, and properties such as a transient solution and joint generating function were given. The concept of monitoring population processes was established, and related population processes were also discussed.

In this introductory chapter, the continuous and discrete stable distributions are treated as separate entities. This apparent dichotomy is addressed in Chapter 3, which connects the discrete-stable distributions with the one-sided continuous-stable distributions through a Poisson transform interrelationship.

3. The Gaussian and Poisson transforms

3.1 Introduction

So far we have only examined the case of continuous stable distributions for which the scale parameter a is fixed. The term 'doubly stochastic' when applied to probability distributions refers to one parameter of a distribution being 'smeared' by another. An example of this, stated by Teich and Diament [107], is the well known result that when the mean of a Poisson distribution is modulated by a gamma distribution, the result is negative binomial. It would be instructive to allow the scale parameter of *stable* distributions to vary according to other stable distributions and examine the results.

This chapter will begin by giving an alternative proof to a result in the literature [41] which uses the one-sided continuous-stable distributions to modulate the variance of the Gaussian distribution, forming a 'Gaussian transform'. It will be shown that in this case, the resultant distribution is another symmetric-stable distribution.

The concept of the 'Gaussian transform' is then extended to the 'Poisson transform', whereby the *mean* of a Poisson distribution is modulated by a one-sided stable distribution. The mathematics of the Poisson transform are given from a photon counting perspective. The intrinsic connection between the discrete and continuous distributions through the Poisson transform is found, and the limit as the power-law

index $\nu \to 1$ (which was shown in Chapter 2 to have singular behaviour) is examined to elucidate the scaling that occurs between the two distributions.

3.2 The Gaussian transform

3.2.1 Definition

The support of the one-sided continuous stable distributions covers all allowable values of the variance of a Gaussian distribution, so it is logical to consider a 'Gaussian transform' where the *variance* of a Gaussian is modulated by a one-sided continuous distribution. To do this, we first start by defining the Gaussian transform, which takes a (one-sided) continuous distribution and outputs a symmetric distribution. Recall that a Gaussian distribution of variance $\sigma^2 = 2a$ has characteristic function $C(u) = \exp(-au^2)$ and density given by

$$p(x,2,0,a) = \frac{1}{2\sqrt{a\pi}} \exp\left(-\frac{x^2}{4a}\right).$$

If the value of a is itself a random variable whose PDF is $\bar{p}(a)$ then the 'Gaussian transformed' probability density function is:

$$p(x) = \int_0^\infty \bar{p}(a) \frac{1}{2\sqrt{a\pi}} \exp\left(-\frac{x^2}{4a}\right) da\,. \tag{3.1}$$

It is clear that in the case when $\bar{p}(a)$ is a delta function, $p(x)$ is again a Gaussian distribution as expected.

Given that $p(x)$ is an even function, its odd moments are zero – evaluation of the even moments of the new distribution can be obtained through direct integration of the PDF:

$$\begin{aligned}\int_{-\infty}^{\infty} p(x)x^{2r}dx &= \int_{-\infty}^{\infty}\left(\int_{0}^{\infty}\overline{p}(a)\frac{1}{2\sqrt{a\pi}}\exp\left(-\frac{x^2}{4a}\right)da\right)x^{2r}dx \\ &= \int_{0}^{\infty}\overline{p}(a)\left(\int_{-\infty}^{\infty}\frac{1}{2\sqrt{a\pi}}\exp\left(-\frac{x^2}{4a}\right)x^{2r}dx\right)da \\ &= \frac{(2r)!}{r!}\int_{0}^{\infty}\overline{p}(a)a^{r}da.\end{aligned} \tag{3.2}$$

Hence the moments of the Gaussian transformed distribution are proportional to that of the one-sided continuous distribution, except that the order of each moment is doubled.

The characteristic function can be evaluated easily using the form of the Gaussian transform (3.1):

$$\begin{aligned}C(u) &= \int_{-\infty}^{\infty}\left(\int_{0}^{\infty}\overline{p}(a)\frac{1}{2\sqrt{a\pi}}\exp\left(-\frac{x^2}{4a}\right)da\right)\exp(ixu)dx \\ &= \int_{0}^{\infty}\overline{p}(a)\left(\int_{-\infty}^{\infty}\exp(ixu)\frac{1}{2\sqrt{a\pi}}\exp\left(-\frac{x^2}{4a}\right)dx\right)da \\ &= \int_{0}^{\infty}\overline{p}(a)\exp\left(-au^2\right)da \\ &= \int_{0}^{\infty}\overline{p}(a)c(u,2,\beta,a)da\end{aligned} \tag{3.3}$$

and is effectively the Laplace transform of $\overline{p}(a)$. This shows that the Gaussian transform can be thought of as a weighed average of Gaussian distributions with different variances.

Having now laid the foundations for the Gaussian transform, we may proceed to apply it to the one-sided stable distributions.

3.2.2 Gaussian transforms of one-sided stable distributions

To evaluate the Gaussian transform of the one-sided continuous-stable distributions, we need to first obtain their PDFs $p(a,\nu,1,b)$. This is done by setting $\beta = 1$ in the characteristic function (2.1) and using the inverse Fourier transform (2.3) when $0 < \nu < 1$, using w as the Fourier variable, and b as the scale factor:

$$p(a,\nu,1,b) = \frac{1}{2\pi}\int_{-\infty}^{\infty} \exp(-iaw)\exp\left(-b|w|^{\nu}\left(1 - i\,\mathrm{sgn}(w)\tan\left(\frac{\pi\nu}{2}\right)\right)\right)dw. \qquad (3.4)$$

We then use this PDF as the one-sided distribution $\overline{p}(a)$ in (3.3). Upon noting that the integrations over a and w are independent, we may exchange their order:

$$\begin{aligned} C(u) &= \frac{1}{2\pi}\int_{0}^{\infty}\left[\int_{-\infty}^{\infty} \exp(-iaw)\exp\left(-b|w|^{\nu}\left(1 - i\,\mathrm{sgn}(w)\tan\left(\frac{\pi\nu}{2}\right)\right)\right)dw\right]\exp\left(-au^2\right)da \\ &= \frac{1}{2\pi}\int_{-\infty}^{\infty}\left[\int_{0}^{\infty} \exp(-iaw)\exp\left(-au^2\right)da\right]\exp\left(-b|w|^{\nu}\left(1 - i\,\mathrm{sgn}(w)\tan\left(\frac{\pi\nu}{2}\right)\right)\right)dw \\ &= \frac{1}{2\pi}\int_{-\infty}^{\infty}\frac{1}{u^2 + iw}\exp\left(-b|w|^{\nu}\left(1 - i\,\mathrm{sgn}(w)\tan\left(\frac{\pi\nu}{2}\right)\right)\right)dw \end{aligned}$$

This integral does not readily yield to direct evaluation, however as there is a term in $(u^2 + iw)^{-1}$, an alternative method using contour integration is possible. To that end, we remove the modulus and sign functions by splitting the integral into two parts and transform $w \to -w$ in the integral over negative w. This then gives:

$$C(u) = \int_0^\infty \frac{1}{2\pi}\left\{\frac{1}{(u^2 - iw)}\exp\left(-bw^v\left(1 + i\tan\left(\frac{\pi v}{2}\right)\right)\right)\right. \\ \left. + \frac{1}{(u^2 + iw)}\exp\left(-bw^v\left(1 - i\tan\left(\frac{\pi v}{2}\right)\right)\right)\right\}dw \tag{3.5}$$

Since this is the sum of a complex term and its complex conjugate, it follows that an alternative expression for $C(u)$ which highlights the fact that it is real is:

$$C(u) = \int_0^\infty \mathrm{Re}\left\{\frac{1}{\pi}\frac{1}{(u^2 + iw)}\exp\left(-bw^v\left(1 - i\tan\left(\frac{\pi v}{2}\right)\right)\right)\right\}dw \tag{3.6}$$

For the contour integration of (3.5), we define Γ to be the contour along the real line from 0 to A, anticlockwise along an arc from A to $A\exp(i\theta)$, then returning along a line from $A\exp(i\theta)$ to 0. These curves are shown on the Argand diagram in Figure 3.1 below.

The simple closed contour Γ is then comprised of the three curves $\Gamma_1, \Gamma_2, \Gamma_3$ in the complex plane. Residue theorem then states that the integral along the contour Γ is the sum of the residues of the integrand of (3.5) inside Γ. The only singularity is at $w = iu^2$, the residue of which we shall denote as R. In order that the contour encloses

the singularity, we require that $\theta > \pi/2$ – for the sake of simplicity, we shall work in the limit $\theta \to (\pi/2)^+$. If we take another limit as $A \to \infty$, the integral along Γ_1 is equal to that of the characteristic function $C(u)$, given by (3.5).

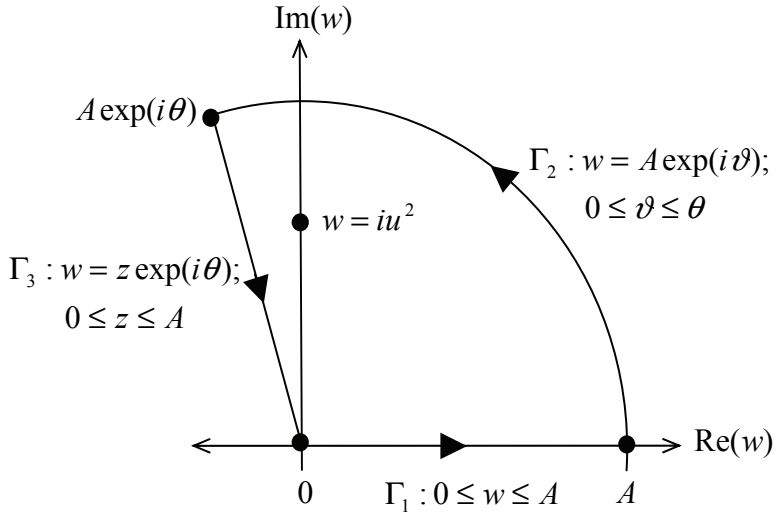

Figure 3.1

The path of the contour Γ on an Argand diagram

Hence by denoting the integrals over the curves $\Gamma_{1,2,3}$ in the limits to be $I_{1,2,3}$, we write:

$$\begin{aligned}\lim_{\substack{A\to\infty \\ \theta\to(\pi/2)^+}} \int_\Gamma \cdots du &= \lim_{\substack{A\to\infty \\ \theta\to(\pi/2)^+}} \left[\int_{\Gamma_1} \cdots du + \int_{\Gamma_2} \cdots du + \int_{\Gamma_3} \cdots du\right] \\ &= I_1 + I_2 + I_3 \\ &= 2\pi i \operatorname{Res}(\cdots)\big|_{w=iu^2} \\ &= R\end{aligned} \tag{3.7}$$

or, alternatively,

$$C(u) = R - I_2 - I_3$$

where the ellipsis refers to the integrand in (3.5), or equivalently, (3.6). The first term is easily evaluated:

$$\begin{aligned} R &= 2\pi i \operatorname{Res}\left(\frac{1}{2\pi}\left\{ \frac{1}{(u^2 - iw)} \exp\left(-bw^v \left(1 + i\tan\left(\frac{\pi v}{2}\right)\right)\right)\right.\right. \\ &\qquad \left.\left. + \frac{1}{(u^2 + iw)} \exp\left(-bw^v \left(1 - i\tan\left(\frac{\pi v}{2}\right)\right)\right)\right\}\right)\Bigg|_{w=iu^2} \\ &= \exp\left(-bw^v \left(1 - i\tan\left(\frac{\pi v}{2}\right)\right)\right)\Bigg|_{w=iu^2} \\ &= \exp\left(-b(iu^2)^v \left\{ 1 - i\tan\left(\frac{\pi v}{2}\right)\right\}\right). \end{aligned}$$

The above may be further simplified by noting that the imaginary term and the term within the braces may be written in exponential forms, revealing their arguments and moduli:

$$\begin{aligned} R &= \exp\left(-bu^{2v} \exp\left[\frac{i\pi}{2}v\right] \sqrt{1 + \tan^2\left(\frac{\pi v}{2}\right)} \exp\left[-\frac{i\pi v}{2}\right]\right) \\ &= \exp\left(-bu^{2v} \sec\left(\frac{\pi v}{2}\right)\right) \end{aligned}$$

Having now found the residue of the pole, the next step is to evaluate the integral over the contour Γ_2. Here it is most logical to use polar coordinates in the real integral form (3.6), and integrate over the angular variable ϑ, which runs from 0 to θ:

$$w = A\exp(i\vartheta); \qquad dw = d\vartheta \cdot iA\exp(i\vartheta)$$

The integral can then be written in the following form:

$$I_2 = \lim_{\substack{A\to\infty \\ \theta\to(\pi/2)^+}} \int_0^{\theta} \mathrm{Re}\left\{ \frac{i}{\pi} \frac{\exp(i\vartheta)A}{u^2 + i\exp(i\vartheta)A} \exp\left(-bA^{\nu} \exp(i\vartheta\nu)\left(1 - i\tan\left(\frac{\pi\nu}{2}\right)\right)\right)\right\} d\vartheta$$

Given that we are interested in the limit as $A \to \infty$, the first terms in the integrand are:

$$\lim_{A\to\infty}\left(\frac{i}{\pi} \frac{\exp(i\vartheta)A}{u^2 + i\exp(i\vartheta)A} \right) = \frac{1}{\pi}.$$

Upon substituting $\exp(i\vartheta\nu) = \cos(\vartheta\nu) + i\sin(\vartheta\nu)$ and splitting the exponential term into a product of real and imaginary exponentials, we have:

$$I_2 = \lim_{\substack{A\to\infty \\ \theta\to(\pi/2)^+}} \frac{1}{\pi} \int_0^{\theta} \mathrm{Re}\left\{ \exp\left[-bA^{\nu}\left(\cos(\vartheta\nu) + \sin(\vartheta\nu)\tan\left(\frac{\pi\nu}{2}\right)\right)\right] \right.$$
$$\left. \times \exp\left[ibA^{\nu}\left(\cos(\vartheta\nu)\tan\left(\frac{\pi\nu}{2}\right) - \sin(\vartheta\nu)\right)\right]\right\} d\vartheta$$

The real exponential must tend to zero if $A \to \infty$ and $\theta \to (\pi/2)^+$ since $b > 0$ and when $0 \le \vartheta \le \pi$ and $0 < \nu < 1$,

$$\cos(\vartheta\nu) + \sin(\vartheta\nu)\tan\left(\frac{\pi\nu}{2}\right) > 0.$$

Therefore the integrand must be zero, i.e.

$$I_2 = 0.$$

The final integral to close the contour Γ is over the curve Γ_3. For this, it is most convenient to transform to a new coordinate z which runs along the curve and use the parameterisation (3.6):

$$w = z\exp(i\theta); \qquad dw = dz\cdot\exp(i\theta).$$

$$\begin{aligned} I_3 &= \mathrm{Re}\int_A^0 \frac{1}{\pi}\frac{\exp(i\theta)}{u^2 + i\exp(i\theta)z}\exp\left(-bz^\nu\exp(i\theta\nu)\left(1 - i\tan\left(\frac{\pi\nu}{2}\right)\right)\right)dz \\ &= \mathrm{Re}\int_A^0 \frac{1}{\pi}\frac{\exp(i\theta)}{u^2 + i\exp(i\theta)z}\left\{\exp\left(-bz^\nu\left[\cos(\theta\nu) + \sin(\theta\nu)\tan\left(\frac{\pi\nu}{2}\right)\right]\right)\right. \\ &\qquad\left.\times\exp\left(ibz^\nu\left[\cos(\theta\nu)\tan\left(\frac{\pi\nu}{2}\right) - \sin(\theta\nu)\right]\right)\right\}dz \end{aligned}$$

As we are examining the contour in the limit $\theta \to (\pi/2)^+$, the above may be simplified greatly since:

$$\lim_{\theta\to(\pi/2)^+}\left(\frac{\exp(i\theta)}{u^2 + i\exp(i\theta)z}\right) = \frac{i}{u^2 - z}$$

$$\lim_{\theta\to(\pi/2)^+}\left(\cos(\theta\nu) + \sin(\theta\nu)\tan\left(\frac{\pi\nu}{2}\right)\right) = \sec\left(\frac{\pi\nu}{2}\right)$$

$$\lim_{\theta\to(\pi/2)^+}\left(\cos(\theta\nu)\tan\left(\frac{\pi\nu}{2}\right) - \sin(\theta\nu)\right) = 0$$

Thus, the integral is entirely imaginary and so the contribution from the contour Γ_3 is zero:

$$\begin{aligned} I_3 &= \mathrm{Re}\int_0^\infty \frac{1}{\pi}\frac{i}{u^2 - z}\exp\left(-b\sec\left(\frac{\pi\nu}{2}\right)z^\nu\right)\times\exp\left(ibz^\nu\cdot 0\right)dz \\ &= 0 \end{aligned}$$

Given that $I_2 = I_3 = 0$, it follows that:

$$\begin{aligned} C(u) &= 2\pi i \operatorname{Res}(\cdots)\big|_{w=iu^2} \\ &= \exp\left(-b\sec\left(\frac{\pi\nu}{2}\right)u^{2\nu}\right), \qquad 0<\nu<1 \end{aligned} \tag{3.8}$$

$$= C\left(u, 2\nu, 0, b\sec\left(\frac{\pi\nu}{2}\right)\right) \tag{3.9}$$

which is the characteristic function of a symmetric-stable distribution (2.1) with power-law index 2ν, symmetry parameter $\beta = 0$ and scale parameter given by $a = b\sec(\pi\nu/2)$.

This shows that the 'Gaussian transform' of a one-sided stable distribution of index ν is a continuous-stable distribution whose index is 2ν. The scaling of the scale factor must occur since in the limit as $\nu \to 1$, the mode of the one-sided stable distributions tends to infinity (see Figure 2.2). Consequently, when taking the Gaussian transform of a one-sided stable distribution with $\nu \to 1$, the scale parameter of the resulting symmetric-stable distribution must also diverge.

Having now found the relationship between the one-sided and symmetric-stable distributions via the 'Gaussian transform', we shall now consider the case of a 'Poisson transform' which transforms continuous distributions into discrete distributions through modulating the mean of a Poisson distribution.

3.3 The Poisson transform

3.3.1 Definition

The Poisson transform was introduced by Cox [58] when he studied the breakdown of cotton looms. If the quality of the cotton was constant, the breakdown could be modelled simply as a Poisson process with a constant rate. Cox found, however, that the number of breakdowns over a certain time period varied, and described a Poisson process whose mean was a stochastic variable which depended on the quality of the cotton. Hence this loom breakdown process is known as a Cox process, or more commonly, a Doubly Stochastic Poisson Process.

Another physically occurring example of the Doubly Stochastic Poisson Process arises in photon counting and was first described by Mandel et al. [108] as follows. The photoelectric effect [e.g. 59] describes the release of electrons from metals when hit by light of certain frequencies. A positively charged 'photocathode' attracts the electrons emitted by the metal – if the metal undergoing the photoelectric effect is the anode, then a current is induced between the two. Since single electrons are hard to detect individually, a photomultiplier is placed between the anode and the cathode to amplify the current. An electron counter is then able to register the resultant pulse of electrons from the anode. This is illustrated schematically in Figure 3.2:

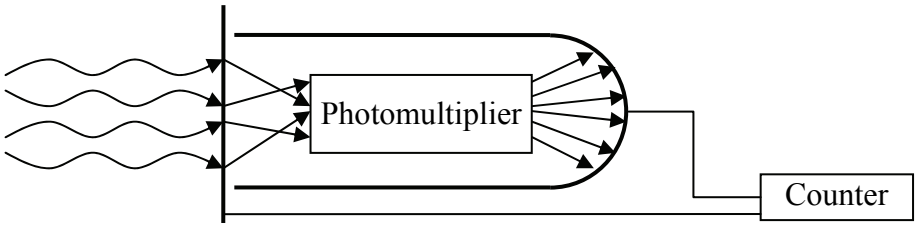

Figure 3.2

Illustrating the photon counting mechanism. The electrons given off through the photoelectric effect from the anode are amplified by the photomultiplier and reach the cathode. The corresponding electric current is measured by an electronic counter. For a full treatment of this, see [59, §9.1].

Defining $p(w)$ to be the probability density function of the light intensity w, the distribution of the number of counts over the interval is then [59]:

$$P(N) = \int_0^\infty p(w) \frac{w^N \exp(-w)}{N!} dw. \tag{3.10}$$

This result is termed the 'Poisson transform' and is general in that it can be used to model counting statistics of a field that fluctuates over time. In the case that the intensity is time-independent, the integrated light intensity is constant, and hence $p(w)$ describes a delta function, and the distribution of the number of counts is Poisson.

Calculating the generating function $Q(s)$ from the Poisson transformed distribution (3.10), we have:

$$
\begin{aligned}
Q(s) &= \sum_{N=0}^{\infty} (1-s)^N \left(\int_0^{\infty} p(w) \frac{w^N \exp(-w)}{N!} dw \right) \\
&= \int_0^{\infty} p(w) \exp(-w) \left(\sum_{N=0}^{\infty} (1-s)^N \frac{w^N}{N!} \right) dw \\
&= \int_0^{\infty} p(w) \exp(-w) \exp\big((1-s)w\big) dw \\
&= \int_0^{\infty} p(w) \exp(-ws) dw
\end{aligned}
\tag{3.11}
$$

which is simply the Laplace transform of the intensity $p(w)$. It must follow then, that the intensity $p(w)$ can be recovered through the inverse Laplace transform of $Q(s)$:

$$p(w) = L^{-1}\big(Q(s)\big). \tag{3.12}$$

The Poisson transform is not only valuable as it relates discrete distributions to continuous ones through a physical process – it also has the property (which can be verified by differentiation of $Q(s)$) that the integer moments of the intensity $p(x)$ is equal to the factorial moments of the distribution $P(N)$, so

$$\int_0^{\infty} p(w) w^r dw = \sum_{N=0}^{\infty} P(N) \cdot N(N-1) \cdots (N-r+1).$$

Having established the necessary tools to convert from discrete to continuous (and vice-versa) one-sided distributions, we shall apply them to the one-sided stable distributions.

3.3.2 Poisson transforms of one-sided stable distributions

Recall that the one-sided stable distributions are defined by setting $\beta = 1$ in (2.1) so that $p(x)$ is defined only for $x \geq 0$. Upon application of (3.11) to (2.3), we obtain the generating function of a Poisson transformed stable distribution:

$$Q(s) = \int_0^\infty \exp(-sx)\left[\frac{1}{2\pi}\int_{-\infty}^{\infty}\exp(-ixu)C(u)du\right]dx \qquad 0 < \nu < 1 \tag{3.13}$$

where

$$C(u) = \exp\left(-a|u|^{\nu}\left(1 - i\beta\,\mathrm{sgn}(u)\tan\left(\frac{\pi\nu}{2}\right)\right)\right).$$

Noting that the integrations over x and u are independent, we exchange the order of integration and evaluate the integral over x first:

$$Q(s) = \frac{1}{2\pi}\int_{-\infty}^{\infty}\frac{1}{s+iu}\exp\left(-a|u|^{\nu}\left(1 - i\,\mathrm{sgn}(u)\tan\left(\frac{\pi\nu}{2}\right)\right)\right)du\,. \tag{3.14}$$

Splitting the integral over positive and negative u and transforming $u \to -u$ in the latter, this becomes:

$$Q(s) = \frac{1}{2\pi}\int_{-\infty}^{\infty}\left\{\frac{1}{s-iu}\exp\left(-a|u|^{\nu}\left(1 + i\,\mathrm{sgn}(u)\tan\left(\frac{\pi\nu}{2}\right)\right)\right)\right.$$
$$\left. + \frac{1}{s+iu}\exp\left(-a|u|^{\nu}\left(1 - i\,\mathrm{sgn}(u)\tan\left(\frac{\pi\nu}{2}\right)\right)\right)\right\}du$$

This integral is of the same form as that which gives the characteristic function of the Gaussian transform of the one-sided stable distributions (3.5), so

$$Q(s) = \exp\left(- a \sec\left(\frac{\pi\nu}{2} \right) s^{\nu} \right)$$

$$= Q\left(s, \nu, a \sec\left(\frac{\pi\nu}{2} \right) \right), \quad 0 < \nu < 1 \tag{3.15}$$

which is exactly the generating function of a discrete-stable distribution (2.8) with power-law index ν. Therefore, the Poisson transforms of the one-sided Levy distributions are the discrete-stable distributions; the two scale parameters being linked through:

$$a = A \cos(\pi\nu / 2). \tag{3.16}$$

It must then follow that the Laplace transform of the one-sided continuous-stable distributions is:

$$\int_0^{\infty} p(x, \nu, 1, a) \exp(-sx) dx = \exp\left(- a \sec\left(\frac{\pi\nu}{2} \right) s^{\nu} \right). \tag{3.17}$$

This result, which is disseminated in Lee, Hopcraft and Jakeman [109] is significant since it links the one-sided continuous-stable distributions (2.1 with $\beta = 1$) to the discrete-stable distributions (2.8) via a Poisson transform, despite the fact that both distributions have infinite means, and hence all other moment-based measures are undefined.

A corollary of the Laplace transform result (3.17) is that the one-sided continuous-stable distributions can also be defined as the *inverse*-Laplace transform of $Q(s) = \exp(-s^{\nu})$. In this case, we write, for convenience, the group of distributions

$$\begin{aligned} p_{\nu}(x) &= \underset{s \to x}{\mathcal{L}^{-1}}\left(\exp\left(-as^{\nu}\right)\right) \\ &= p\left(x, \nu, 1, a\cos\left(\frac{\pi\nu}{2}\right)\right). \end{aligned} \tag{3.18}$$

3.3.3 A new discrete-stable distribution

The above Poisson transform interrelationship between one-sided continuous-stable distributions and discrete-stable distributions can be used to find the expression of a previously unknown discrete-stable distribution.

Recall that in §2.4 the one-sided continuous-stable distribution of index $\nu = 1/3$ is given in terms of modified Bessel functions of the second kind by (2.17):

$$p\left(x, \frac{1}{3}, 1, 1\right) = \frac{1}{\pi}\frac{2^{3/2}}{3^{7/4}}x^{-3/2}K_{1/3}\left(\frac{2^{5/2}}{3^{9/4}}x^{-1/2}\right).$$

If we use (2.5) to permit the scale parameter a to vary using (2.5), we obtain:

$$p\left(x, \frac{1}{3}, 1, a\right) = \frac{1}{\pi}\frac{2^{3/2}a^{3/2}}{3^{7/4}}x^{-3/2}K_{1/3}\left(\frac{2^{5/2}a^{3/2}}{3^{9/4}}x^{-1/2}\right).$$

Poisson transforming the resulting distribution using (3.10) obtains:

$$\int_0^\infty p\left(x,\frac{1}{3},1,a\right)\frac{x^N\exp(-x)}{N!}dx$$
$$=\int_0^\infty \frac{1}{\pi}\frac{2^{3/2}a^{3/2}}{3^{7/4}}x^{-3/2}K_{1/3}\left(\frac{2^{5/2}a^{3/2}}{3^{9/4}}x^{-1/2}\right)\frac{x^N\exp(-x)}{N!}dx$$
$$=\frac{1}{\pi}\frac{2^{3/2}a^{3/2}}{3^{7/4}N!}\int_0^\infty x^{N-3/2}K_{1/3}\left(\frac{2^{5/2}a^{3/2}}{3^{9/4}}x^{-1/2}\right)\exp(-x)dx \qquad (3.19)$$

Using (3.16) to relate the scale parameters a and A, we obtain $a = A\sqrt{3}/2$. An evaluation of the above integral in Mathematica then gives:

$$P\left(N,\frac{1}{3},A\right)=\frac{A^{3N}}{(3N)!}{}_0F_2\left(N+\frac{1}{3},N+\frac{2}{3};-\frac{A^3}{27}\right)$$
$$+\frac{A^2\Gamma(-1/3)\Gamma(N-2/3)}{6\sqrt{3}\pi N!}{}_0F_2\left(\frac{4}{3},\frac{5}{3}-N;-\frac{A^3}{27}\right)$$
$$-\frac{A\Gamma(-2/3)\Gamma(N-1/3)}{3\sqrt{3}\pi N!}{}_0F_2\left(\frac{2}{3},\frac{4}{3}-N;-\frac{A^3}{27}\right)$$

which is a new result for the discrete-stable distribution of index $\nu = 1/3$. The form of the one-sided continuous-stable distribution for which $\nu = 2/3$ does not lend itself easily to evaluation of the Poisson transform.

3.3.4 In the Poisson limit

Recall that as the power-law index ν approaches unity, the mode of the one-sided continuous-stable distributions diverges (c.f. Figure 2.2). The effect of this divergence of the mode can be seen in the Poisson transform of the same continuous-stable distributions. Figure 3.3 shows the discrete and stable-continuous distributions with $a = 1$ and $\nu = 0.99$; the mode of both being approximately $\tan(0.99\pi/2) \approx 64$.

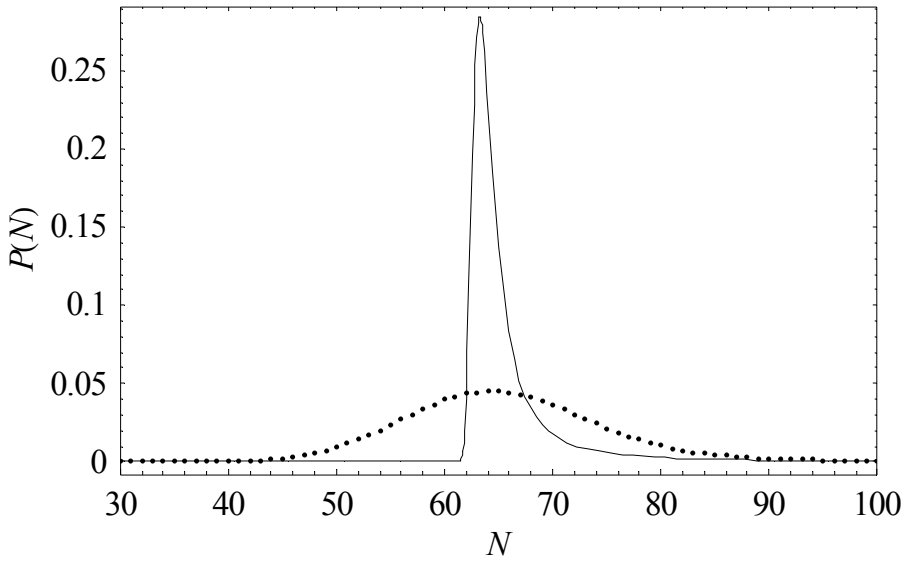

Figure 3.3

Comparison of the discrete (dots) and continuous-stable (line) distributions, with ν = 0.99 and scale parameter a = 1.

We can use the scaling relation (3.16) to resolve the issue of the diverging modes. Recall (e.g. Figure 2.4) that for the discrete-stable distributions, as $\nu \to 1$ the changeover between Poissonian to power-law behaviour occurs at larger values of N, but the mode remains the same. It then stands to reason that by keeping the value of A fixed, and setting the scale parameter of the continuous-stable distribution to be $a = A\cos(\pi\nu/2)$, the continuous-stable distributions must then tend to a Dirac delta function centred at A. This rescaling is demonstrated in Figure 3.4, which shows the continuous-stable distributions for $A = 1$ and ν = 0.7, 0.8, and 0.9. For comparison, the distribution $p(x,1,1,1)$, which marks the boundary between one-sidedness and two-sidedness is also plotted.

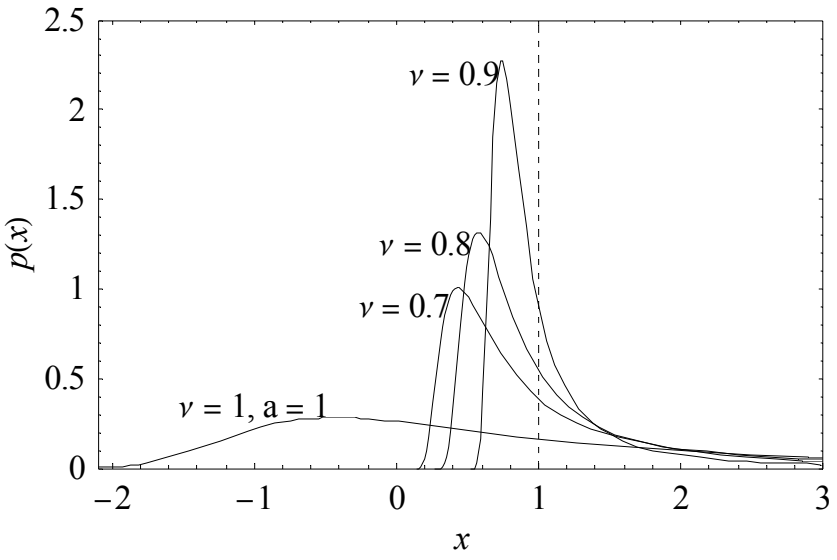

Figure 3.4

Showing the one-sided continuous-stable distributions with scale parameter $a = \cos(\pi v/2)$ as v tends to 1. The limiting case $v = 1$, which does not scale and is two-sided is also shown. The dotted line represents the delta function limit as $v \to 1$.

Using the scaling relation (2.5), it is clear that this scaling is equivalent to setting:

$$p\left(x,\nu,1,a\cos\left(\frac{\pi\nu}{2}\right)\right) \to p\left(r'x,\nu,1,a\right)\cdot r' \qquad r' = \sec^{\frac{1}{\nu}}\left(\frac{\pi\nu}{2}\right).$$

It can be readily shown using trigonometric identities that the effective scale parameter r' satisfies:

$$\lim_{\nu\to 1} r' = \lim_{\nu\to 1} \sec^{\frac{1}{\nu}}\left(\frac{\pi\nu}{2}\right) = \tan\left(\frac{\pi\nu}{2}\right) \tag{3.20}$$

which gives an intuitive interpretation of the rate of divergence of the mode of the one-sided continuous-stable distributions $p\left(x,\nu,1,a\right)$ as $\nu \to 1$.

Setting $\nu = 1$ in (2.8) or (3.15) describes a Poisson distribution. Recall that according to the Poisson transform (3.10), to have Poisson distributed counts, the continuous distribution to be Poisson transformed must be a delta function. Setting $\nu = \beta = 1$ in (2.1) gives the two-sided distribution shown in Figure 3.4 which is clearly not a delta function. According to the scaling relation (3.16), for the continuous-stable distribution to have a Poisson distributed Poisson transform, its scale parameter a must be zero. This degenerate case is not permitted, however, since it would then not have a power-law tail; the restriction that $a > 0$ for all the continuous-stable distributions means that all but the Gaussian have power-law tails.

An auxiliary advantage of knowing the form of the Poisson transform of one-sided stable distributions is that the generating function of the transform is identical to its Laplace transform (e.g. 3.11). For $1 \le \nu \le 2$ and $\beta = \pm 1$, the continuous-stable distributions are not one-sided, and so the traditional Laplace transform is undefined. One may instead consider a *bilateral* Laplace transform for which the limits of integration range from $-\infty$ to ∞. Samorodnitsky and Taqqu [39] provide without proof the *bilateral* Laplace transforms for the continuous-stable distributions with $\beta = 1$, $1 \le \nu \le 2$, i.e.:

$$Q(s) = \int_{-\infty}^{\infty} \exp(-sx)\, p(x) dx = \begin{cases} s^{\left(\frac{2as}{\pi}\right)} & \nu = 1 \\ \exp\left(-a \sec\left(\frac{\pi\nu}{2}\right) s^{\nu} \right) & 1 < \nu \le 2 \end{cases}$$

The form of the bilateral Laplace transform for $1 < \nu \leq 2$ is identical to that of the earlier result (3.8) for $0 < \nu < 1$. Since the PDF of the one-sided continuous-stable distributions are zero for negative x, the expression for $1 < \nu < 2$ given above may be extended to $0 < \nu < 1$.

3.4 'Stable' transforms

Having found the Gaussian and Poisson transform of the one-sided continuous-stable distributions, for which the power-law index is in the range of $0 < \nu < 1$, one may ask the question – can these transform methods be applied to *other* stable distributions? Recall that the characteristic function of the Gaussian transform of a one-sided distribution $\overline{p}(a)$ is (3.3) a Laplace transform:

$$C(u) = \int_0^\infty \overline{p}(a) \exp\left(-au^2\right) da$$

and that the generating function of the Poisson transform of a one-sided distribution is another Laplace transform (3.11), i.e.

$$Q(s) = \int_0^\infty \overline{p}(a) \exp\left(-as\right) da \,.$$

Either of these results could be derived from noting that they are weighted averages of either characteristic or generating functions, and thus do not require the form of $p(x)$ or $P(N)$ to be known. The form of the symmetric continuous-stable distributions' characteristic function is

$$C(u,\nu,0,a) = \exp(-a|u|^{\nu}); \qquad 0 < \nu \le 2,\ \text{a} > 0$$

and the discrete-stable distributions' generating function can also be written:

$$\begin{aligned} Q(s,\nu,A) &= \exp(-As^{\nu}) \\ &= \exp(-A|s|^{\nu}); \qquad 0 < \nu \le 1,\ \text{A} > 0. \end{aligned}$$

We can therefore state without loss of generality that the transforms (3.3) and (3.11) can be extended to the *symmetric-stable* transform

$$C(u) = \int_0^{\infty} \bar{p}(a) \exp\left(-a|u|^{\nu}\right) da; \qquad 0 < \nu \le 2 \tag{3.21}$$

or a *discrete-stable* transform of $\bar{p}(a)$:

$$Q(s) = \int_0^{\infty} \bar{p}(a) \exp\left(-a|s|^{\nu}\right) da; \qquad 0 < \nu \le 1. \tag{3.22}$$

Equations (3.21) and (3.22) describe allowing the scale parameters of symmetric-stable and discrete-stable distributions to be modulated by the distribution $\bar{p}(a)$, supposing that $\bar{p}(a)$ is one-sided. The integrals are identical in form, save for the fact that the ranges of ν differ. The effect of setting $\bar{p}(a)$ to be a one-sided stable distribution of index η can then be found for both transforms upon using their probability density functions (3.4):

$$\bar{p}(a) = p(a,\eta,1,b) = \frac{1}{2\pi} \int_{-\infty}^{\infty} \exp(-iaw) \exp\left(-b|w|^{\eta}\left(1 - i\,\text{sgn}(w)\tan\left(\frac{\pi\eta}{2}\right)\right)\right) dw.$$

Substitution of the PDF into (3.21) gives

$$C(u) = \int_0^\infty \left[\frac{1}{2\pi} \int_{-\infty}^{\infty} \exp(-iaw) \exp\left(-b|w|^\eta \left(1 - i\,\mathrm{sgn}(w) \tan\left(\frac{\pi\eta}{2} \right) \right) \right) dw \right] \exp\left(-a|u|^\nu \right) da$$

$$= \frac{1}{2\pi} \int_0^\infty \left\{ \frac{1}{|u|^\nu - iw} \exp\left(-b|w|^\eta \left(1 + i\,\mathrm{sgn}(w) \tan\left(\frac{\pi\eta}{2} \right) \right) \right) \right.$$

$$\left. + \frac{1}{|u|^\nu + iw} \exp\left(-b|w|^\eta \left(1 - i\,\mathrm{sgn}(w) \tan\left(\frac{\pi\eta}{2} \right) \right) \right) \right\} dw$$

which is of the same form as (3.5), hence

$$C(u) = \exp\left(-b \sec\left(\frac{\pi\eta}{2} \right) u^{\eta\nu} \right)$$

$$= C\left(u, \eta\nu, 0, b \sec\left(\frac{\pi\eta}{2} \right) \right); \qquad 0 < \nu \le 2,\ 0 < \eta \le 1 .$$

The same applies for the generating function of the *discrete*-stable transform, i.e.

$$Q(s) = \exp\left(-b \sec\left(\frac{\pi\eta}{2} \right) s^{\eta\nu} \right)$$

$$= Q\left(s, \eta\nu, b \sec\left(\frac{\pi\eta}{2} \right) \right); \qquad 0 < \nu \le 1,\ 0 < \eta \le 1 .$$

The corresponding identities for the stable probability density function and generating functions are then:

$$p(x, \eta\nu, 0, b) = \int_0^\infty p(x, \nu, 0, a) \cdot p\left(a, \eta, 1, b \cos\left(\frac{\pi\eta}{2} \right) \right) da \tag{3.23}$$

$$P(N, \eta\nu, B) = \int_0^\infty P(N, \nu, A) \cdot p\left(A, \eta, 1, B \cos\left(\frac{\pi\eta}{2} \right) \right) dA . \tag{3.24}$$

Equations (3.23) and (3.24) are therefore able to generate closed-form expressions (or at least formulae for) symmetric or discrete-stable distributions. Successive applications of (3.24) or (3.23) can therefore be used (in principle) to provide integral relations for symmetric or discrete-stable distributions for which the index ν are products of existing distributions.

Recall that in the Poisson limit, the inverse Poisson transform of the discrete-stable distributions tends to, but never becomes a delta function. The generating function of the form of the discrete-stable transform is given by (3.22), so taking the inverse Laplace transform, this corresponds to a one-sided continuous-stable distribution modulating the scale parameter of *another* one-sided continuous-stable distribution. This then gives

$$p(x,\eta\nu,1,b)=\int_0^\infty p(x,\nu,1,a)\cdot p\left(a,\eta,1,b\cos\left(\frac{\pi\eta}{2}\right)\right)da$$

which, provided that $\nu<1$ and $\eta<1$, show that the one-sided continuous-stable distributions are a closed-set under transformations with themselves.

The results within this chapter are substantial since they show a deeper connection between the different classes of stable distributions, in particular that the discrete-stable distributions and one-sided continuous-stable distributions are linked through the Poisson transform.

3.5 Summary

The Gaussian transform can be thought of as the 'smearing' of a continuous distribution upon the variance of a Gaussian. It was seen that the Gaussian transforms of the class of one-sided stable distributions of power-law index $0 < \nu < 1$ are symmetric-stable distributions of index 2ν and a different scale parameter. This result implies that when the variance of Gaussian distributed processes are modulated according to one-sided continuous-stable distributions, the resultant processes are still symmetric and continuous-stable, but no-longer Gaussian.

Similarly, the Poisson transform can be thought of as a 'smearing' of one distribution on the mean of a Poisson variable. Teich and Diament [107] describe a wider class of distribution transforms, whereby the variable whose mean is 'smeared' can be *any* distribution, though they consider the cases when the variance is finite. Through this formulation, they show how many classes of distribution can be constructed through transforms of two or more other distributions. Their interpretation of this is a scattering medium, which imposes a modulation on the mean irradiance W of a light source that passes through it. This modulation can either be measured in terms of the integrated irradiance of the resultant light, *or* through the photon count mechanism described previously.

It has been shown that the discrete and one-sided continuous-stable distributions are connected through the Poisson transform, the scaling for which elucidates the behaviour of the one-sided stable distributions in the delta function limit.

The results found in this chapter are best summarised in schematic form in Figure 3.5, which shows the effect of the modulation of the scale parameters of symmetric-stable (or discrete-stable) distributions by one-sided continuous-stable distributions. For instance, the Poisson transform is shown by an arrow from a Poisson distribution to another discrete-stable distribution.

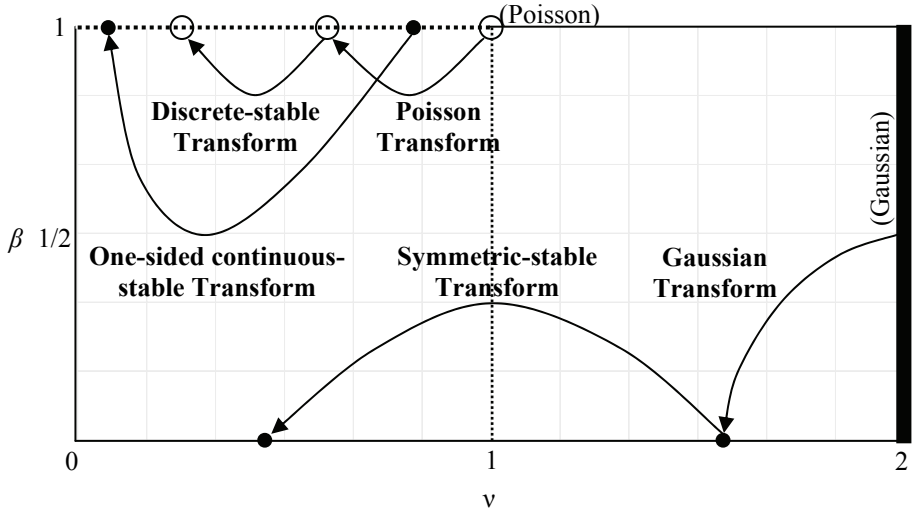

Figure 3.5

Illustrating the stable-transform results. Arrows represent the effect of the modulation of the scale parameter of one distribution by a one-sided continuous-stable distribution.

Having made these connections between stable distributions, a method of generating discrete-stable variables can be inferred – this will be investigated in §5. We shall now use the Poisson transform interrelationship to generate a continuous-stable *process*, finding its multiple-interval statistics via the (discrete) DMI population process upon which this work is partly based.

4. Continuous-stable processes and multiple-interval statistics

4.1 Introduction

The key to understanding physical processes is creating, studying and refining suitable models. The ubiquity of stable distributions found in nature [1] means that a mathematical model for a Markovian, continuous-stable process is a powerful one indeed.

Through the Poisson transform interrelationship developed in Section 3.3.2, this chapter will create a one-sided continuous-stable *process*. Its transient solution and Fokker-Planck style equation is found. Finally, the n-fold generating function for the continuous-stable process is given, expanding on the Markovian nature of the processes. These results use the formulation for the *discrete*-stable process (outlined in §2.5) as a basis.

4.2 A transient solution

The transient solution of the discrete-stable DMI process is given as a generating function by (2.35):

$$\begin{aligned} Q(s,t) &= \exp\left(-A(1-\theta(t)^{\nu})s^{\nu}\right)Q_0\left(s\theta(t)\right) \\ &= \exp\left(-\omega(t)^{\nu}s^{\nu}\right)Q_0\left(s\theta(t)\right) \end{aligned} \tag{4.1}$$

where $A = \varepsilon / \mu\nu$, $\omega(t) = \left[A(1-\theta(t)^{\nu})\right]^{1/\nu}$ and $\theta(t) = \exp(-\mu t)$ define the time scale of the process and $Q_0(s)$ is the generating function corresponding to the initial condition of the system. Following the Poisson transform result, it is possible to inverse Laplace transform (4.1) to obtain the transient solution $p(x,t)$ of a one-sided continuous-stable process. The result is a convolution of the initial condition and the stable distribution:

$$p(x,t) = \frac{1}{\omega(t)} \frac{1}{\theta(t)} \int_0^x p_{\nu}\left(\frac{x'}{\omega(t)}\right) p_0\left(\frac{x-x'}{\theta(t)}\right) dx' \tag{4.2}$$

where $p_0(x)$ is the initial condition of the process and has Laplace transform $Q_0(s)$, and $p_{\nu}(x)$ is the inverse Laplace transform of $\exp(-s^{\nu})$, as defined by (3.18). Note that the transient solution gives $p(0,t) = 0$ for all $t > 0$, except for the degenerate case $p_0(x) = \delta(0)$, which will not be considered.

A simple case to consider is when the initial condition $p_0(x)$ is uniform on [0,1]. In this case, the initial distribution and transient solution are:

$$p_0(x) = H(x) - H(x-1)$$

$$p(x,t) = \frac{1}{\omega(t)} \frac{1}{\theta(t)} \int_{\max(x-\theta(t),0)}^{x} p_{\nu}\left(\frac{x'}{\omega(t)}\right) dx' \tag{4.3}$$

It can be seen from the form of (4.3) that for $t > 0$ and $x >> 0$, the power-law is established immediately. In the case $\nu = 1/2$, the integral for the transient solution can be evaluated exactly since [110]:

$$\int p_{1/2}(x)dx = \int \frac{1}{2\sqrt{\pi}} x^{-3/2} \exp\left(\frac{1}{4x}\right)dx$$
$$= -\operatorname{erf}\left(\frac{1}{2\sqrt{x}}\right)$$

where $\operatorname{erf}(x)$ is the error function [93, 110]. This gives:

$$p(x,t) = \begin{cases} \dfrac{1}{\theta(t)}\left\{1 - \operatorname{erf}\left(\dfrac{1}{2}\sqrt{\dfrac{\omega(t)}{x}}\right)\right\} & 0 \le x \le \theta(t) \\ \dfrac{1}{\theta(t)}\left\{\operatorname{erf}\left(\dfrac{1}{2}\sqrt{\dfrac{\omega(t)}{x-\theta(t)}}\right) - \operatorname{erf}\left(\dfrac{1}{2}\sqrt{\dfrac{\omega(t)}{x}}\right)\right\} & x > \theta(t) \end{cases}$$

The dynamics of this transient solution to the continuous-stable process can be seen in Figure 4.1, which shows the rapid convergence to the stationary solution.

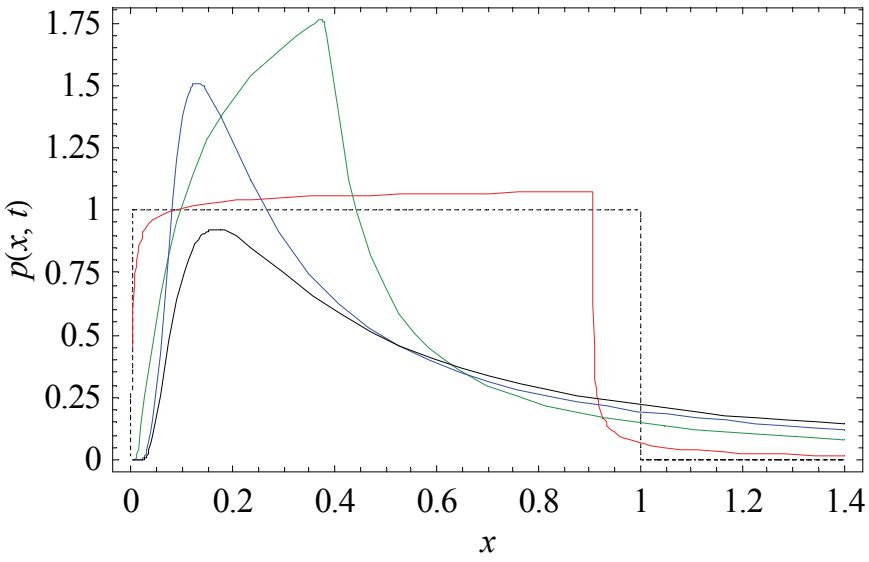

Figure 4.1

Illustrating the evolution of $p(x,t)$ when the initial distribution (dotted lines) is uniform on [0,1]. The parameters are $A = \mu = 1$, and $\mu t = 0.1$, 1, and 3 (red, green and blue lines respectively). The stationary state is also plotted (solid black line).

The behaviour when the initial condition is a delta function is particularly interesting. The dynamics in this case are shown for when the delta function is centred on $x = 1$, though the results are general:

$$p_0(x) = \delta(x-1)$$

$$p(x,t) = \frac{1}{\omega(t)}\frac{1}{\theta(t)}\int_0^x p_\nu\left(\frac{x'}{\omega(t)}\right)\delta\left(\frac{x-x'}{\theta(t)}-1\right)dx'$$

$$= \begin{cases} 0 & 0 \le x \le \theta(t) \\ \dfrac{1}{\omega(t)}\, p_\nu\left(\dfrac{x-\theta(t)}{\omega(t)}\right) & x > \theta(t). \end{cases}$$

This shows that in this case, the transient solution attains the shape of the stable distribution instantaneously, but with a scale change and a shift. This is shown in Figure 4.2.

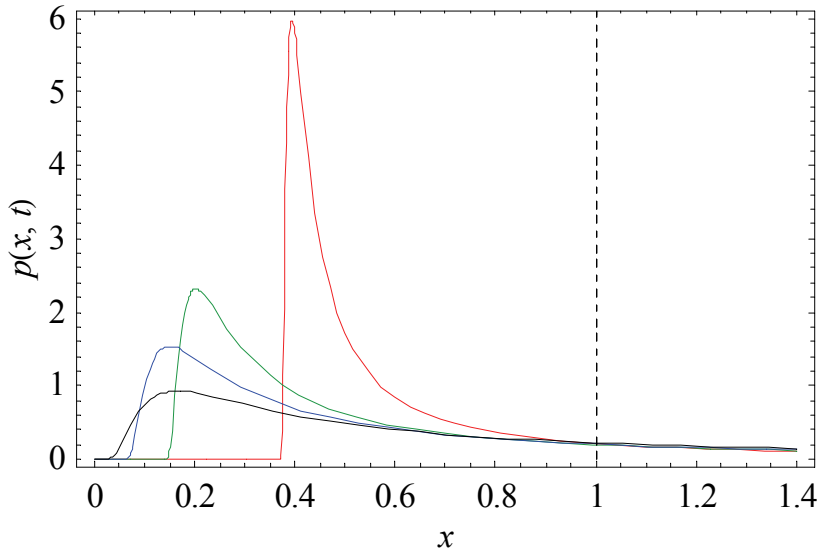

Figure 4.2

Showing the rapid convergence to the stationary solution when the initial distribution (dotted line) is a delta function. Plotted is the distribution for μt = 1, 2 and 3, and the stationary solution (red, green blue and black lines, respectively).

4.3 A one-sided stable Fokker-Planck style equation

We have seen previously that the PDE for the stable DMI population model's generating function is given by (2.29) and (2.32):

$$\frac{\partial}{\partial t}Q(s,t) = -\mu s\frac{\partial}{\partial s}Q(s,t) - \varepsilon s^{\nu}Q(s,t). \tag{4.4}$$

Since the above is the PDE which governs a discrete-stable process, it must follow from the Poisson transform interrelationship that Laplace inversion of (4.4) will yield a Fokker-Planck equation [16] for the continuous-stable process $p(x,t)$. *Direct* inversion of (4.4) is not possible since the final term cannot then be evaluated. However, it is possible to first divide by s and then evaluate the inverse Laplace transform:

$$\frac{\partial}{\partial t}\int_0^x p(x',t)dx' = \mu x p(x,t) - \frac{\varepsilon}{\Gamma(1-\nu)}\int_0^x \frac{p(x',t)}{(x-x')^{\nu}}dx'.$$

Differentiating with respect to x the above becomes:

$$\frac{\partial}{\partial t}p(x,t) = \mu\frac{\partial}{\partial x}(xp(x,t)) - \frac{\varepsilon}{\Gamma(1-\nu)}\frac{\partial}{\partial x}\left(\int_0^x \frac{p(x',t)}{(x-x')^{\nu}}dx'\right).$$

The final term may be evaluated by transforming $x' = x - y$:

$$\begin{aligned}\frac{\partial}{\partial x}\left(\int_0^x \frac{p(x',t)}{(x-x')^{\nu}}dx'\right) &= \frac{\partial}{\partial x}\left(\int_0^x \frac{p(x-y,t)}{y^{\nu}}dy\right)\\ &= \int_0^x\left(\frac{\partial}{\partial x}\frac{p(x-y,t)}{y^{\nu}}\right)dy + \frac{p(0,t)}{x^{\nu}}\\ &= \int_0^x\left(\frac{1}{(x-x')^{\nu}}\frac{\partial p(x',t)}{\partial x'}\right)dx'\end{aligned}$$

where the last line results from transforming back to x' and recalling that $p(0,t)=0$. The corresponding Fokker-Planck style equation for the one-sided continuous-stable process is then:

$$\frac{\partial}{\partial t}p(x,t)=\mu\frac{\partial}{\partial x}\left(xp(x,t)\right)-\frac{\varepsilon}{\Gamma(1-\nu)}\int_0^x\left(\frac{1}{(x-x')^{\nu}}\frac{\partial p(x',t)}{\partial x'}\right)dx' \tag{4.5}$$

The convolution in the final term highlights the nonlinear dependence between different values of x corresponding to different points in space as time evolves. Indeed the non-local effects of the evolution of the process over time allude to some more complex behaviour than that seen in 'standard' Fokker-Planck equations involving only drift and diffusion terms.

The validity of the Fokker-Planck style equation (4.5) can be tested by setting the PDF $p(x,t)$ of the process to be equal to the Lévy-Smirnov distribution (2.14), which is one-sided continuous-stable with index 1/2:

$$\begin{aligned}p(x,t)&=p\left(x,\frac{1}{2},1,a\right)\\&=\frac{a}{\sqrt{2\pi}}x^{-3/2}\exp\left(-\frac{a^2}{2x}\right).\end{aligned}$$

The time derivative in (4.5) should then be zero when setting $\nu=1/2$ and $\varepsilon=A\mu\nu$ (according to (2.33)), and $A=a\sec(\pi\nu/2)=a\sqrt{2}$, according to (3.16), so that:

$$\frac{\partial}{\partial t}p(x,t) = \mu\frac{\partial}{\partial x}\left(\frac{a}{\sqrt{2\pi}}x^{-1/2}\exp\left(-\frac{a^2}{2x}\right)\right)$$
$$-\frac{a\mu}{\sqrt{2\pi}}\int_0^x\left(\frac{1}{(x-x')^{1/2}}\frac{\partial}{\partial x'}\left[\frac{a}{\sqrt{2\pi}}x'^{-3/2}\exp\left(-\frac{a^2}{2x'}\right)\right]\right)dx'$$
$$=\frac{a\mu}{2\sqrt{2\pi}}x^{-5/2}\left(a^2-x\right)\exp\left(-\frac{a^2}{2x}\right)$$
$$-\frac{a\mu}{\sqrt{2\pi}}\int_0^x\left(\frac{1}{(x-x')^{1/2}}\left(\frac{a^3}{2\sqrt{2\pi}}x'^{-7/2}-\frac{3a}{2\sqrt{2\pi}}x'^{-5/2}\right)\exp\left(-\frac{a^2}{2x'}\right)\right)dx'$$

Upon transforming $x' = a^2x/(a^2+z)$ in the integral, the final term is:

$$-\frac{a\mu}{\sqrt{2\pi}}\int_0^x\left(\frac{1}{(x-x')^{1/2}}\left(\frac{a^3}{2\sqrt{2\pi}}x'^{-7/2}-\frac{3a}{2\sqrt{2\pi}}x'^{-5/2}\right)\exp\left(-\frac{a^2}{2x'}\right)\right)dx'$$
$$=-\frac{a\mu}{\sqrt{2\pi}}\frac{1}{2\sqrt{2\pi}a^2x^3}\exp\left(-\frac{a^2}{2x}\right)\int_0^\infty\exp\left(-\frac{z}{2x}\right)\frac{\left(z+a^2\right)\left(z+a^2-3x\right)}{\sqrt{z}}dz$$
$$=-\frac{a\mu}{2\sqrt{2\pi}}x^{-5/2}\left(a^2-x\right)\exp\left(-\frac{a^2}{2x}\right)$$

so $\partial p(x,t)/\partial t = 0$, i.e. the Lévy-Smirnov distribution (2.14) is a solution to the Fokker-Planck style equation (4.5), as expected.

A Fokker-Planck equation for *symmetric*-stable processes was developed by West [111, 112], but the nonlinear dependence in x which manifests itself in the integral is different, and does not involve a drift term. The form of the Fokker-Planck Equation given is:

$$\frac{\partial}{\partial t}p(x,t) = C\cdot\int_{-\infty}^{\infty}\frac{p(x',t)}{\left|x-x'\right|^{\nu+1}}dx'$$

though upon closer examination, this cannot be correct, since the integrand is singular when $x' = x$.

4.4 *r*-fold generating functions

4.4.1 The joint generating function

We have seen that a Fokker-Planck style equation for a continuous-stable process can be formed by taking the inverse Laplace transform of the stable Death-Multiple-Immigration model's PDE. The joint statistics for the continuous-stable process can also be formed from inverse-Laplace transforming the joint generating function (2.37) using the Poisson transform relationship. To produce *multiple*-interval statistics of the stable processes, we begin by obtaining the multiple-interval generating function of general stochastic, Markovian population processes. All of the results in this section pertain to Markovian discrete and continuous processes.

Recall that the joint probability $P(N, N'; t)$ of a process describes the probability that a population has sizes N and N' following a separation time t. The joint generating function $Q(s, s'; t)$ corresponding to the joint probability is defined by:

$$\begin{aligned} Q(s, s'; t) &= \sum_{N=0}^{\infty} (1-s)^N \sum_{N'=0}^{\infty} (1-s')^{N'} P(N, N'; t) \\ &= \sum_{N=0}^{\infty} (1-s)^N \sum_{N'=0}^{\infty} (1-s')^{N'} P_N P(N' | N; t) \end{aligned} \tag{4.6}$$

where P_N is the distribution of the stationary state of the process, and $P(N' | N; t)$ is the probability that the population has size N' on the condition that a time t ago, the

size was N. The joint distribution $P(N,N';t)$ of a population process can be recovered upon using (2.10) *twice* on (4.6) – once for the s variable and again for the s' variable.

The transient generating function gives the distribution of the population size after a time t, on the condition that the population had size N at time 0, and is defined:

$$Q^{[N]}(s;t) = \sum_{N'=0}^{\infty} (1-s)^{N'} P(N'|N;t)$$

and can be shown to always be of the form

$$Q^{[N]}(s;t) = (1-\Psi(s,t))^{N} \xi(s,t), \tag{4.7}$$

where the functions $\Psi(s,t)$ and $\xi(s,t)$ depend on the particular process considered. Supposing a stationary solution exists, in the infinite time limit, the functions satisfy $\Psi(s,\infty) = 0$ and $\xi(s,\infty) = Q_{st}(s)$.

Thus the joint generating function is

$$\begin{aligned} Q(s,s';t) &= \sum_{N=0}^{\infty} (1-s)^{N} P_N \times Q^{[N]}(s';t) \\ &= \xi(s',t) \times \sum_{N=0}^{\infty} (1-s)^{N} P_N (1-\Psi(s',t))^{N} \\ &= \xi(s',t) \times \sum_{N=0}^{\infty} P_N ((1-\Psi(s',t))(1-s))^{N} \\ &= \xi(s',t) \times \sum_{N=0}^{\infty} P_N (1-S)^{N} \\ &= \xi(s',t)\xi(S,\infty) \end{aligned}$$

where $S = 1-(1-\Psi(S';t))(1-s)$. The result of the final summation over N is $\xi(S,\infty)$ since it is simply the stationary solution of the population, and $Q_{st}(S) = \xi(S,\infty)$.

Note, however that despite its derivation from Markov processes, the result for the joint generating function holds true even when the Markov property does not.

4.4.2 The 3-fold generating function

We now consider the 3-fold generating function $Q(s,s',s'';t,t')$ of a Markovian process. This describes the probability that there are initially N members in the population, then N' following a separation time t, *then* N'' following another separation time t'. This is shown schematically in Figure 4.3:

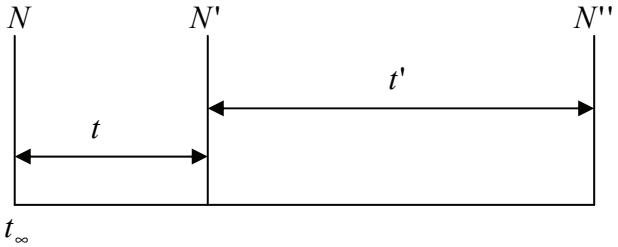

Figure 4.3

The formulation of a 3-fold generating function.

The 3-fold generating function is defined:

$$Q(s,s',s'';t,t') = \sum_{N=0}^{\infty}(1-s)^N P_N \sum_{N'=0}^{\infty}(1-s')^{N'} P(N'|N;t)\sum_{N''=0}^{\infty}(1-s'')^{N''} P(N''|N';t')$$

The summations over N'' and N' may be evaluated by the same reasoning as in the two-fold generating function:

$$\begin{aligned} Q(s,s',s'';t,t') &= \sum_{N=0}^{\infty}(1-s)^N P_N \sum_{N'=0}^{\infty}(1-s')^{N'} P(N'|N;t)\times Q^{[N']}(s'';t') \\ &= \left[\sum_{N=0}^{\infty}(1-s)^N P_N \sum_{N'=0}^{\infty}(1-s')^{N'} P(N'|N;t)(1-\Psi(s'';t'))^{N'}\right]\xi(s'',t') \\ &= \left[\sum_{N=0}^{\infty}(1-s)^N P_N \sum_{N'=0}^{\infty}(1-S')^{N'} P(N'|N;t)\right]\xi(s'',t') \end{aligned}$$

therefore

$$\begin{aligned} Q(s,s',s'';t,t') &= \left[\sum_{N=0}^{\infty}(1-s)^N P_N \times Q^{[N]}(S';t)\right]\xi(s'',t') \\ &= \left[\sum_{N=0}^{\infty}(1-s)^N P_N \times (1-\Psi(S';t))^N\right]\xi(S',t)\xi(s'',t') \\ &= \left[\sum_{N=0}^{\infty}(1-S)^N P_N\right]\xi(S',t)\xi(s'',t') \end{aligned}$$

where $S = 1-(1-s)(1-\Psi(S';t))$ and $S' = 1-(1-s')(1-\Psi(s'';t'))$.

The final summation over N also follows that of the two-fold result. Thus, if we write $S'' = s''$, we have:

$$Q(s,s',s'';t,t') = \xi(S,\infty)\xi(S',t)\xi(S'',t').$$

4.4.3 The *r*-fold generating function

It is straightforward to continue the concept of the generating function to $r+1$ different population sizes, separated by r time intervals. To prevent cumbersome notation as r grows large, we denote

$$N^{[0]} = N \qquad s^{[0]} = s \qquad S^{[0]} = S$$
$$N^{[1]} = N' \qquad s^{[1]} = s' \qquad S^{[1]} = S'$$
$$N^{[2]} = N'' \qquad s^{[2]} = s'' \qquad S^{[2]} = S''$$
$$\cdots \qquad \cdots \qquad \cdots$$

and set

$$P(\mathbf{N};\mathbf{t}) = P\left(N^{[0]}, N^{[1]} \cdots N^{[r-1]}, N^{[r]}; t^{[0]}, t^{[1]}, \cdots, t^{[r-2]}, t^{[r-1]}\right)$$

to be the probability of the population having sizes $N^{[0]}, N^{[1]} \cdots N^{[r-1]}, N^{[r]}$ following separation times $t^{[0]}, t^{[1]}, \cdots, t^{[r-2]}, t^{[r-1]}$.

This can be illustrated in the following diagram:

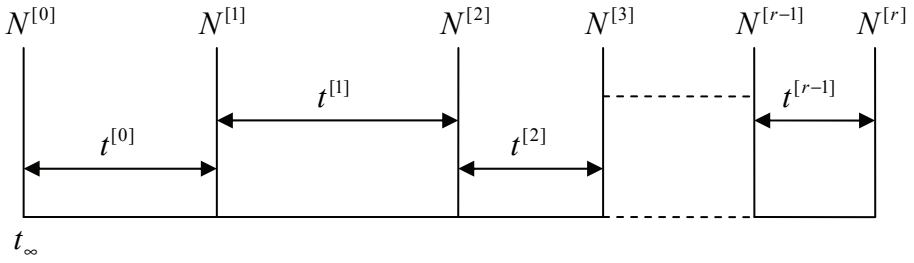

Figure 4.4

The formulation of an *n*-fold generating function.

The r-fold generating function for $P(\mathbf{N};\mathbf{t})$ is then:

$$Q(\mathbf{s};\mathbf{t}) = \prod_{k=0}^{r} \xi\left(S^{[k]}, t^{[k-1]}\right) \tag{4.8}$$

where

$$S^{[k]} = \begin{cases} s^{[r]} & k = r \\ 1 - \left(1 - s^{[k]}\right)\left(1 - \Psi\left(S^{[k+1]}, t^{[k]}\right)\right) & 0 \le k \le r-1 \end{cases} \tag{4.9}$$

and $t^{[-1]} = \infty$ so that the population is initially at equilibrium. From the results (4.8, 4.9), it is then possible to examine the r–fold interval statistics of *any* Markovian discrete process.

4.4.4 Application to the DMI model

For the Death, Multiple Immigration process, the functions $\Psi(s,t)$ and $\xi(s,t)$ can be obtained using (2.36) and (4.7) to be:

$$\Psi(s;t) = s \cdot \theta(t)$$
$$\xi(s,t) = \exp\left[-As^{\nu}\left(1-\theta^{\nu}(t)\right)\right]$$

where $\theta(t) = \exp(-\mu t)$.

The r-fold generating function for the DMI process is then

$$\begin{aligned} Q(\mathbf{s};\mathbf{t}) &= \prod_{k=0}^{r} \xi\left(S^{[k]}, t^{[k-1]}\right) \\ &= \prod_{k=0}^{r} \exp\left[-AS^{[k]\nu}\left(1-\theta^{\nu}\left(t^{[k-1]}\right)\right)\right] \\ &= \exp\left[-A\sum_{k=0}^{r} S^{[k]\nu}\left(1-\theta^{\nu}\left(t^{[k-1]}\right)\right)\right]. \end{aligned} \tag{4.10}$$

Having now obtained the form of the r-fold generating function for the DMI process, we can consider using the Poisson transform interrelationship to obtain the r-fold statistics of the *continuous*-stable process. However, care must be taken when inverse-Laplace transforming the above generating function, due to the terms which arise solely from the discrete nature of the process. For instance, when considering the Poisson case (i.e. $\nu = 1$), the continuous analogue must be a product of

uncorrelated delta functions, since the Poisson process is memoryless. The terms involving products of s are responsible for these inherently discrete properties, hence we require a rescaling of the s terms to suppress them. One such scaling is

$$s^{[k]} \to \left(\frac{a}{A}\right)^{\frac{1}{\nu}} s^{[k]} \tag{4.11}$$

in the limit $A \to \infty$.

The r-fold generating function for which the inverse Poisson transform *can* be performed is then:

$$Q(\mathbf{s};\mathbf{t}) = \exp\left[-a\sum_{k=0}^{r}\left(1-\theta^{\nu}\left(t^{[k-1]}\right)S^{[k]^{\nu}}\right)\right] \tag{4.12}$$

and the linearised $S^{[k]}$ terms are

$$S^{[k]} = \begin{cases} s^{[r]} & k = r \\ s^{[k]} + S^{[k+1]}\theta\left(t^{[k]}\right) & 0 \le k \le r-1 \end{cases}$$
$$= \begin{cases} s^{[r]} & k = r \\ s^{[k]} + \sum_{l=k+1}^{r} s^{[l]}\theta\left(\sum_{m=k}^{l-1} t^{[m]}\right) & 0 \le k \le r-1 \end{cases}$$

The correctly linearised r-fold generating function is then:

$$Q(\mathbf{s},\mathbf{t}) = \exp\left\{-a\sum_{k=0}^{r}\left(1-\theta\left(t^{[k-1]}\nu\right)\right)\left[s^{[k]} + \sum_{l=k+1}^{r} s^{[l]}\theta\left(\sum_{m=k}^{l-1} t^{[m]}\right)\right]^{\nu}\right\}. \tag{4.13}$$

In this linearised form, the r-fold generating function is of the same form as that of the Birth, Death, Multiple-Immigration (BDMI) process. For instance, taking the case $r = 2$, the joint generating functions for the DMI and BDMI processes are [6]:

$$Q(s,s',t) = \exp\left(-A\left\{s'^{\nu}\left[1-\theta(t)^{\nu}\right]+\left[s+(1-s)s'\theta(t)\right]^{\nu}\right\}\right)$$

and

$$Q(s,s',t) = \exp\left[-\frac{A}{\nu(\mu-\lambda)}\left\{s'^{\nu}\left(1-\frac{\exp(-\nu(\mu-\lambda)t)}{(1+bs'(1-\theta(t)))^{\nu}}\right)+\left(s+\frac{(1-s)s'\theta(t)}{1+bs'(1-\theta(t))}\right)^{\nu}\right\}\right]$$

respectively.

Upon suppressing the product terms using (4.11), the joint generating functions both reduce to the form:

$$Q(s,s',t) = \exp\left(-a\left\{s'^{\nu}\left[1-\theta(t)^{\nu}\right]+\left[s+s'\theta(t)\right]^{\nu}\right\}\right) \tag{4.14}$$

which implies that the intrinsic differences between the processes which arise from the inclusion of the birth term do not carry through to the continuous processes.

4.4.5 *r*-fold distributions for the one-sided continuous-stable process

To take the inverse Poisson transform of the r-fold generating function (4.13), we use the definition (3.18) for $p_{\nu}(x)$ and note that the only contribution of $s^{[0]}$ occurs when $k = 0$. Then, upon using the relation [93] for Laplace inversion:

$$\mathsf{L}^{-1}\left[f(c(s+b))\exp(-ds)\right] = F\left(\frac{x-d}{c}\right)\cdot\frac{1}{c}\cdot H(x-d)\cdot\exp(-b(x-d)) \tag{4.15}$$

where $H(x)$ is the Heaviside step function [93], $f(s)$ is the Laplace transform of $F(x)$, and

$$b = \left[\sum_{l=k+1}^{r} s^{[l]} \theta\left(\sum_{m=k}^{l-1} t^{[m]} \right) \right]_{k=0}$$
$$c = a^{1/\nu} \left(1 - \theta\left(t^{[k-1]} \nu\right)\right)^{1/\nu} \Big|_{k=0}$$
$$d = 0$$

we obtain

$$\mathsf{L}^{-1}_{s^{[0]} \to x^{[0]}} Q(\mathbf{s}, \mathbf{t}) = p_\nu \left(\frac{x^{[0]}}{a^{1/\nu}} \right) \cdot \frac{1}{a^{1/\nu}} \cdot H\left(x^{[0]}\right)$$
$$\times \exp\left\{ -a \sum_{k=1}^{r} \left(1 - \theta\left(t^{[k-1]} \nu\right)\right) \left[s^{[k]} + \sum_{l=k+1}^{r} s^{[l]} \theta\left(\sum_{m=k}^{l-1} t^{[m]} \right) \right]^{\nu} \right\}$$
$$\times \exp\left(-x^{[0]} \left[\sum_{l=k+1}^{r} s^{[l]} \theta\left(\sum_{m=k}^{l-1} t^{[m]} \right) \right]_{k=0} \right)$$

Inversion with respect to $s^{[1]}$ is facilitated by noting that the only $s^{[1]}$ contributions occur when $k = 1$ in the first exponential term and $l = 1$ in the second. Substituting

$$b = \left[\sum_{l=k+1}^{r} s^{[l]} \theta\left(\sum_{m=k}^{l-1} t^{[m]} \right) \right]_{k=1}$$
$$c = a^{1/\nu} \left(1 - \theta\left(t^{[k-1]} \nu\right)\right)^{1/\nu} \Big|_{k=1}$$
$$d = x^{[0]} \theta\left(t^{[0]}\right)$$

into (4.15) one obtains the second-order inversion:

$$\underset{\substack{s^{[0]}\to x^{[0]}\\ s^{[1]}\to x^{[1]}}}{\mathcal{L}^{-1}}\ Q(\mathbf{s},\mathbf{t}) = \left[\begin{array}{l} P_\nu\left(\dfrac{x^{[0]}}{a^{1/\nu}}\right)\cdot\dfrac{1}{a^{1/\nu}}\cdot H\left(x^{[0]}\right) \\ \times P_\nu\left(\dfrac{x^{[1]}-x^{[0]}\theta\left(t^{[0]}\right)}{a^{1/\nu}\left(1-\theta\left(t^{[0]}\nu\right)\right)^{1/\nu}}\right)\cdot\dfrac{1}{a^{1/\nu}\left(1-\theta\left(t^{[0]}\nu\right)\right)^{1/\nu}}\cdot H\left(x^{[1]}-x^{[0]}\theta\left(t^{[0]}\right)\right) \end{array}\right]$$

$$\times\exp\left\{-\frac{a}{\nu\mu}\sum_{k=2}^{r}\left(1-\theta\left(t^{[k-1]}\nu\right)\right)\left[s^{[k]}+\sum_{l=k+1}^{r}s^{[l]}\theta\left(\sum_{m=k}^{l-1}t^{[m]}\right)\right]^{\nu}\right\}$$

$$\times\left[\begin{array}{l} \exp\left(-x^{[0]}\left[\sum_{l=k+1}^{r}s^{[l]}\theta\left(\sum_{m=k}^{l-1}t^{[m]}\right)\right]_{k=1}\right) \\ \times\exp\left(-\left(x^{[1]}-x^{[0]}\theta\left(t^{[0]}\right)\right)\left[\sum_{l=k+1}^{r}s^{[l]}\theta\left(\sum_{m=k}^{l-1}t^{[m]}\right)\right]_{k=1}\right) \end{array}\right]$$

Note that the last two exponential terms simplify, thus

$$\underset{\substack{s^{[0]}\to x^{[0]}\\ s^{[1]}\to x^{[1]}}}{\mathcal{L}^{-1}}\ Q(\mathbf{s},\mathbf{t}) = \left[\begin{array}{l} P_\nu\left(\dfrac{x^{[0]}}{a^{1/\nu}}\right)\cdot\dfrac{1}{a^{1/\nu}}\cdot H\left(x^{[0]}\right) \\ \times P_\nu\left(\dfrac{x^{[1]}-x^{[0]}\theta\left(t^{[0]}\right)}{a^{1/\nu}\left(1-\theta\left(t^{[0]}\nu\right)\right)^{1/\nu}}\right)\cdot\dfrac{1}{a^{1/\nu}\left(1-\theta\left(t^{[0]}\nu\right)\right)^{1/\nu}}\cdot H\left(x^{[1]}-x^{[0]}\theta\left(t^{[0]}\right)\right) \end{array}\right]$$

$$\times\exp\left\{-\frac{a}{\nu\mu}\sum_{k=2}^{r}\left(1-\theta\left(t^{[k-1]}\nu\right)\right)\left[s^{[k]}+\sum_{l=k+1}^{r}s^{[l]}\theta\left(\sum_{m=k}^{l-1}t^{[m]}\right)\right]^{\nu}\right\}$$

$$\times\exp\left(-x^{[1]}\left[\sum_{l=k+1}^{r}s^{[l]}\theta\left(\sum_{m=k}^{l-1}t^{[m]}\right)\right]_{k=1}\right)$$

Successive inversions are then performed with respect to increasing values of k using (4.15) with

$$b = \sum_{l=k+1}^{r} s^{[l]} \theta\left(\sum_{m=k}^{l-1} t^{[m]} \right)$$

$$c = a^{1/\nu} \left(1 - \theta\left(t^{[k-1]} \nu\right)\right)^{1/\nu}$$

$$d = x^{[k-1]} \theta\left(t^{[k-1]}\right)$$

This method may be continued arbitrarily many times as required using the same technique and thus, without loss of generality, the r-fold distribution is:

$$P(\mathbf{x}, \mathbf{t}) = \prod_{k=0}^{r} \left[\frac{H\left(x^{[k]} - x^{[k-1]} \theta\left(t^{[k-1]}\right)\right)}{a^{1/\nu} \left(1 - \theta\left(t^{[k-1]} \nu\right)\right)^{1/\nu}} \times P_{\nu}\left(\frac{x^{[k]} - x^{[k-1]} \theta\left(t^{[k-1]}\right)}{a^{1/\nu} \left(1 - \theta\left(t^{[k-1]} \nu\right)\right)^{1/\nu}} \right) \right] \tag{4.16}$$

upon setting $t^{[-1]} = \infty$ as before and noting that $x^{[-1]}$ terms are always multiplied by zero, and therefore ignored.

This result (4.16) is enormously significant since it gives an explicit factorisation of the r-fold probability density function of a one-sided continuous-stable process, from which (in principle) suitably defined correlations can be found. Indeed, if the value of a one-sided continuous-stable process at n points in time, separated by $n-1$ intervals is known, (4.16) can be used to predict the probability density function of the process at any given point.

4.5 Summary

Having discovered the significance of the Poisson transform in relating continuous- and discrete-stable distributions in Chapter 3, the concept of a one-sided continuous-stable *process* was introduced. The corresponding Fokker-Planck style equation for

the process is given, and compared with a proposed symmetric-stable counterpart found in the literature. The r-fold probability density function of the process, which gives the probability that the process takes on values x, x', x''… after separation times t, t'… is derived from the corresponding discrete-stable process. Though this is an extension of the Markovian properties of the discrete-stable process, a rescaling of the variables to remove intrinsically discrete properties was undertaken.

Another such discrete property which is destroyed when undertaking the Poisson transform is the distribution of the number of emigrants into the DMI process, which has generating function $Q_f(s) = 1 - s^{\nu}$, for which the *inverse* Laplace transform cannot be found. This implies that though the one-sided continuous-stable arises from a discrete-stable DMI process, the continuous-stable process cannot be thought of as a *continuous* DMI process. The mechanism which drives the increases in the *value* of the process (in the case of the DMI process, this is the multiple immigrations) is something which is inherently continuous.

5. Simulating discrete-stable variables

5.1 Introduction

The simulation of variates to aid the application of processes provides an invaluable insight into their behaviours; power-law distributed variates in particular, not least because such niceties as the means and higher moments are undefined. Despite the propensity of methods to generate *continuous* variates [e.g. 113], the same cannot be said for discrete variates. They can be simulated, however, on the provisions that their (discrete) distribution can be formed through a doubly-stochastic Poisson process, and that the corresponding variates from the corresponding continuous distribution can be simulated. The simulation is *exact* in the sense that the discrete variates generated follow the discrete distribution exactly and are not approximations. In particular, following from the results in Chapter 3, discrete-*stable* random variates will be generated using an existing algorithm which generates *continuous*-stable random variates.

5.2 The algorithm

We are interested in generating independent, identically distributed (i.i.d.) discrete variates from i.i.d. continuous variates using Poisson transform interrelationships. A method of doing this can be inferred directly from the Poisson transform (3.10):

$$P(N) = \int_0^\infty p(w) \frac{w^N \exp(-w)}{N!} dw .$$

Suppose that there is a method of generating a continuous variate x_1 from a distribution $p_c(x)$. The variate x_1 may be thought of as having a delta function as its probability density function, i.e. $\tilde{p}(w) = \delta(w - x_1)$. Since $\tilde{p}(w)$ is a delta function, its Poisson transform $\tilde{P}(N)$ is Poisson distributed with mean x_1. A discrete variate n_1 (with value N) drawn from the distribution $\tilde{P}(N)$ is doubly stochastic since *two* variates need to be drawn from distributions to generate it – x_1, and n_1, which itself is dependent on x_1. The variate n_1 therefore has a distribution given by the Poisson transform of $p_c(x)$:

$$P_{(T)}(N) = \int_0^\infty p_c(x) \frac{x^N \exp(-x)}{N!} dx \,. \tag{5.1}$$

Repeating this process with new independent variates $x_2, x_3 \ldots x_m$ drawn from the distribution $p_c(x)$ will then generate new discrete variates $n_2, n_3 \cdots n_m$, drawn from independent Poisson distributions with mean $x_2, x_3 \cdots x_m$. The variates $n_1, n_3 \cdots n_m$ are i.i.d. since each variate is distributed according to (5.1).

By dividing the count C_N of the occurrence of each value of N by the number of variates m, the ensemble distribution is $P_{(E)}(N) = C_N \cdot m^{-1}$. In the limit as m tends to infinity, the distribution $P_{(E)}(N)$ of the ensemble of $n_1, n_2, n_3 \cdots n_m$ will be equal to $P_{(T)}(N)$, the Poisson transform of $p_c(x)$. It is important to stress that though the distribution of the *ensemble* $P_{(E)}(N)$ only becomes the theoretical distribution

$P_{(T)}(N)$ when $m \to \infty$, *each* variate is drawn from the distribution $P_{(T)}(N)$ by virtue of the Poisson transform. The algorithm is shown schematically in Figure 5.1 below.

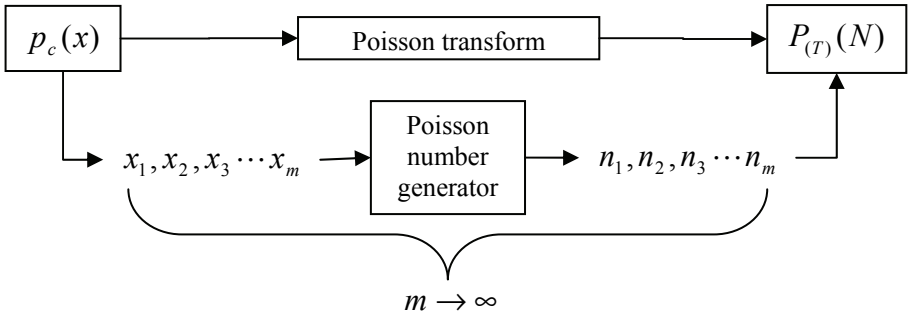

Figure 5.1

Illustrating the method of generating discrete variates drawn from the (discrete) Poisson transform of a continuous variate. As the number *m* of discrete variates drawn tends to infinity, the distribution of the ensemble of discrete variates tends to the Poisson transform of the continuous distribution.

There exist many algorithms for generating Poisson variables of arbitrary mean λ in the literature. One such very simple generator is given by Knuth [114] for which the complexity (i.e. the running time) is $O(\lambda)$. Clearly when the distribution of the mean λ is continuous-stable, and hence has a power-law tail, this method is rather inefficient. A more suitable method with a complexity of $O(\log(\lambda))$ is given by Devroye [113]. This is far more appealing when power-law tails (or indeed large values of the mean λ) are involved, and it is the algorithm used by MATLAB.

The ensemble distributions will be compared to theoretical distributions via the χ^2 test statistic:

$$\chi^2 = \sum_{N=0}^{\infty} \frac{\left(P_{(T)}(N) - P_{(E)}(N)\right)^2}{P_{(T)}(N)} . \tag{5.2}$$

It is clear from its form that the smaller the value of χ^2, the better the fit between theoretical and empirical results.

The χ^2 statistic is sensitive to behaviour in the *tail*(s) of distributions – this can be seen from its form. Supposing we write $T_N = m \cdot P_{(T)}(N)$, (where the values of T_N need not be integers, as opposed to the counts C_N, which must be integer), then the individual contributions to the χ^2 statistic (5.2) are

$$\begin{aligned} \chi^2_N &= \frac{\left(P_{(T)}(N) - P_{(E)}(N)\right)^2}{P_{(T)}(N)} \\ &= \frac{\left(T_N \cdot m^{-1} - C_N \cdot m^{-1}\right)^2}{T_N \cdot m^{-1}} \\ &= \frac{\left(T_N - C_N\right)^2}{T_N \cdot m} . \end{aligned}$$

Clearly for moderately large values of m, $T_N \approx C_N$ for all N, so the value of χ^2_N is small. Large contributions χ^2_N arise when T_N is *small*, corresponding to small values of the theoretical probabilities such as at the tails of distributions. In particular, if there are many values of N for which $P_{(T)}(N) \approx m^{-1}$ (e.g. if the distribution has a *slowly* decaying tail), a large χ^2 statistic is to be expected. In the limit $T_N \to 0$ (for

which $P_{(T)}(N) << m^{-1}$), the count C_N of the occurrences of N will also tend to zero, in which case the contribution χ^2_N is T_N / m, which is vanishingly small.

Having now outlined the algorithm for numerically simulating discrete distributions via the Poisson transform and discussed the χ^2 statistic, we shall examine the case of generating negative binomial distributions, whose mean and all other higher moments exist, in order to test and validate the algorithm.

5.3 Simulating negative-binomial distributed variates

Recall that the Poisson transform of a gamma distribution is negative binomial – a special case of this is when an exponential distribution transforms to a Bose-Einstein distribution. This result is easily proven by calculating the Laplace transform of a gamma-distribution. A gamma-distribution of shape parameter k and mean Ak is [e.g. 93]:

$$p_{(g)}(x,k,A) = \frac{\exp(-x/A)}{\Gamma(k)A^k} x^{k-1}.$$

and has Laplace transform

$$Q(s) = \frac{1}{(1+As)^k}.$$

According to (3.11), the Laplace transform of a continuous distribution is also the generating function of its Poisson transformed distribution, so the Poisson transform of a gamma distribution must be a negative binomial distribution [93]:

$$P(N) = \frac{A^N}{(A+1)^{k+N}} \frac{\Gamma(k+N)}{\Gamma(k)\Gamma(1+N)}$$

$$= P_{(NB)}(N,k,A).$$

The transformation from a gamma to a negative binomial distribution can be seen in Figure 5.2 below, and shows that though the distributions resemble each other, the Poisson transform does more than sample the continuous distribution at integer values. This is obvious when considering the limit $k \to \infty$ when Ak is fixed – the gamma distributions become delta functions, and the negative binomial distributions become Poisson.

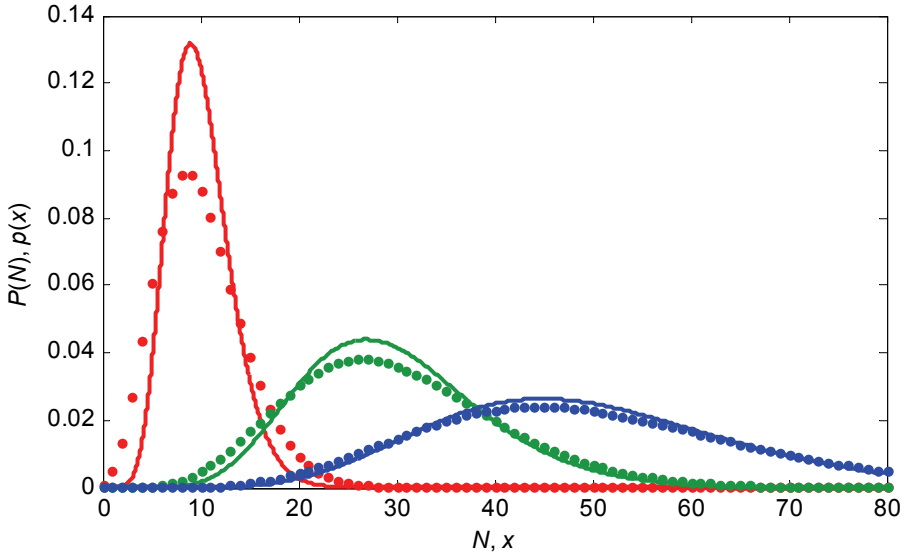

Figure 5.2

Plotting gamma and negative binomial distributions with shape parameter k = 10, and means Ak = 10, 20 and 30 (red, green and blue lines and points, respectively).

A gamma distributed variable of shape parameter k (when k is an integer) and mean Ak can be generated [e.g. 113] by summing k exponentially distributed variables of

mean A. Non-integer values of k require additional steps in the generation of the gamma variates, and will not be considered since they are not special cases of the gamma and negative binomial distributions. Exponentially distributed variates are readily generated by many computer packages, provided a method of generating uniformly distributed variates U on [0, 1] exist: $X = -\lambda \log(U)$ has an exponential distribution of mean λ.

5.4 Results

The algorithm was used to generate negative binomial distributed variates with $A = 1,5,10,100$ and $k = 1,5,10,100$ in ensembles of 10^6 and 10^{10} variates.

The results in Table 5.1 suggest an excellent agreement between the simulated ensembles' and the theoretical distributions for 10^6 variates. As expected, when the mean Ak of the distributions increases, the χ^2 statistic increases also.

$\chi^2 \times 10^5$		K			
		1	5	10	100
A	1	4.2391	3.8318	2.6362	16.061
	5	7.9201	12.454	16.641	59.233
	10	17.205	29.711	37.774	210.6
	100	150.83	230.11	343.45	1048.5

Table 5.1

The χ^2 statistics for the ensembles of 10^6 simulated negative binomial variates. Note that the values are scaled by 10^5 to aid comparison.

Table 5.2 shows the effect of the resolution of the distribution on the χ^2 statistic, this time with 10^9 variates. It is clear that even when A and k are 100 (i.e. the mean is 10,000), the simulations provide excellent agreement with theoretical results.

$\chi^2 \times 10^8$		K			
		1	5	10	100
A	1	2.0532	3.4268	6.4461	15.711
	5	14.123	17.015	40.180	65.851
	10	23.529	33.964	42.674	126.94
	100	185.56	314.85	443.08	1281.5

Table 5.2

The χ^2 statistics for the ensembles of 10^9 simulated negative binomial variates. Note that the values are scaled by 10^8 to aid comparison.

Figure 5.3 shows the excellent agreement between theoretical and simulated results of the negative binomial distributions when the ensemble size is 10^6, $A = 5$ and $k = 10$. The difference between theoretical and simulated distributions is barely discernable.

Having shown the efficacy of the method of generating discrete distributions via a Poisson transform method, we shall now examine the case of *stably* distributed discrete distributions; since the moments are all infinite, it is expected that the heavier tails will require much larger ensemble sizes to provide small values of the χ^2 statistics.

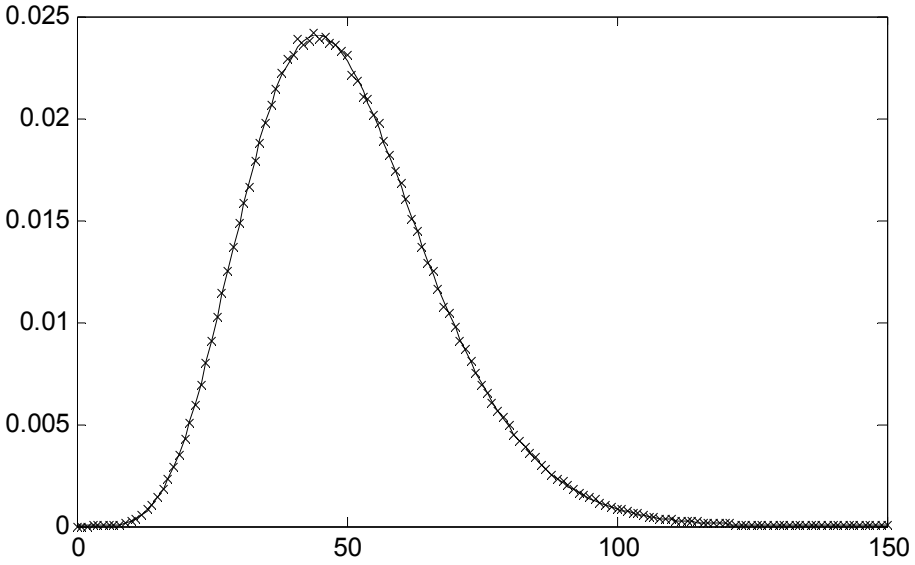

Figure 5.3

Comparing theoretical (joined) and ensemble (crosses) negative binomial distributions of 10^6 variates, with $A = 5$ and $k = 10$. In this instance, $\chi^2 \approx 10^{-4}$.

5.5 Simulating *continuous*-stable distributed variates

We have seen that it is possible to use the Poisson transform relationship to generate discrete-stable variates, provided that a method for generating one-sided continuous-stable variates exists. In the literature there are several methods for generating continuous-stable variates of specific values of ν and β. For instance, the famous Box-Muller method [115] generates Gaussian distributed variates X_g, from which Lévy distributed variates (for which $\nu = 1/2$, $\beta = 1$) can be simulated though $X_L = 1/X_g^2$. It is also known [e.g. 40] that Cauchy variates can be generated by dividing one Gaussian variate by another independent Gaussian variate.

Methods exist to generate continuous-stable distributed variates of *any* values of the parameters ν and β. The first such method was discovered by Kanter [116] and generates one-sided continuous-stable variates (i.e. those for which $0<\nu<1$ and $\beta=1$). It relies on an integral representation of the *one-sided* continuous-stable distributions given (with an error in the proof, corrected below) by Ibragimov and Chernin [117]:

$$p_\nu(x)=\frac{1}{\pi}\left(\frac{\nu}{1-\nu}\right)x^{-\frac{1}{1-\nu}}\int_0^\pi a(\varphi)\exp\left(-x^{-\frac{\nu}{1-\nu}}a(\varphi)\right)d\varphi \tag{5.3}$$

where

$$a(\varphi)=\left(\frac{\sin(\nu\varphi)}{\sin(\varphi)}\right)^{\frac{1}{1-\nu}}\left(\frac{\sin((1-\nu)\varphi)}{\sin(\nu\varphi)}\right) \tag{5.4}$$

and $p_\nu(x)$ is as defined in (3.18).

Kanter used this representation to deduce a method of simulating the one-sided continuous-stable distributions: if U is a variable uniformly distributed on $[0,\pi]$ and W is an independent, exponentially distributed variable of unit mean, then the random variable

$$X=\left(\frac{a(U)}{W}\right)^{\frac{1-\nu}{\nu}}$$

has distribution $p_\nu(x)$. The proof of this is as follows:

Define a random vector $\mathbf{Y}=(W,U)$ which has values x and u with joint probability

$$f(x,u) = \exp(-x)\cdot\frac{1}{\pi} \qquad x \geq 0, 0 \leq u \leq \pi$$

and a vector function of $\mathbf{Y}$

$$\mathbf{Z}(\mathbf{Y}) = \mathbf{Z}(W,U) = \left(\left(\frac{a(U)}{W}\right)^{\frac{1-\nu}{\nu}}, U\right) = (X,\Phi)$$

which has an inverse

$$\begin{aligned}\mathbf{G}(X,\Phi) &= \left(\frac{a(\Phi)}{X^{\frac{\nu}{1-\nu}}}, \Phi\right) = \mathbf{X} = \mathbf{Y}^{-1}(X,\Phi)\\ &= (g_1(X,\Phi), g_2(X,\Phi)).\end{aligned}$$

The Jacobian determinant of $\mathbf{G}$ is

$$\begin{aligned}|\mathbf{J}| &= \begin{vmatrix}\frac{\partial g_1(X,\Phi)}{\partial X} & \frac{\partial g_1(X,\Phi)}{\partial \Phi}\\ \frac{\partial g_2(X,\Phi)}{\partial X} & \frac{\partial g_2(X,\Phi)}{\partial \Phi}\end{vmatrix} = \begin{vmatrix}\frac{\partial g_1(X,\Phi)}{\partial X} & \frac{\partial g_1(X,\Phi)}{\partial \Phi}\\ 0 & 1\end{vmatrix}\\ &= \frac{\partial g_1(X,\Phi)}{\partial Z}\\ &= \frac{\nu}{\nu-1}\cdot\frac{a(\Phi)}{X^{\frac{1}{1-\nu}}}.\end{aligned}$$

The joint distribution of X and Φ having values x and φ is, by Theorem 4.2 of [113]:

$$\begin{aligned}h(x,\varphi) &= f(g_1(x,\varphi), g_2(x,\varphi))\cdot|\mathbf{J}|\\ &= \frac{1}{\pi}\left(\frac{\nu}{\nu-1}\right)\exp\left(-\frac{a(\varphi)}{x^{\frac{\nu}{1-\nu}}}\right)\cdot\frac{a(\varphi)}{x^{\frac{1}{1-\nu}}}\end{aligned}$$

and thus the marginal distribution of the variable X being equal to x is found by integrating over φ, which is uniform on $[0,\pi]$:

$$\frac{1}{\pi}\left(\frac{\nu}{1-\nu}\right)x^{-\frac{1}{1-\nu}}\int_0^{\pi} a(\varphi)\exp\left(-x^{-\frac{\nu}{1-\nu}}a(\varphi)\right)d\varphi$$

which is exactly the form of (5.3) above, thus completing the proof.

The parameterisation (5.3), [117] is defined as giving one-sided continuous-stable distributions $p_\nu(x)$ with Laplace transform $\exp(-s^\nu)$, which, by (3.18) corresponds to $p(x,\nu,1,\cos(\pi\nu/2))$. In order to obtain variates for which the probability density function is $p(x,\nu,1,a)$ – i.e. for which the scale parameter may be varied, we use the scaling relation (2.5) to obtain

$$X = \left[a\cdot\sec\left(\frac{\pi\nu}{2}\right)\right]^{\frac{1}{\nu}}\left(\frac{a(U)}{W}\right)^{\frac{1-\nu}{\nu}}$$

$$= \left(\frac{a}{\cos(\pi\nu/2)}\right)^{\frac{1}{\nu}}\times\frac{\sin(\nu U)}{\sin(U)^{1/\nu}}\times\left(\frac{\sin((1-\nu)U)}{W}\right)^{\frac{1-\nu}{\nu}} \qquad (5.5)$$

for which the distribution is $p(x,\nu,1,a)$.

Chambers, Mallows and Stuck [118] extended this result to the entire parameter range of ν and β using a similar technique, this time relying on a different integral representation of the continuous-stable distributions given by Zolotarev [119]. If γ and W are random, independent variables drawn from a uniform distribution on

$[-\pi/2, \pi/2]$ and an exponential distribution of unit mean, respectively, then a slight modification of their formula gives [e.g. 120, 121, 122] the random variable

$$X = \begin{cases} a^{1/\nu} \times D_{\nu,\beta} \times \dfrac{\sin\left(\nu(\gamma + C_{\nu,\beta})\right)}{\cos(\gamma)^{1/\nu}} \times \left(\dfrac{\cos\left(\gamma - \nu(\gamma + C_{\nu,\beta})\right)}{W} \right)^{(1-\nu)/\nu} & \nu \neq 1 \\ a^{1/\nu} \times \dfrac{2}{\pi}\left[\left(\dfrac{\pi}{2} + \beta\gamma \right) \tan(\gamma) - \beta \log\left(\dfrac{W\cos(\gamma)}{1 + (2\beta\gamma/\pi)} \right) \right] & \nu = 1 \end{cases} \tag{5.6}$$

where

$$\begin{aligned} C_{\nu,\beta} &= \frac{\arctan\left(\beta \tan(\pi\nu/2)\right)}{\nu} \\ D_{\nu,\beta} &= \left(\cos\left(\arctan\left(\beta \tan(\pi\nu/2)\right)\right)\right)^{-1/\nu} \end{aligned} \tag{5.7}$$

which has distribution $p(x, \nu, \beta, a)$.

The full proof of this result is similar to that for the one-sided variates, and is omitted for the sake of brevity. As expected, in the case when $0 < \nu < 1$ and $\beta = 1$, (5.6) is of the same form as (5.5). Setting $\beta = 0$ to obtain a simulator for the symmetric-stable distributions, (5.6) reduces to:

$$X = \begin{cases} a^{1/\nu} \times \dfrac{\sin(\nu\gamma)}{\cos(\gamma)^{1/\nu}} \times \left(\dfrac{\cos(\gamma(1-\nu))}{W} \right)^{(1-\nu)/\nu} & \nu \neq 1 \\ a^{1/\nu} \times \tan(\gamma) & \nu = 1 \end{cases} \tag{5.8}$$

The method above is one which is most commonly found in the literature for generating symmetric-stable distributions [e.g. 39, 120, 122] – in the case when $\nu = 2$, it simplifies to.

$$X = W^{1/2} \sin(2\gamma)$$

which is the Box-Muller method [115] for generating Gaussian distributed variates.

With the foundations for simulating continuous-stable distributed variates laid, we may now progress to the simulation of *discrete*-stable distributed variates.

5.6 Simulating *discrete*-stable distributed variates

Having found a method of generating one-sided continuous-stable random variates and discovered the Poisson transform interrelationship between the one-sided continuous and discrete-stable distributions, we may proceed to generate *discrete*-stable variates. A random Poisson variable with mean governed by a one-sided continuous-stable variable has, by the Poisson transform interrelationship, a discrete-stable distribution.

Since the discrete-stable distributions are defined entirely through their scale parameter A and power-law index ν, it is necessary to use the scaling relation (3.16) to define the random variable X in terms of the scale parameter A rather than a.

Hence setting $a = A\cos(\pi\nu/2)$ in (5.5) gives:

$$X = A^{1/\nu} \times \frac{\sin(\nu U)}{\sin(U)^{1/\nu}} \times \left(\frac{\sin((1-\nu)U)}{W} \right)^{\frac{1-\nu}{\nu}} \tag{5.9}$$

Note that (5.9) illustrates clearly the role of the discrete scale parameter A on the variable X. The specific dependence on the scale parameter A by the discrete-stable

distributions on the *shape* of the distributions cannot be derived from the generating function (2.8), and so this gives a new meaning to the dependence on the scale parameter of the discrete-stable distributions.

Note also that upon setting $\nu = 1$, (5.9) reduces to $X = A$, which alludes to the delta function limit of the scaled continuous-stable distributions as $\nu \to 1$. This has the effect of extending the range of the discrete-stable variate simulator to include the Poisson case despite the fact that the corresponding continuous distribution is a delta function.

Calculation of a new value of X is required for each successive discrete-stable variable. Whilst this method requires the creation of three independent random variables to create one, this method is very flexible in that it generates discrete-stable distributions of *any* valid parameter, and does not require the use of look-up tables or other such computationally expensive methods. Nor is it an approximation based simply on power-law tails; the variates generated *are* discrete-stable distributed.

The efficacy of the simulator is of the most interest as $\nu \to 1$, as the discrete-stable distributions are Poisson-like for small values of N (see Figure 2.4). In this limit, we require that the generator of the one-sided stable distributions produce variables from a distribution which is *almost* a delta function in x (see Figure 3.4). The algorithm outlined above is accurate only if the ensemble distributions of the generated variates

as $\nu \to 1$ have both the Poisson behaviour for small N and the power-law behaviour for large N.

5.7 Results

The values of the power-law index chosen to investigate a range of values across the parameter space are ν = 0.1, 0.3, 0.5, 0.7 and 0.9, and to investigate the Poisson limit, ν is of the form $1-10^{-m}$ for m = 1, 3, 5, 7, and 9. The scale parameter A is set to 10 throughout.

Theoretical results are found by exploiting the form of the generating function of the discrete-stable distributions (2.8) in Mathematica. The `Expand` command can be used to produce Taylor-series expansions the generating functions $Q(s)$ at the point $s=1$. Since $Q(s)$ is defined (2.7):

$$\begin{aligned} Q(s) &= \sum_{N=0}^{\infty} (1-s)^N P(N) \\ &= (1-s)^0 P(0) + (1-s)^1 P(1) + (1-s)^2 P(2) + (1-s)^3 P(3) + \ldots \end{aligned}$$

the coefficients of $(1-s)^N$ in the expansion are the $P(N)$ terms.

The χ^2 statistics of the simulations are given in Table 5.3. It is apparent that for a fixed values of A and m, as the power-law index ν approaches unity, the correspondence of the ensemble distributions to the theoretical distributions increases. This is due to the fact that as the index approaches unity, the Poissonian portion of the

distribution dominates for small N, where $P(N) >> m^{-1}$. Denoting k to be the value of N for which the power-law tail begins, the 'weight' of the power-law tail, which is given by the partial sum

$$\sum_{N=k}^{\infty} P_{(T)}(N) \tag{5.10}$$

decreases as $\nu \to 1$ – this can be inferred from Figure 2.4.

	χ^2	
ν	$m = 10^9$	$m = 10^{11}$
0.1	1.0573×10^{-3}	1.0014×10^{-5}
0.3	9.9912×10^{-4}	1.0042×10^{-5}
0.5	9.9654×10^{-4}	1.0001×10^{-5}
0.7	6.1361×10^{-4}	1.0005×10^{-5}
0.9	9.9081×10^{-4}	1.2048×10^{-5}
0.999	8.3549×10^{-4}	9.3910×10^{-6}
0.99999	1.0381×10^{-4}	9.8812×10^{-6}
0.9999999	9.2061×10^{-6}	4.9494×10^{-7}
0.999999999	3.0443×10^{-8}	2.8680×10^{-8}

Table 5.3

The χ^2 statistics for generated ensembles of discrete-stable variates. The value of A chosen is 10 throughout.

The effect of the index on the χ^2 statistic can be seen in Figure 5.4 below, which shows the distribution of ensembles of $m = 10^6$ variates for $A = 10$ with $\nu = 0.5$, $\nu = 0.9$ and $\nu = 0.999$. The corresponding χ^2 statistics are 0.985, 1.02 and 0.010

respectively. When $\nu = 0.5$ the tail behaviour begins at $N \approx 100$ – in this case the 'weight' of the tail given by (5.10) is approximately 0.52, so there is a far greater probability of a variate being in the tail. This can be seen in Figure 5.4; the error in the ensemble distribution is noticeably larger here.

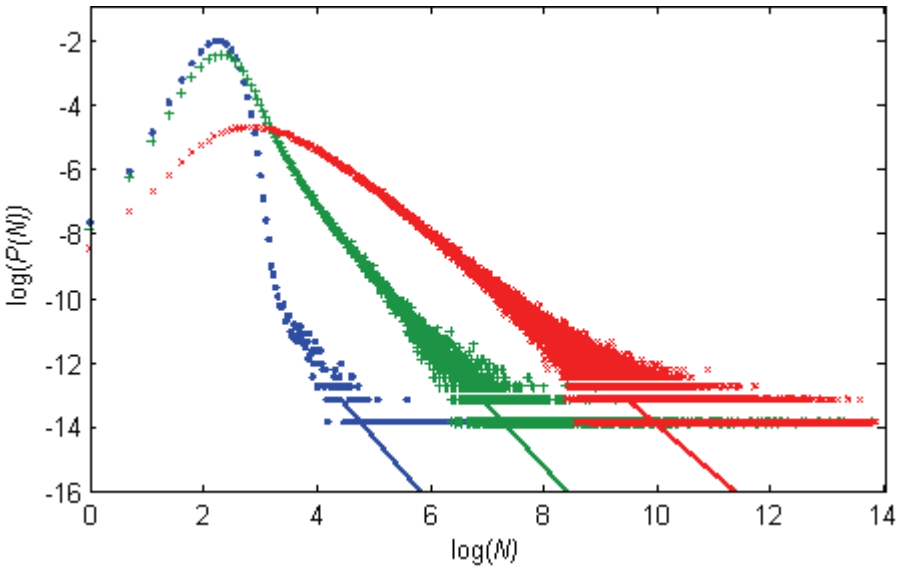

Figure 5.4

Illustrating the contributing factors to the lower χ^2 statistics as v approaches unity. Plotted are the distributions of ensembles of 10^6 simulated variates for which $A = 10$ and $v = 0.5$, 0.9 and 0.999 (red crosses, green plus signs and blue points, respectively). The power-law tails for each distribution are also plotted (lines).

5.8 Summary

The method of generating discrete distributions using Poisson transform interrelationships is outlined, and applied firstly to generate negative binomial variates, then to discrete-stable variates. For each point in each parameter space, large

numbers of the variates were collected to form an ensemble, the distribution of which was compared to theoretical distributions found via analytical methods.

For a fixed ensemble size m, it was shown that as the mean (and hence the variance) of the negative binomial distribution decreases, the accuracy of the ensemble distribution increases. As the power-law index ν of the discrete-stable distribution approached unity, the accuracy increased. This is to be expected, since the 'weight' of the tail and the number of values of N for which $P_{(T)}(N) \approx m^{-1}$ both decrease in this limit.

It is important to state that despite the fact that the χ^2 statistics are non-zero for the ensemble distributions, this is a type of sampling error; the variates are independent, and identically distributed, and the algorithm is an *exact* (as opposed to approximate) method for generating discrete-stable variates.

We have now described a novel method to generate discrete-stable distributed variates of *arbitrary* scale parameter A or power-law index ν without the use of cumbersome lookup tables or approximations. This is significant since the discrete-stable distributions underpin so many processes in nature – the ability to generate discrete-stable *variat*es enables, for instance, Monte Carlo modelling [123] of real-world discrete-stable processes. For this reason alone, the usefulness of this method cannot be exaggerated.

6. Crossing statistics

6.1 Introduction

In Chapter 5 a method of generating variates from discrete-stable distributions via the Poisson transform was described – however this is a mechanism for the simulation of random variates. A discrete-stable random process based on a multiple-immigration population model, for which the counted emigrants also form a discrete-stable process was described in Section 2.5. Yet another method of generating (asymptotically) discrete-stable distributions was found by Hopcraft, Ingrey and Jakeman [84] when studying continuous processes whose correlation function has fractal properties. They found that the level crossing statistics of these processes have power laws, and are thus asymptotically stable. The crossing behaviour of such processes can be thought of as a model for extremal behaviour in nature, where processes which have power-law tails are common. Smith, Hopcraft and Jakeman [83] found that for Gaussian processes which have *non* fractal correlation functions, the distribution of the number of *zero* crossings is either binomial, negative binomial or (exceptionally) Poisson.

These results have been based on well-studied processes for which, in general, the Probability Density Function (PDF) of the intensity has been known analytically. One process whose PDF is *not* analytically known, but which can be numerically simulated with ease is the phase-screen model [124]. This is an optical paradigm in

which a plane wave is scattered through a phase perturbing screen which changes the phase of the wave according to a given continuous process. This scattering is demonstrated schematically in Figure 6.1. As the phase of a plane wave is altered by the phase screen, contributions from different points of the phase screen interfere with each other on propagating from the screen. As a result, focusing or 'bright spots' are seen. By examining the intensity of light, in particular the distribution of level crossings, (which occur when the intensity exceeds, or falls below a certain level), we are examining the discrete properties of a continuous process, a recurrent theme of this thesis.

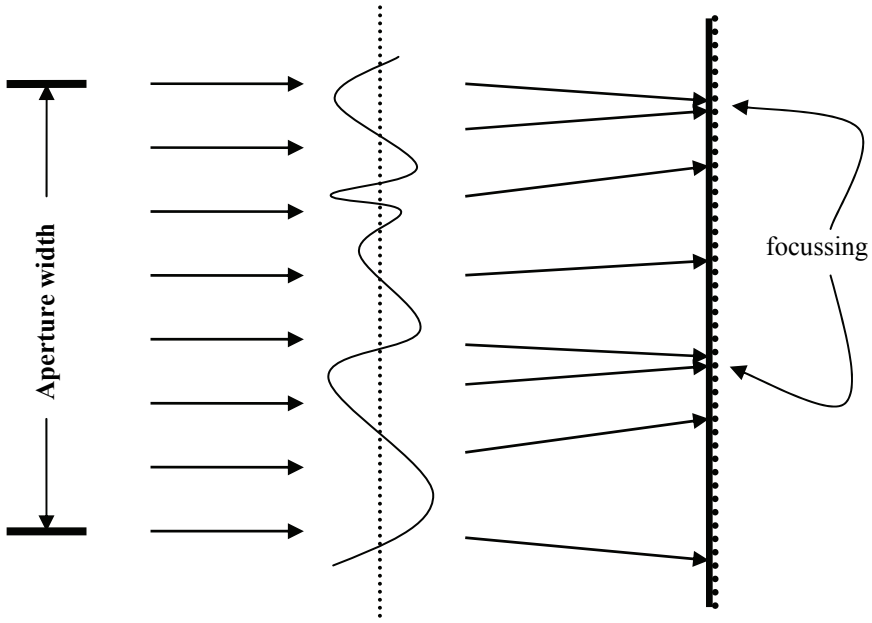

Figure 6.1

A schematic demonstration of the effect of a random phase screen on a plane wave

It has been seen that negative binomial distributions in number fluctuations of processes and the so-called *K* distributions [20] are intimately linked. The *K*

distributions have deep roots in the context of scattering, initially proposed as a model for sea echo, they also arise as the distribution of the slope of gamma processes [125] and a wealth of other areas [e.g. 107, 126].

This chapter will begin by introducing the K distributions, then will outline the algorithm used to simulate the phase-screen process. The intensity of the process will firstly be analysed and its density compared to known distributions. After examination of their means and Fano factors, the level crossing distributions will be compared to binomial and negative binomial distributions. Finally, the asymptotic properties of the *inter*-event times will be considered and estimated.

6.2 The *K* distributions

In Chapter 1 the K distributions were introduced as being an excellent model for the statistics of 'clutter' (unwanted returns from radars), where the surface of the sea was modelled as an ensemble of individual 'scatterers' of the radar signal. A heuristic model [127] of this scattering paradigm arises when considering the *number* of scatterers to have a negative binomial distribution, and the contribution of the signal from each scatterer has finite variance.

This is analogous to a random walk model [97, 126] in which the sum of N independent n-dimensional Gaussian processes is considered. The displacement of the process is K distributed (after a suitable rescaling of the parameters) if N is a negative binomially distributed statistical variable of mean $\overline{N}$, and $\overline{N} \to \infty$.

We have already seen that the concept of 'multiply stochastic' processes and distributions can produce new distributions from combinations of simpler ones. One such multiply stochastic distribution which results in K distributed statistics occurs when considering an exponential distribution whose mean is modulated by an independent gamma distribution. Suppose we consider an exponential distribution of mean A, where A is a gamma distributed random variable with shape parameter α and mean α / b, then the multiply stochastic distribution is [e.g. 107, 125]:

$$K(x,\alpha,b) = \int_0^\infty \frac{1}{A}\exp\left(-\frac{x}{A}\right) p_{(g)}\left(A,\alpha,\frac{1}{b}\right) dA$$

$$= \frac{2b}{\Gamma(\alpha)}(bx)^{\frac{\alpha-1}{2}} K_{\alpha-1}\left(2\sqrt{bx}\right). \tag{6.1}$$

where as before, $K_\nu(x)$ is a modified Bessel function [93]. The moments of these K distributions are easily obtained to be:

$$< x^m >= \frac{m!}{b^m}\frac{\Gamma(m+\alpha)}{\Gamma(\alpha)}. \tag{6.2}$$

An alternative parameterisation of the K distributions arises from their roots in the context of scattering. Supposing the variable x represents the *intensity* (i.e. the square of the amplitude) of a return signal, and y is the *amplitude* of the signal, then upon transforming $x = y^2$, the distribution of the amplitude y is:

$$\tilde{K}(y,\alpha,b) = \frac{4b^{(\alpha+1)/2}}{\Gamma(\alpha)} y^\alpha K_{\alpha-1}\left(2\sqrt{b}y\right). \tag{6.3}$$

and the moments are:

$$< y^{2m} >= \frac{m!}{b^m}\frac{\Gamma(m+\alpha)}{\Gamma(\alpha)}$$

It is in this parameterisation that the $\widetilde{K}$ distributions reduce to Rayleigh distributions as $\alpha \to \infty$ [72]. In the same limit, the K distributions reduce to exponential distributions.

Both parameterisations $K(x,\alpha,b)$ and $\widetilde{K}(y,\alpha,b)$ occur in a wide variety of experimental data [e.g. 20]; the specifics of the mode of measurement determine *which* is appropriate for the situation.

The K distributions have arisen in a wealth of areas, as diverse as human migration [128], and satellite imaging [129]. It would therefore be instructive to examine the connection between negative binomial number fluctuations and K distributions.

6.3 A nonlinear filter model of a phase screen

A nonlinear filter model was introduced by Jakeman and Ridley [124] to numerically investigate some properties of phase screen scattering such as far-field statistics. The filter they describe, which is essentially a band-pass Lorentzian filter of width λ of a signal $\phi(t)$, is given by the integral

$$S(t) = \lambda \int_{-\infty}^{t} \exp[i\phi(t') + \lambda(t'-t)]dt'. \tag{6.4}$$

This integral is analogous to the amplitude of a plane wave when scattered into the far field by a corrugated random phase-changing screen, as illustrated in Figure 6.1.

Denoting the aperture width of the wave to be W, the filter width can be thought of as being $\lambda \sim W^{-1}$ – this can be inferred from the integral for the filter (6.4).

The discrete analogue of this filter can be derived since:

$$\frac{dS(t)}{dt} = \lambda \exp(i\phi(t')) - \lambda \cdot S(t).$$

Supposing that $\phi(t)$ and $S(t)$ are discretised as $\phi(n)$ and $S(n)$ for $1 \le n \le N$, it then follows that

$$S(n) - S(n-1) = \lambda \delta t \exp(i\phi(n)) - \lambda \delta t \cdot S(n-1)$$
$$S(n) = \lambda \delta t \exp(i\phi(n)) + (1 - \lambda \delta t) S(n-1).$$

To maintain accuracy in the discretisation, the quantity $\lambda \delta t$ must be small, or the phase $\phi(t)$ must be slowly changing. For simplicity, δt is set to unity, so the corresponding recurrence relation is:

$$S(n) = \begin{cases} \lambda \exp(i\phi(1)) & n = 1 \\ \lambda \exp(i\phi(n)) + (1-\lambda) S(n-1) & 1 < n < N \end{cases} \tag{6.5}$$

Note that the lower limit of the integral (6.4) is $-\infty$, and the process $S(n)$ has a lower limit of $n = 1$. Due to the exponentially decaying nature of the filter, for $n' > n$ and $(n' - n) >> 1/\lambda$, $S(n)$ and $S(n')$ are independent. Hence if the initial values of $S(n)$ are discarded (e.g. for $n < 3/\lambda$), the filtered signal is statistically stationary.

We are interested in studying the *intensity* of the filtered signal, which is found by setting

$$I(n) = |S(n)|^2$$

from which the pertinent statistics can be found.

6.4 Simulating a Gaussian process

Having discussed a nonlinear filtering model of a phase screen, the next logical step is to discuss the generation of the random process which corresponds to the phase $\phi(t)$. A suitable process is the Gaussian process, for which generation methods exist. One such method which allows the rapid generation a Gaussian process with a prescribed autocorrelation was introduced by Liu and Manson [130]. Firstly, a vector V_1 of i.i.d. Gaussian variables of unit variance and zero mean is created, then padded with zeros. V_1 is then convolved with a filter vector V_2 which contains all the information regarding the autocorrelation of the required process. The result, V_3 is now a Gaussian process with the specified correlation function. A portion of V_3 is removed so that end effects from the convolution are removed.

6.5 Level crossing detection

We are now in a position where we are given the intensity as a time series and are thus able to find the level crossings. Given a series of values $I(n)$, an efficient way to find the level crossings at an arbitrary level u is demonstrated by Smith [131]. The procedure of finding crossings of the level $u = 1$ for a series of eight values is illustrated below:

0.1	1.5	1.9	3.0	0.9	0.3	2	0.1	$I(n)$

Firstly, take the sign of the values of the difference between the values and the level: $I_d = \mathrm{sgn}(I(n) - u)$.

-1	1	1	1	-1	-1	1	-1	$I_d(n) = \mathrm{sgn}(I(n) - u)$

Next define $I_d^{'}(n) = I_d(n) \times I_d(n+1)$, ignoring the terms that do not overlap (in grey):

-1	1	1	1	-1	-1	1	-1		$I_d^{'}(n) = I_d(n) \times I_d(n+1)$
				×					
	-1	1	1	1	-1	-1	1	-1	
				=					
	-1	1	1	-1	1	-1	-1		

Finally, subtract one from each point in the series, and divide by minus two.

	1	0	0	1	0	1	1		$I_c(n) = \left(I_d^{'}(n) - 1\right)/(-2)$

The corresponding train of zeros and ones gives the locations of the level crossings. For instance, $I_c(n) = 1$ indicates that there is a crossing of the level u between $I(n)$ and $I(n+1)$. Thus the number of crossings of the series $I(n)$ of the level u is simply the sum over the series $I_c(n)$. This method of analysis does not in general need to be

performed in an element-by-element fashion, as many mathematical packages such as MATLAB and Mathematica allow operations to be performed on entire vectors simultaneously.

6.6 Results

For the purposes of the results in this chapter, the correlation function of the Gaussian process is itself chosen to be Gaussian – this facilitates the fastest computation of the Gaussian process itself. The particular correlation function chosen is of the form:

$$< \phi(0)\phi(\tau) >= \varphi^2 \exp\left(-\frac{\tau^2}{2L^2} \right)$$

where the value of φ is taken to be 20, and the correlation length scale L is 100 steps so that the difference in value between each step in the discretised process is small. Values of the filter width λ in (6.4) and (6.5) are chosen from the range [0.001, 0.1].

Each simulation is run over 87,381 steps, with the first 7381 steps discarded so that the signal (comprised of 80,000 steps) is statistically stationary. Each realisation of the filtered process is therefore run over 800 correlation lengths of the Gaussian process. To generate the following results, 100,000 realisations are run for each chosen value of λ, totalling $8\text{x}10^9$ steps.

For further examination later, nine points have been chosen which depict a range of behaviours in the processes, and will be referred to as the test cases. These are when the filter width $\lambda = 0.01,\ 0.025,\ 0.075$, and when the crossing level $u = 0.01,\ 0.1$ and

0.5. These test cases (along the filter widths and crossing levels) are marked on the figures as appropriate.

6.6.1 The intensity and its density

Having outlined the method to generate the filtered process, it is instructive to examine the effect of the filter width λ on the intensity. For the same discretised Gaussian process $\phi(n)$, Figure 6.2 shows the processed signal $I(n)$ for the chosen values of λ. Note that peaks in the intensity, regardless of the value of λ, correspond to stationary points in the phase.

For small λ (corresponding to large apertures in the phase screen), the process has more fine-scale structure that is not present as λ increases. This is because for larger apertures, many different points in the field contribute to create interference effects which are not seen for smaller apertures (large values of λ).

In the limit $\lambda \to 0$, the filtered signal is termed 'Gaussian' or 'fully developed speckle' [e.g. 132], for which the intensity has a negative exponential density. This can be seen from the kernel of the integral (6.4) as $\lambda \to 0$, from which it can be inferred that the signal $I(t)$ has a longer memory of the phase $\phi(t)$, resulting in interference from many correlation lengths of the Gaussian process.

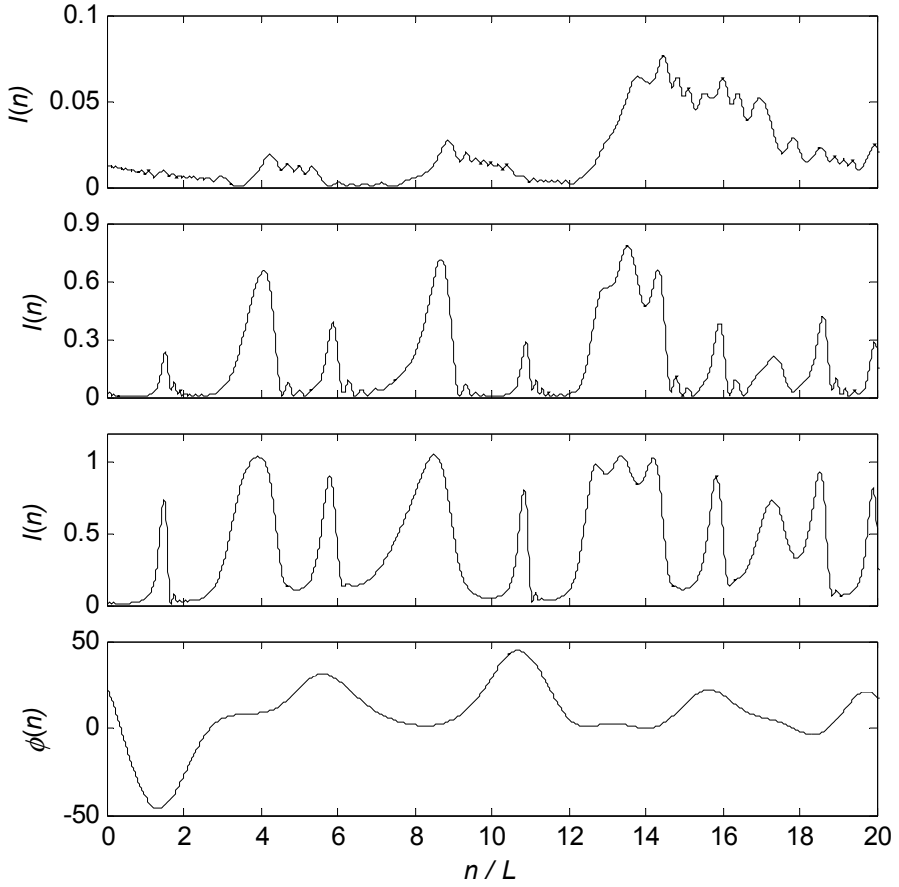

Figure 6.2

Individual realisations of the process for λ = 0.002 (top box), 0.025 (second), 0.075 (third), and the Gaussian phase itself (bottom box). Note the different vertical scales.

The logarithm of the probability density function of $I(n)$ is plotted for the entire parameter range in Figure 6.3. The richness of behaviour can be immediately be seen in the multiple local maxima and minima in the phase space. As expected, the maximum intensity increases as a function of the filter width λ. Figure 6.4 plots the logarithm of the intensity for $0 < u < 0.2$, where there is more structure.

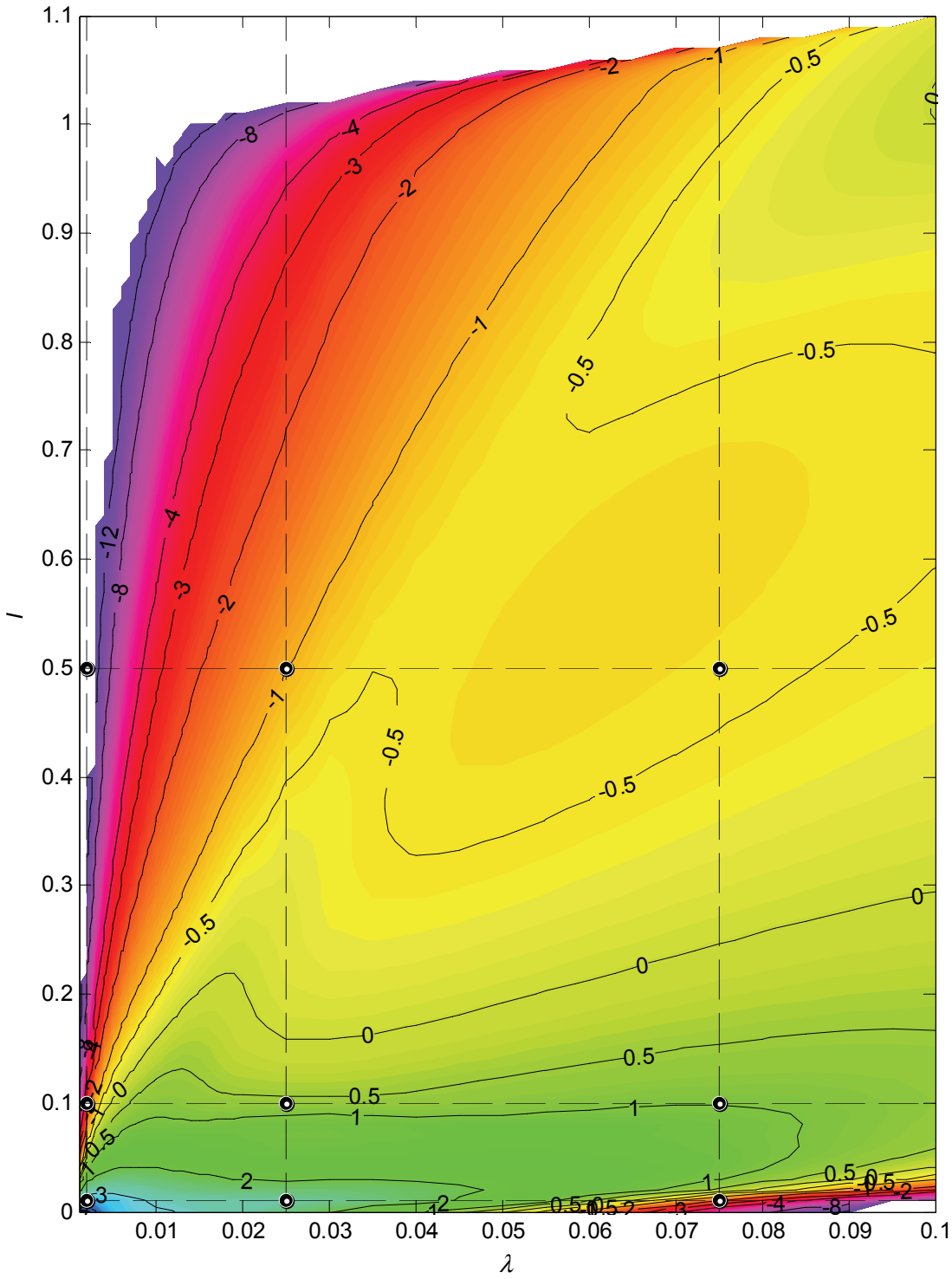

Figure 6.3

A contour plot of the logarithm of the probability density function of the intensity of filtered process for $0 < I < 1.1$. The dots refer to the case studies.

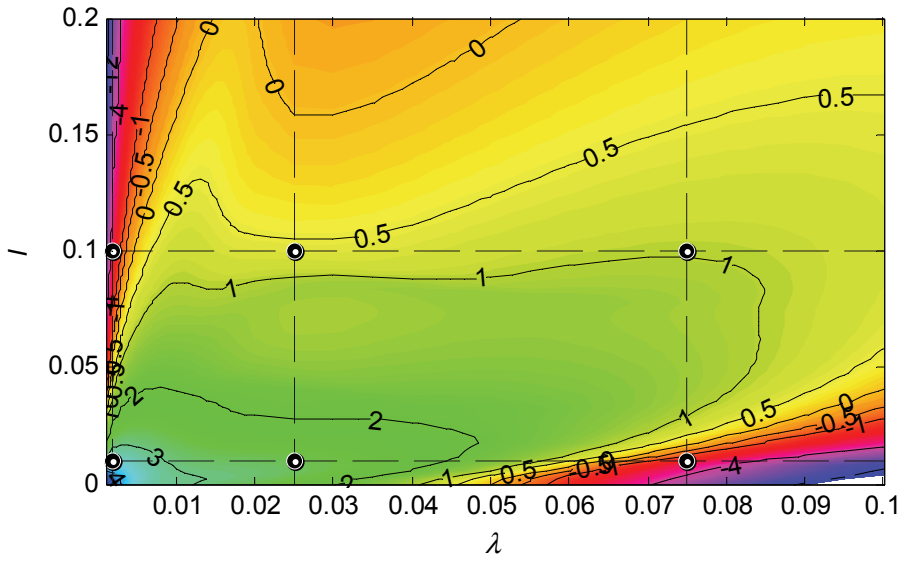

Figure 6.4

A contour plot of the logarithm of the probability density function of the intensity of filtered process for $0 < I < 0.2$.

In order to examine the density $P(I)$ of the intensity $I(n)$ in the large aperture limit, Figure 6.5 plots $P(I)$ for λ = 0.001, 0.002, 0.003 and 0.004. Recall that the K distributions are defined by the two parameters α and b. To fit them to the densities, (6.2) can be manipulated to obtain

$$\alpha = \frac{2 < x >^2}{< x^2 > -2 < x >^2} \tag{6.6}$$

$$b = \frac{\alpha}{< x >}. \tag{6.7}$$

This method of finding α and b to fit K distributions is used in Figure 6.5 below – it is apparent that as λ increases, the fit to the K distribution is less appropriate.

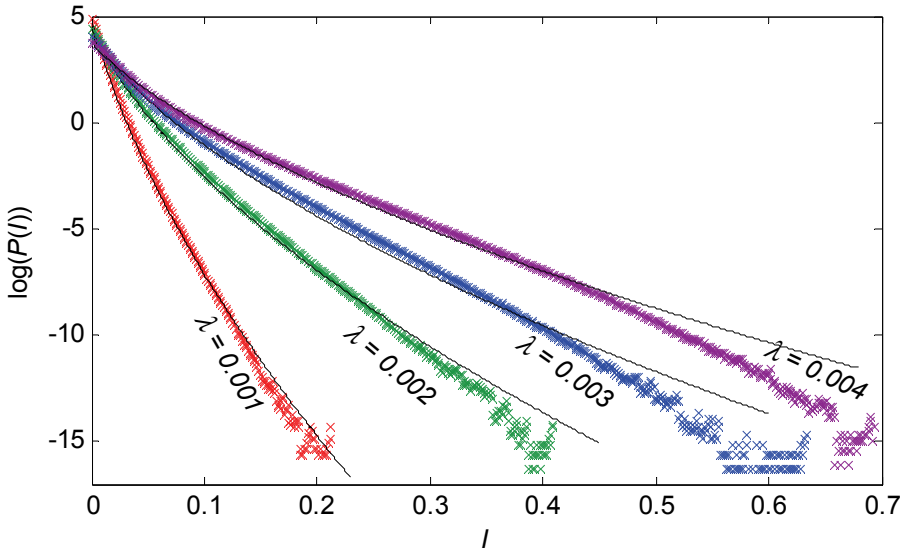

Figure 6.5

Fitting *K* distributions to the density of the intensity when λ = 0.001 (red), 0.002 (green), 0.003 (blue) and 0.004 (purple). The fitted *K* distributions are plotted as solid lines.

The parameters of the *K* distributed fits and the χ^2 statistics of the fit (χ_k^2) are given in Table 6.1. The χ^2 statistics from fitting an exponential distribution of the same mean are also given (χ_e^2). It is clear upon comparison of the χ^2 statistics that for $\lambda > 0.001$ that the *K* distributions provide far better fits than the exponential distributions. When λ = 0.001, the exponential and *K* fits are comparable, which is to be expected given that as $\lambda \to 0$ negative exponential statistics (which *K* distributions attain in the large α limit) are expected from the phase screen model.

λ	0.001	0.002	0.003	0.004
$< x >$	0.00597	0.0120	0.0182	0.0260
α	8.05	5.50	4.72	4.5
b	1349	459	254	173
χ^2_k	81.3	24.8	14.5	15.25
χ^2_e	95.1	108	140	76.1

Table 6.1

Comparing the effectiveness of the fit of the K distribution to an exponential distribution of the same mean for the intensity density of the filtered process.

For the values of λ chosen as test cases, the intensity density is plotted in Figure 6.6.

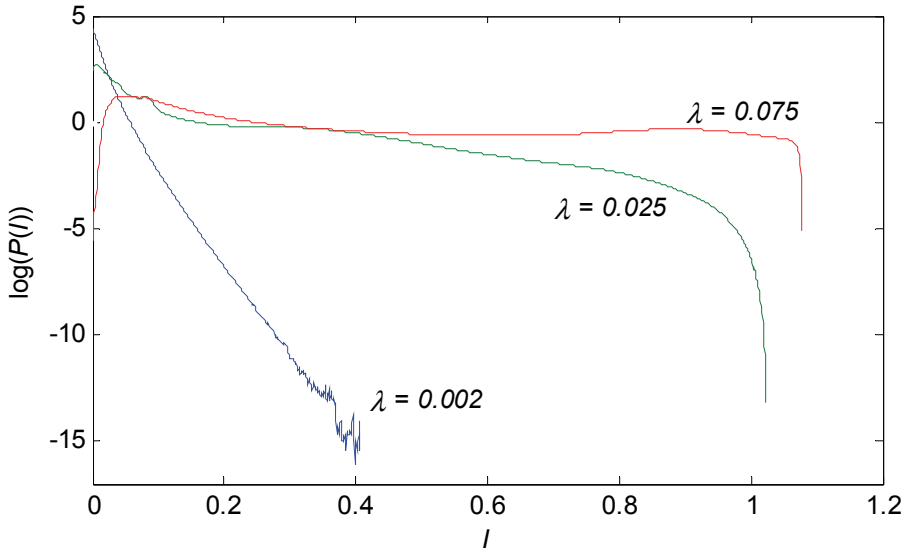

Figure 6.6

Individual probability density functions for λ = 0.002 (blue), 0.025 (green), and 0.075 (red).

In conjunction with Figure 6.5 which examines the intensity for small λ, it is apparent that there are three distinct regimes of behaviour for $P(I)$. For very small

values of λ, the intensity is exponential. When $\lambda \approx 0.002$, $P(I)$ is approximated well by a K distribution. For $\lambda = 0.075$, $P(I)$ resembles a uniform distribution, whereas for $\lambda = 0.025$, $P(I)$ is not like any known distributions.

6.6.2 Level crossing rates

Having investigated some properties of the process $I(n)$, it is instructive to examine its level crossings. Since the number of crossings in each realisation of the process is dependent on the number of samples, it is more useful to consider the number of crossings per correlation length of the Gaussian process, i.e. the crossing *rate*, which is defined:

$$R = \frac{< N >}{L_n}$$

where, for the parameters used for these simulations in §6.6, $L_n = 800$ is the *number* of correlation lengths over which each realisation is run. R is given as a contour plot in Figure 6.7 as a function of the filter of width λ and the crossing level u.

It is noteworthy that for values of λ above 0.04, there is a large range of u for which $R \geq 1$, i.e. where the intensity crosses the level u more than once per correlation length. For a fixed level $u << 1$, the mean decreases as λ increases; this could be inferred from the density of the process itself (Figure 6.3), which also decreases very quickly as the level decreases. Figure 6.8 plots the mean crossing rate R for $0 < u < 0.2$, where the largest value of R is.

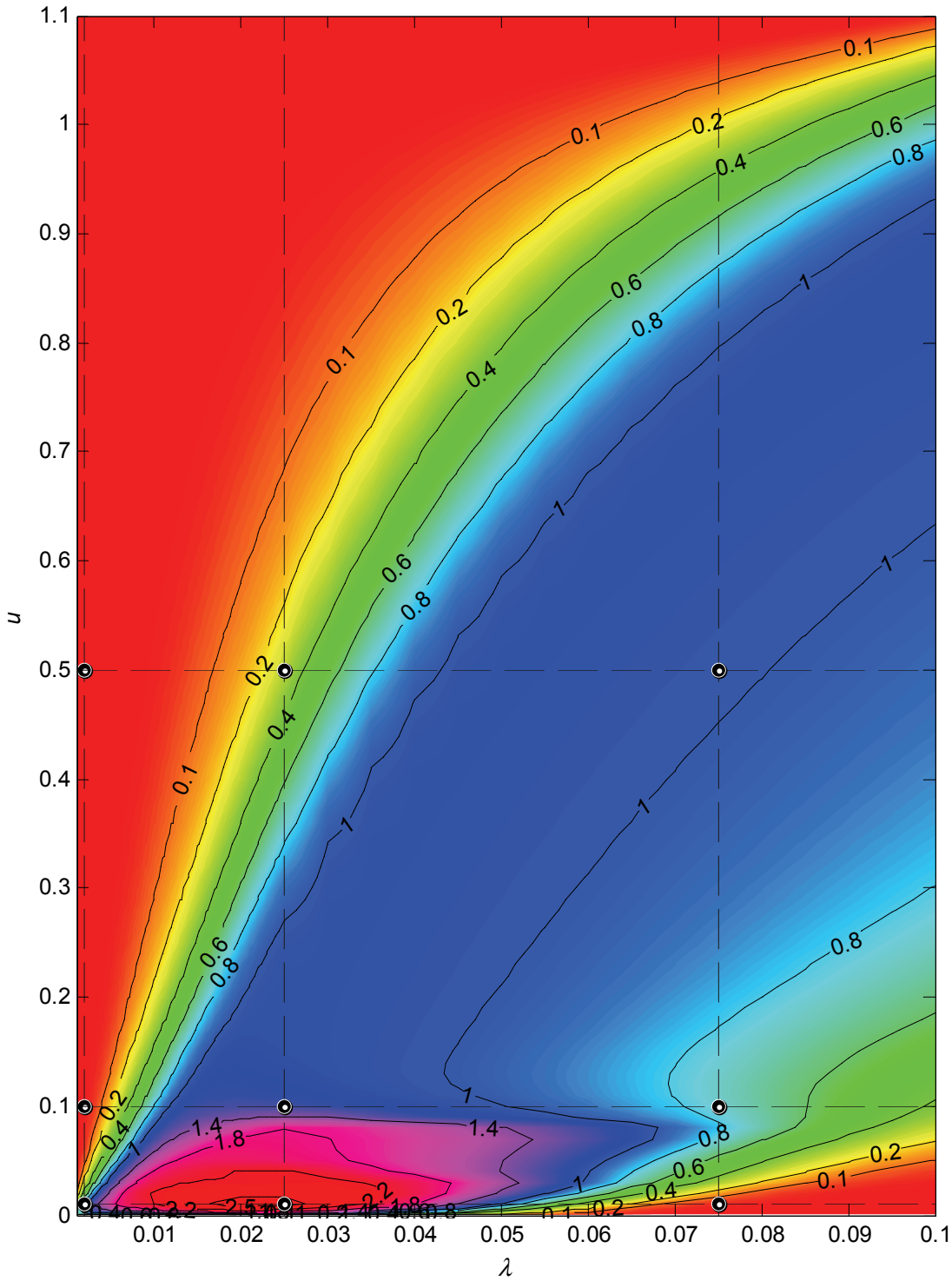

Figure 6.7

A contour plot of the level crossing rate of the filtered process for $0 < u < 1.1$.

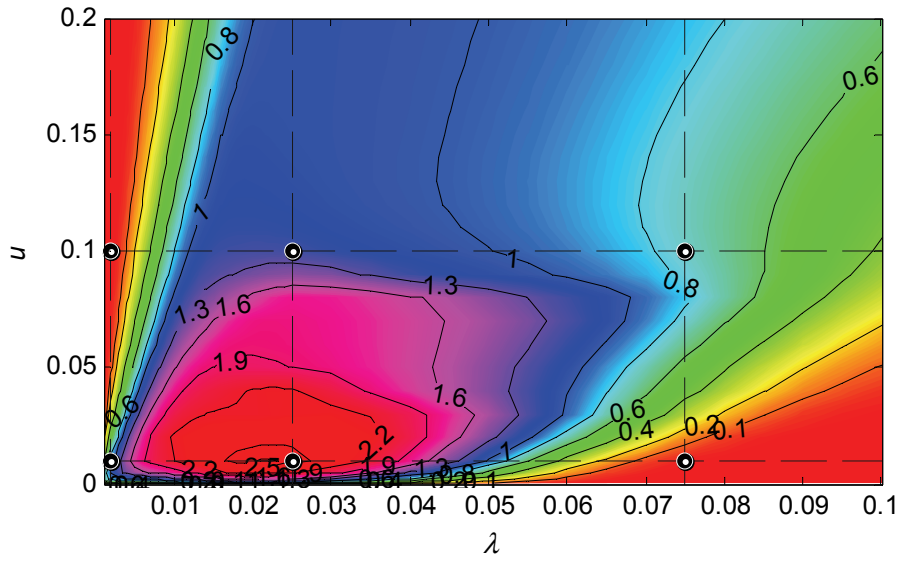

Figure 6.8

A contour plot of the level crossing rate of the filtered process $0 < u < 0.2$.

The intensity of the process for $\lambda = 0.02$, $u = 0.01$ where the crossing rate is near its maximum is plotted in Figure 6.9. There is a large degree of fine scale structure which occurs at almost all levels. This is due to the phase from many different points in time contributing to produce interference effects.

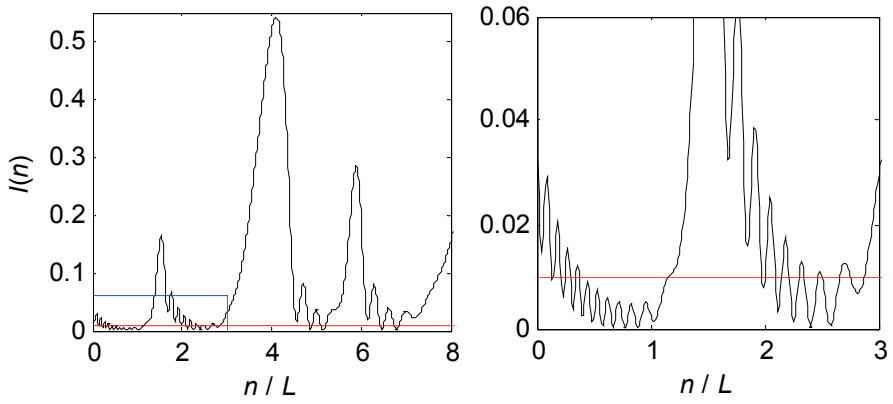

Figure 6.9

Showing the a realisation of the process for which $u = 0.01$ and $\lambda = 0.02$. The region within the blue box on the left plot is expanded on the right.

6.6.3 Fano factors

Recall that the Fano factor is a measure of how Poissonian a discrete distribution is, and is defined as the ratio of the variance to the mean:

$$F = \frac{< N^2 > - < N >^2}{< N >}. \tag{6.8}$$

It might be expected that since the process is measured over a large (800) number of correlation lengths, the fluctuations in the number of level crossings would average each other out, resulting in the crossings having a Poisson distribution, and hence unit Fano factor.

Figure 6.10 shows the Fano factor for the crossings of the intensity of the filtered process for the range $0 < \lambda < 0.1$ and $0 < u < 1.2$, from which it can be seen that the Poisson assumption clearly does not hold, since there are points for which $F < 0.5$ and $F > 6$.

Again, the range of interest seems to be $0 < u < 0.2$ – this is plotted in Figure 6.11. A maximum of the Fano factor plot can be seen to be in the region of $\lambda \approx 0.065$, $u \approx 0.015$. Another region which has a very large Fano factor is at the origin - this can be explained by Figure 6.2, which shows a greater degree of bunching of crossings when λ and u are low. The large variance in the crossing distribution compared to its mean (c.f. Figures 6.7 and 6.8) then results in a large Fano factor.

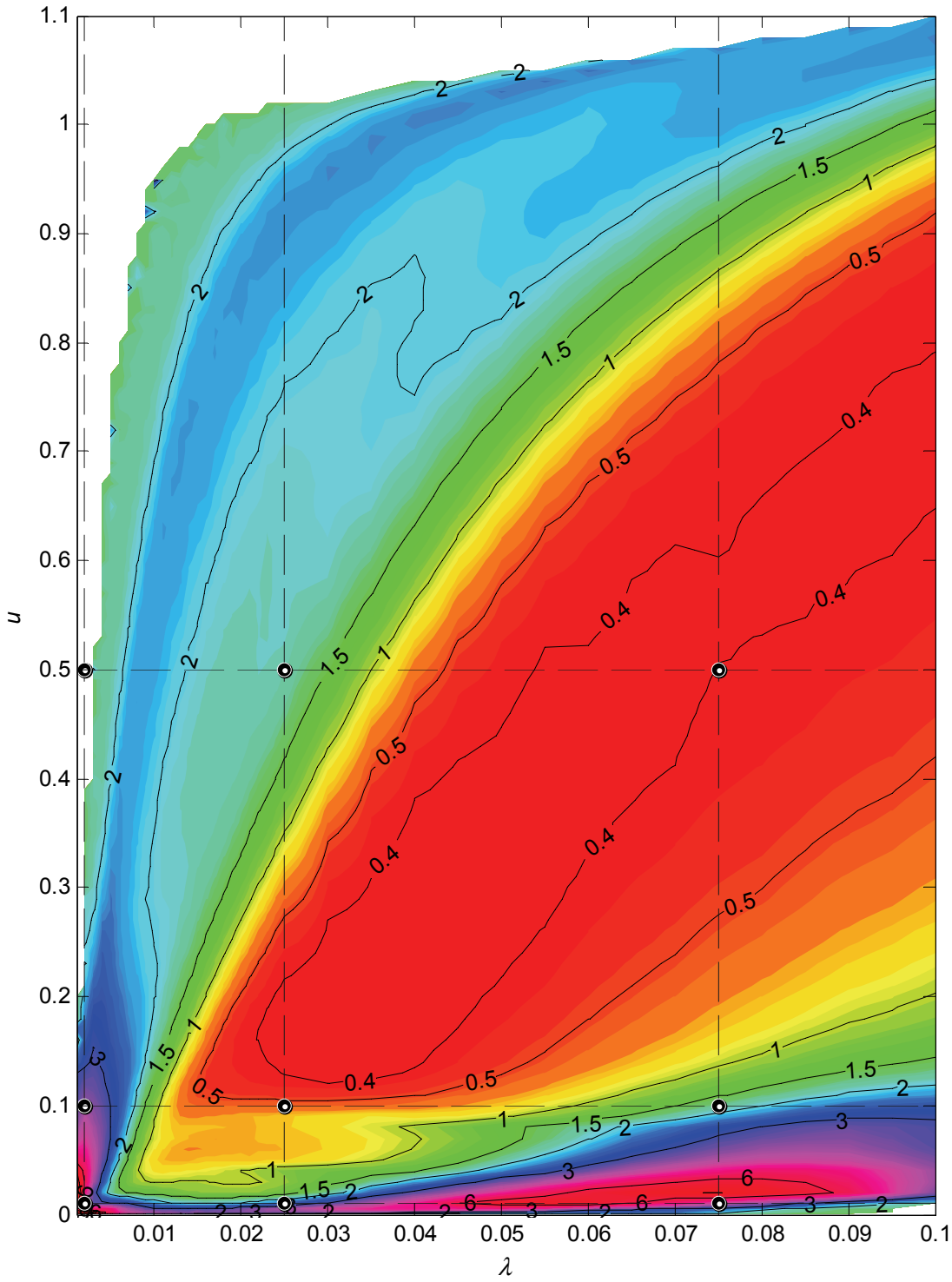

Figure 6.10

A contour plot of the Fano factor of the level crossings distribution of the intensity for $0 < u < 1.1$.

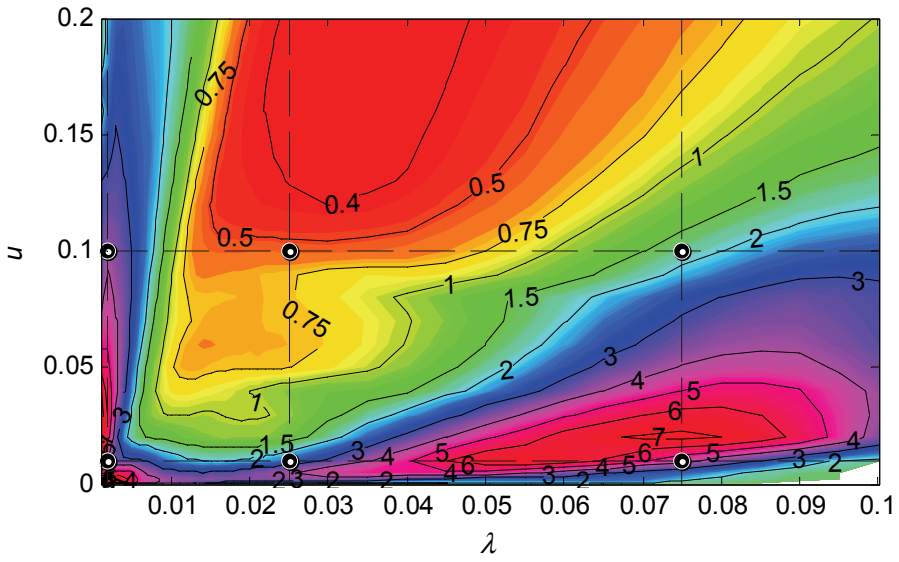

Figure 6.11

A contour plot of the Fano factor of the level crossings distribution of the intensity for $0 < u < 0.2$.

6.6.4 Level crossing distributions

Instead of examining the *global* characteristics of the crossings via their mean and Fano factors, it is instructive to choose points in phase space and consider the level crossing distributions themselves.

Though not apparent from either the crossing rate R or Fano factor F, there are strong odd-even effects in the level crossing distributions. Figure 6.12 plots one such crossing distribution when $\lambda = 0.025$ and $u = 0.5$ which exhibits strong odd-even behaviour – there is a much greater probability of an *even* number of crossings occurring than an *odd* number.

The reasons for the odd-even behaviour can be intuited from the intensity $I(n)$ of the filtered process. Figure 6.13 shows a single realisation of the process when $\lambda = 0.025$, with the level $u = 0.5$ plotted in red. The crossings tend to occur in pairs, with *even* numbers of crossings being more likely than *odd* numbers. This is reminiscent of a population process [61] for which immigrants are only permitted to enter in *pairs*, and the distribution of *emigrants* showed strong odd-even effects.

These odd-even effects can be removed by considering the 'envelope' of the distribution. Defining $P(N)$ to be the probability that there are exactly N crossings of the level u, the envelope is:

$$P_e(N) = \begin{cases} \dfrac{P(0)}{2} & N = 0 \\ \dfrac{P(N) + P(N-1)}{2} & N > 0. \end{cases}$$

The resultant distribution $P_e(N)$ is then 'smoothed' – the envelope of the level crossing distribution for $\lambda = 0.025$ and $u = 0.5$ is plotted as circles in Figure 6.12. It is shown in Appendix A that calculating the envelope of a distribution does not affect its mean or Fano factor greatly except when the mean of $P(N)$ is very small.

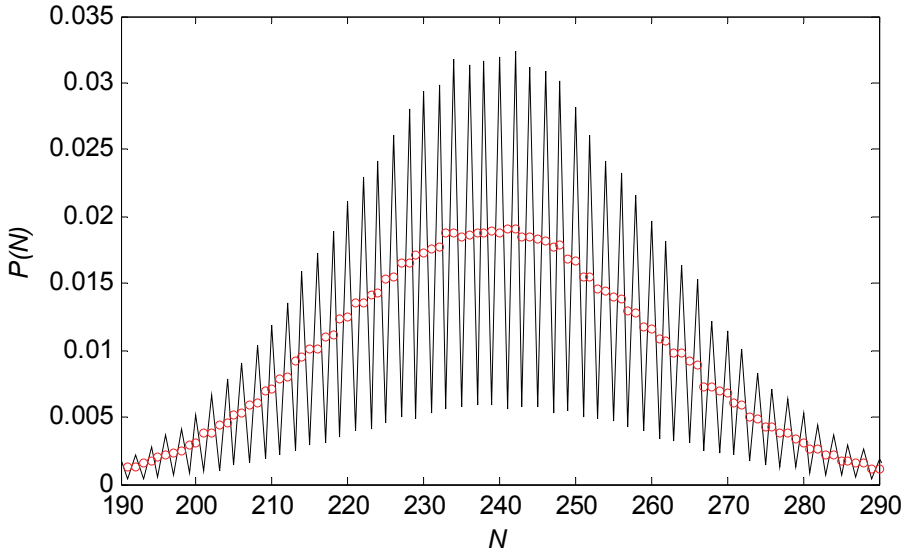

Figure 6.12

Crossing distribution (black line) and envelope (red circles) for $\lambda = 0.025$, $u = 0.5$.

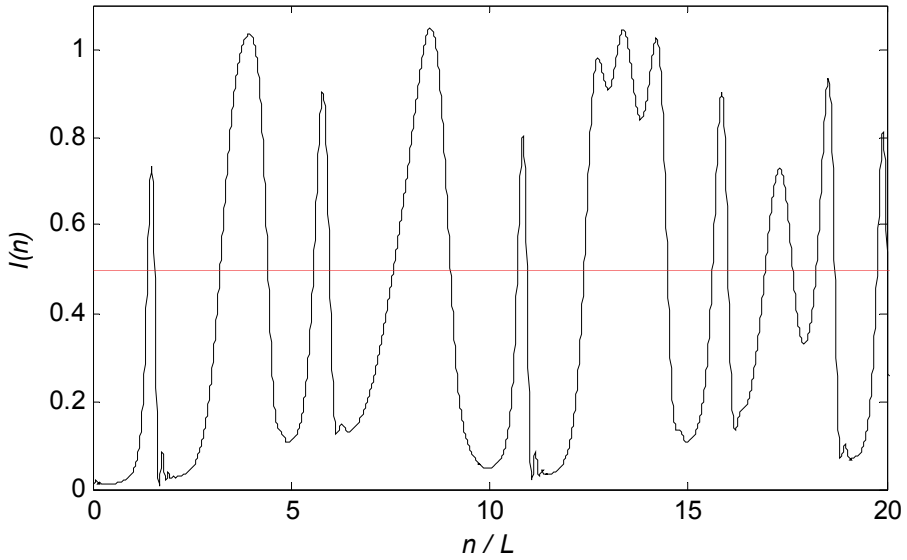

Figure 6.13

A realisation of the process, showing the intensity when $\lambda = 0.025$, and the level $u = 0.5$ (red line).

The fact that the binomial, negative binomial and Poisson distributions have Fano factors less than, greater than and equal to unity respectively makes them suitable

candidate distributions to fit to the envelopes. It is possible [e.g. 83] to parameterise the binomial and negative binomial distributions in terms of their Fano factor F and another parameter α, i.e.:

$$P_b(N) = \frac{\alpha!}{N!(\alpha - N)!} F^{\alpha - N}(1-F)^N; \qquad \alpha = \frac{< N >}{1-F}, F < 1 \tag{6.9}$$

and

$$P_n(N) = \frac{(\alpha - 1 + N)!}{N!(\alpha - 1)!} F^{-\alpha}\left(1 - \frac{1}{F}\right)^N; \qquad \alpha = \frac{< N >}{F-1}, F > 1 \tag{6.10}$$

respectively. In the context of scattering of light by discrete particles, the parameter α can be thought of as the number of coherent scattering centres in the scattering medium, or as another measure of how Poissonian a distribution is. For instance, as $\alpha \to \infty$, (6.9) and (6.10) become Poisson.

For each of the nine test cases, the envelope is calculated, then (depending on the value of the Fano factor) a negative binomial or binomial distribution fit is taken, and the corresponding χ^2 statistics are found. A Poisson distribution of the same mean, and a Gaussian distribution of the same mean and variance are also compared via their χ^2 values – $\chi^2{}_P$ and $\chi^2{}_G$ respectively.

The envelopes of the level crossing distributions for u = 0.01, 0.1 and 0.5 are plotted in Figures 6.14, 6.15 and 6.16 respectively. Also plotted are the Poisson, Gaussian and (depending on the Fano factor) binomial or negative binomial fits. The corresponding statistics for u = 0.01, 0.1 and 0.5 are given in Tables 6.2, 6.3 and 6.4

respectively. Note that when $\lambda = 0.02$, there are *no* crossings of the level $u = 0.5$, so this case is not considered.

The envelopes (plotted as crosses) of the level crossing distributions are barely discernable when plotted alongside the binomial and negative binomial fits (plotted as blue lines). This shows that the binomial and negative binomial distributions provide excellent fits to the envelopes for all of the test cases – regardless of the Fano factor or the mean, and even in the *tails* of the distribution. The χ^2 statistics are therefore consistently better for binomial/negative binomial fits than either Gaussian or Poisson fits.

From the values of $\chi^2{}_G$ it is clear that the Gaussian distribution is bad fit to the envelopes when the mean is small. This is to be expected since it is symmetric – the binomial and negative binomial distributions are not. For larger values of the mean however, the Gaussian distribution provides a better fit, with $\chi^2{}_G \approx \chi^2$, since it can be thought of as a continuum limit to the binomial and negative binomial distributions. Note that irrespective of the value of $\chi^2{}_G$, the number of level crossings is a *discrete* quantity, and thus can never have a true Gaussian distribution. The Poisson distribution has provided poor fits to all the crossing distribution envelopes. This is to be expected since none of the test cases have Fano factors which are close to unity, and hence have relative variances which differ greatly to that of a Poisson.

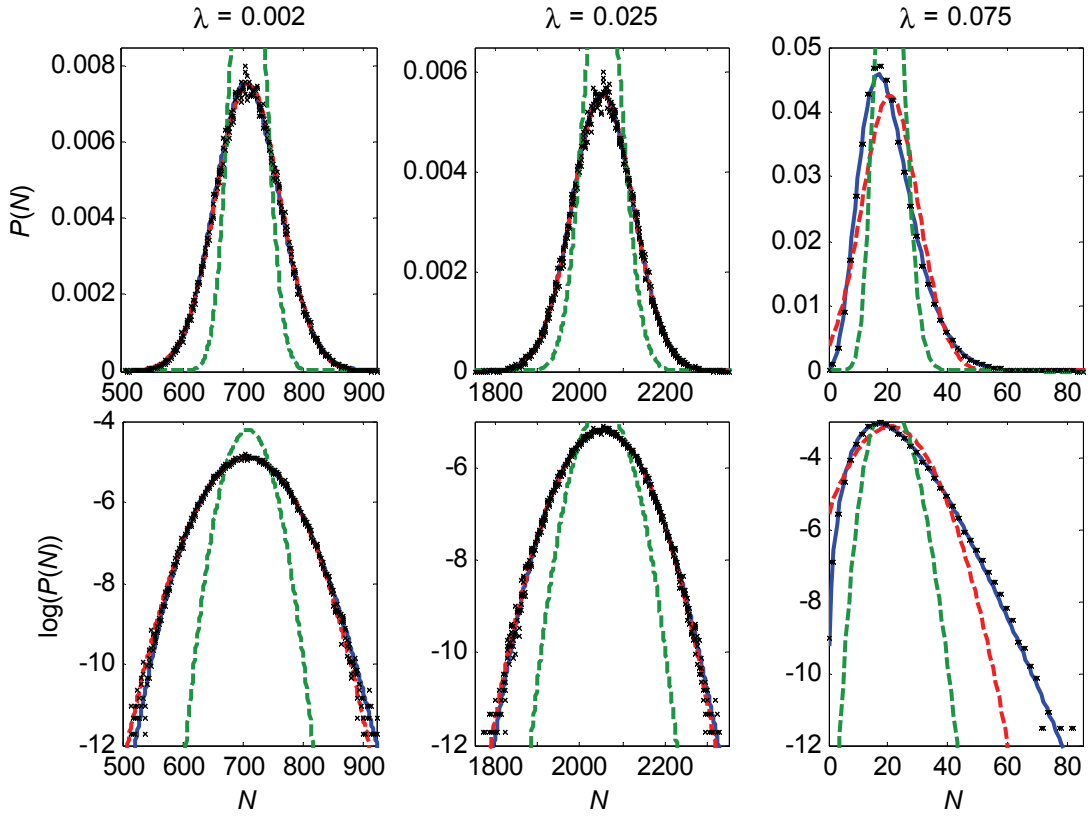

Figure 6.14

Crossing distribution envelopes for λ = 0.002 (left), 0.025 (middle), and 0.075 (right). The crossing level u is 0.01 throughout. Also plotted are Poisson, Gaussian and either binomial or negative binomial fits (green, red and blue lines respectively).

λ	0.002	0.025	0.075
$< N >$	708.8	2054	21.20
F	3.967	2.518	4.130
Fit	Negative binomial	Negative binomial	Negative binomial
χ^2	0.0052	0.3895	1.002
$\chi^2{}_G$	0.0055	0.3987	8911
$\chi^2{}_P$	8.3×10^7	526	1.04×10^{20}

Table 6.2

The mean, Fano factor and χ^2 statistics for the three values of λ when u = 0.01.

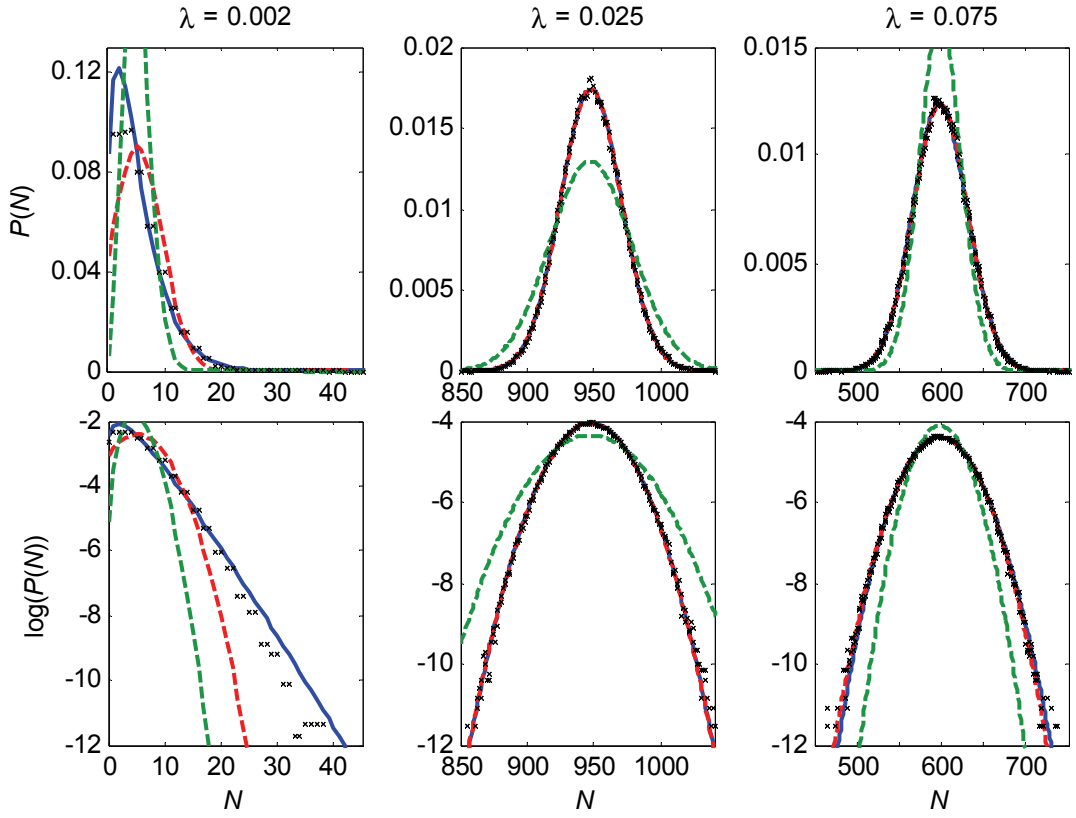

Figure 6.15

Crossing distribution envelopes for λ = 0.002 (left), 0.025 (middle), and 0.075 (right). The crossing level u is 0.1 throughout. Also plotted are Poisson, Gaussian and either binomial or negative binomial fits (green, red and blue lines respectively).

λ	0.002	0.025	0.075
$< N >$	5.569	948.3	599.4
F	3.628	0.5538	1.736
Fit	Negative binomial	Binomial	Negative binomial
χ^2	0.9594	0.0025	0.1585
$\chi^2{}_G$	1194	0.0030	0.1595
$\chi^2{}_P$	2.67×10^{12}	0.120	3.18

Table 6.3

The mean, Fano factor and χ^2 statistics for the three values of λ when u = 0.1.

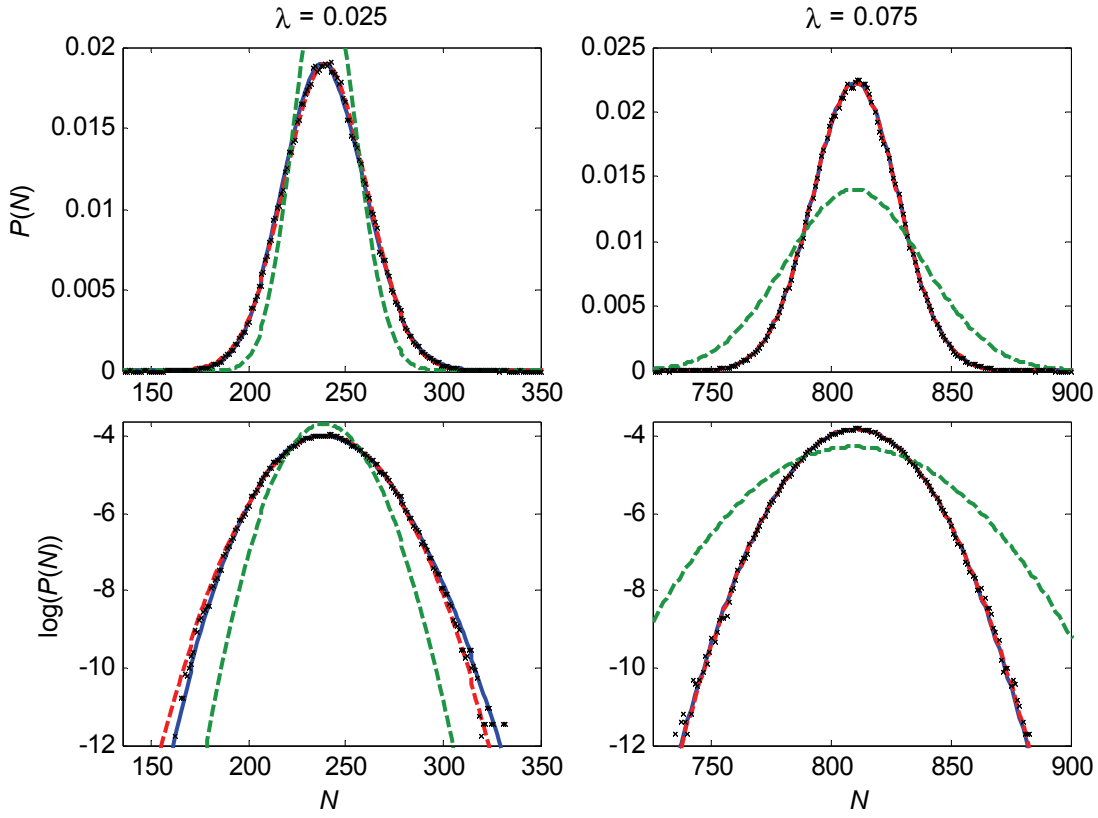

Figure 6.16

Crossing distribution envelopes for λ = 0.025 (left) and 0.075 (right). The crossing level u is 0.5 throughout. Also plotted are Poisson, Gaussian and either binomial or negative binomial fits (green, red and blue lines respectively).

λ	0.025	0.075
$< N >$	240.0	810.4
F	1.842	0.3966
Fit	Negative binomial	Binomial
χ^2	0.4838	0.0022
χ^2_G	0.5010	0.0029
χ^2_P	33.1	0.257

Table 6.4

The mean, Fano factor and χ^2 statistics for the two values of λ when u = 0.5.

Given that the parameters for the binomial and negative binomial fits are completely parameterised by the mean and the Fano factor, it is instructive to plot the Fano factor as a function of the mean; this is shown in Figure 6.17 (note that the Fano factor is plotted on a logarithmic scale).

It can then be seen that for $0.5 < R < 1$ the minimum Fano factor is an exponential function of the crossing rate – this is approximately

$$F = 5\exp(-2.6R)\,. \tag{6.11}$$

Likewise, the maximum crossing rate as a function of the Fano factor is approximately

$$R = 2.65 - \frac{(\log(F/2))^2}{1.6}\,. \tag{6.12}$$

It therefore follows that the maximum value of the mean crossing rate occurs when the Fano factor is two – this can be seen in Figure 6.17, which plots the bounds for F and R. Equation (6.13) can be inverted to give a maximum Fano factor of ~16 – it can be inferred from Figure 6.11 and its discussion that this corresponds to crossings for *very* small values of λ and u.

Recall that the binomial (6.9) and negative binomial (6.10) distributions become Poisson as $\alpha \to \infty$ (e.g. as $F \to 1$), and that χ^2 statistics have shown that they are excellent fits to the test case envelopes (and presumably to the envelopes of any other λ, u combination also). Figure 6.17 shows that there *are* envelopes for which $F \approx 1$, so it therefore follows that for a suitable choice of λ and u, the envelopes are

Poisson distributed, though binomial and negative binomial envelopes are far more abundant.

Small values of α, which imply strongly non-Poissonian statistics, occur either as a result of *small* values of R, or *large* values of $|F-1|$. It is apparent from Figure 6.17 that there is an abundance of negative-binomial envelopes where R (and α) is very small, but the same is *not* true for binomially distributed envelopes, since the lower bound of R is given by (6.11). For instance, the binomial test case with the *smallest* value of α is $\lambda = 0.075$, $u = 0.5$, where $F = 0.397$ and $R = 1.01$, and $\alpha \approx 1300$.

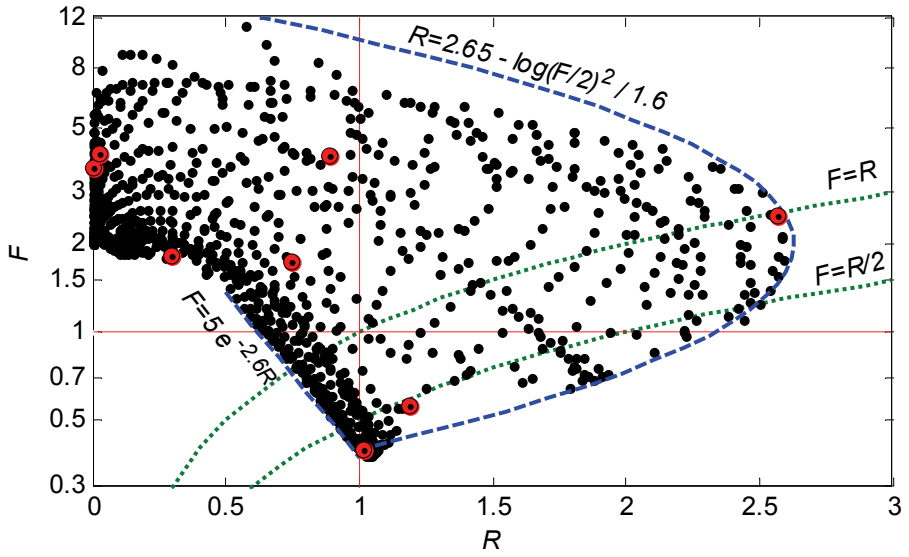

Figure 6.17

Plotting the Fano factor (on a logarithmic scale) as a function of the mean level crossing rate for all sampled points. The blue dashed lines correspond to empirical bounds for the crossing rate and Fano factor. Red lines depicting unit mean rate and unit Fano factor are also plotted, and test cases are marked as red dots. The green dotted lines $F = R$ and $F = R/2$ will be referred to later.

Note that the form of (6.9) and (6.10) imply that as the Fano factor passes through unity from negative binomial to binomial, the value of α will diverge – this divergence can be seen in Figure 6.18. It is especially interesting that for $\lambda = 0.025$ and 0.075, the value of α seems to remain the same for large ranges of u, implying a robustness in the level crossings statistics. That is, though the Fano factor in (6.9) and (6.10) varies as the level increases, α does not vary much, indicating that an underlying feature of the fluctuations of the intensity control the value of α.

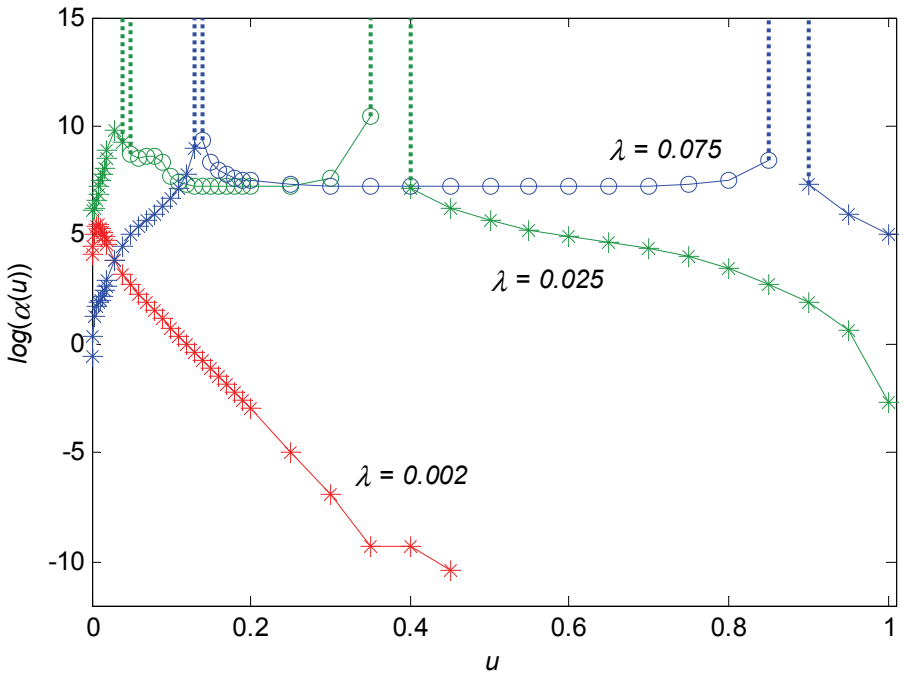

Figure 6.18

Plotting α as a function of the crossing level u for $\lambda = 0.002$ (red), 0.025 (green), and 0.075 (blue). Stars represent negative binomial distributed crossings; circles represent binomial distributed envelopes. A transition from stars to circles (i.e. negative binomial distributed envelopes to binomially distributed envelopes, or vice versa) represents a divergence of α, illustrated by dotted lines.

6.6.5 Inter-event times and persistence

Having considered the distribution of the number of level crossings of the process, it is also useful to examine the distribution of the *intervals* between level crossings. A useful measure of the dynamics of a process its 'persistence exponent', which can be thought of as a measure of how long it tends to stay above/below a set level.

If we define the variable τ to be the interval between two consecutive level crossings, then it can [e.g. 133] be shown that for a wide class of random processes:

$$P(\tau) \sim \exp\left(-\frac{\tau}{L}\theta\right); \qquad \tau \to \infty \tag{6.14}$$

where θ is termed the 'persistence exponent' and L is some scale length of the process at hand (in this case, the correlation length of the Gaussian process). Clearly for large values of θ, the process is more likely to change signs rapidly, which implies that the mean number of crossings will be larger as a result. Likewise, it can be inferred that when θ is large, crossings are more bunched together, which implies a *small* Fano factor. It then follows that the quantity

$$\theta_e = c \cdot \frac{R}{F} \tag{6.15}$$

where c is some constant, is a heuristic estimate of the persistence exponent.

Figure 6.19 plots the inter-event distribution of the level crossings when $\lambda = 0.025$ and $u = 0.01$. Also plotted are straight lines corresponding to exponential tails with persistence exponent θ = 0.9923 which best fits the data (in red) and the estimated

value (with $c = 1$), $\theta_e = 1.020$ (in blue). It is evident that the two values do not differ by much, θ_e *over*-estimating the persistence coefficient. This implies that θ_e is a suitable estimator for the persistence exponent.

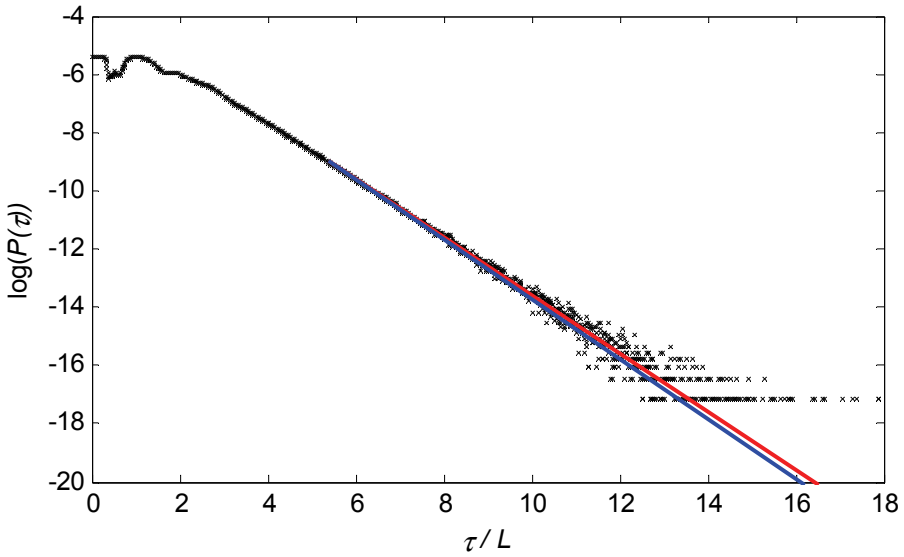

Figure 6.19

Plotting the inter-event distribution when $\lambda = 0.025$, $u = 0.01$ as a function of the normalised interval length τ / L. Straight lines corresponding to the persistence exponent θ (red) and from the estimated persistence θ_e (blue) are also plotted.

Figure 6.20 plots the persistence index θ, the estimated persistence index θ_e, mean crossing rate R and Fano Factor F for $u = 0.01$, 0.1 and 0.5 as a function of the filter width λ for the three chosen crossing levels. For $u = 0.01$, the difference between θ_e and θ is being barely discernable. For $u = 0.1$ and $u = 0.5$, the *form* of θ_e resembles that of the persistence, with the fit being better for small λ.

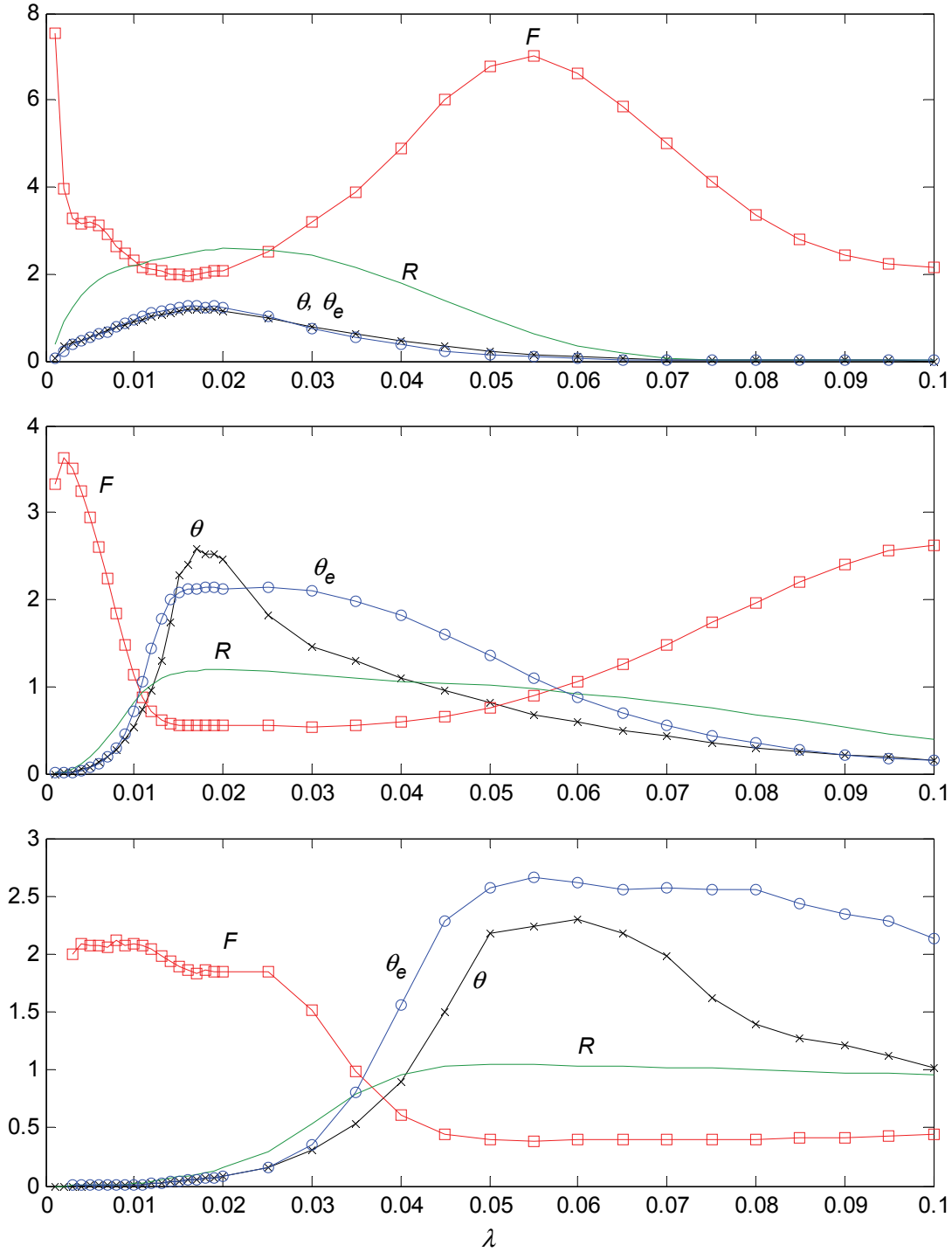

Figure 6.20

Plotting the persistence θ (black line with crosses), the mean crossing rate R (green line), Fano factor F (red line with squares), and the estimator θ_e (blue line with circles) for the three levels 0.01, 0.1, and 0.5 (top, middle and bottom boxes respectively).

Figure 6.21 plots the rescaled persistence $\theta / c(u)$ (where $c(u)$ is some unknown function of the level u) as a function of R/F for the three test case levels. It is apparent that when $R < 2F$, $\theta / c(u) \approx R/F$, so

$$P(\tau) \sim \exp\left(-\frac{c(u)R}{F} \cdot \frac{\tau}{L}\right) \qquad \tau \to \infty,\ R < 2F\,. \tag{6.16}$$

The line $R = 2F$ is plotted in Figure 6.17, from which it can be seen that the majority of points in the λ, u phase space satisfy $R < 2F$, i.e. (6.16) is a good estimate for the asymptotic behaviour of the inter-event times.

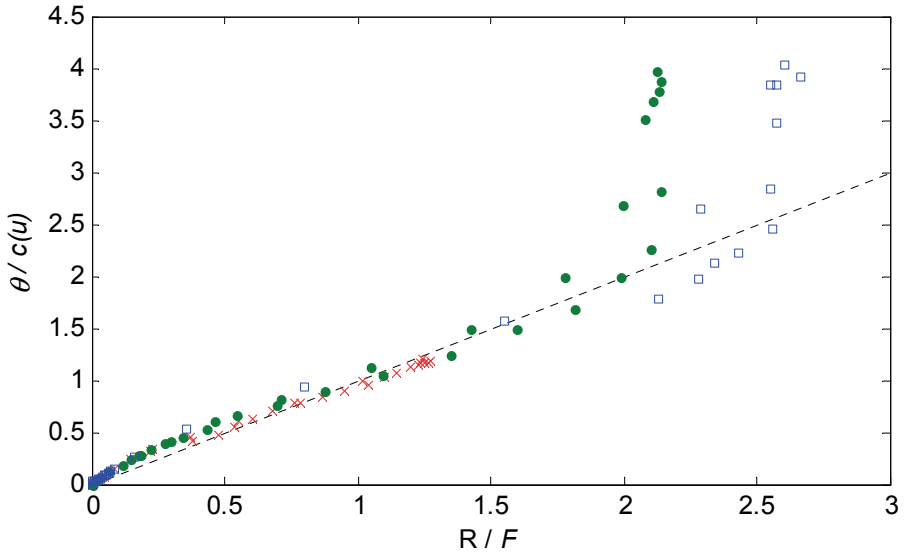

Figure 6.21

Plotting the rescaled persistence exponents θ / $c(u)$ as a function of the ratio of the mean crossing rate to the Fano factor, R / F for the three levels u = 0.01, 0.1 and 0.5 (red crosses, green points and blue squares respectively), the corresponding scales being $c(0.01) = 1$, $c(0.1) = 0.65$ and $c(0.5) = 0.57$.

Analogies to the concept of persistence can be drawn in *discrete* processes also. For instance, Hopcraft considers the counting statistics (see §2.5.3) of different models of

population processes in an unpublished memo [134, pertinent results reproduced in Appendix B] and defines the persistence exponent θ_d of the process through:

$$P(\tau) \sim \exp(-\theta \cdot \tau); \qquad \tau \to \infty$$

where $P(\tau)$ is the inter-event density of the counting process. Three models in particular are of interest, since their count distributions are either binomial, or negative binomial. They are a binomial population process [135], a Birth-Death-Immigration (BDI) process [53] and a Multiple-Immigration (MI) process [53], the latter two having negative binomial counting statistics. The corresponding persistence exponents are:

$$\theta_b = \frac{R}{1-F}\left(1-\sqrt{2F-1}\right); \qquad \frac{1}{2} < F < 1$$

$$\theta_{BDI} = \frac{R}{F-1}\left(\sqrt{2F-1}-1\right); \qquad F > 1$$

$$\theta_{MI} = \frac{2R}{F+1}; \qquad F \geq 1$$

respectively, where R is the *count* rate from monitoring the population, i.e. the number of emigrants per unit time. Without loss of generality, we set $R = 1$ in the above, since we are considering fitting these population model results to the *rescaled* persistence exponents $\theta / c(u)$.

The persistence exponents from the population models are plotted with the rescaled persistence exponents in Figure 6.22. It is clear that when $0 < R/F < 1$ (i.e. $0 < R < F$), the value of the rescaled persistence exponent lies between the estimate R/F (dotted line) and θ_{MI} (the persistence for the multiple immigration model, blue

line). The *average* value of θ_e and θ_{MI} is therefore an improved estimate in this regime. Similarly, it can be seen that for $F < R < 2F$, θ_e is a better estimate for the rescaled persistence exponent than that of the binomial process (red line). Therefore, the persistence exponent θ for the range $0 < R < 2F$ is well approximated by the functions:

$$\begin{aligned} \theta &\approx \frac{\theta_e + c \cdot \theta_{MI}}{2} = \frac{c(u)}{2}\left(\frac{R}{F} + \frac{2}{F+1}\right) && 0 < R < F \\ \theta &\approx \theta_e = c(u) \cdot \frac{R}{F} && F < R < 2F. \end{aligned} \tag{6.17}$$

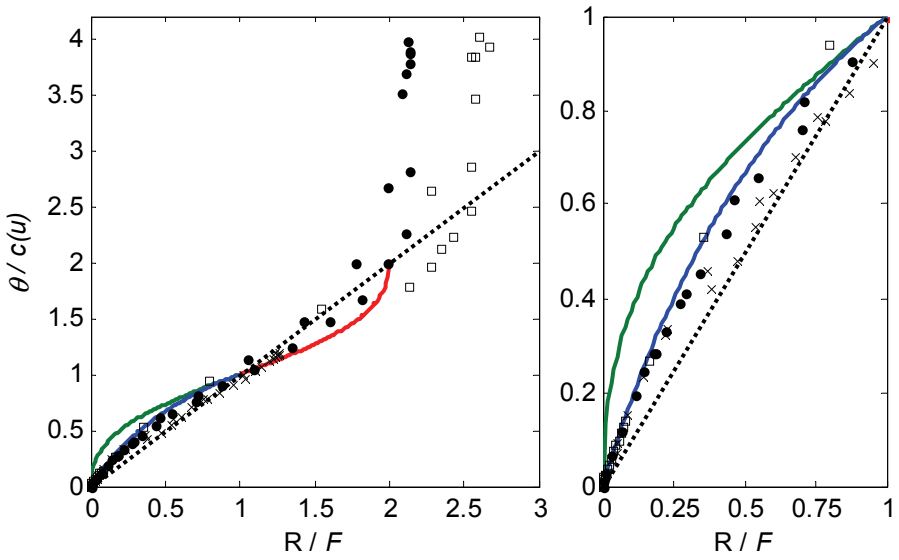

Figure 6.22

Plotting the θ / $c(u)$ as a function of R / F for u = 0.01, 0.1 and 0.5 (crosses, points and squares respectively), the corresponding scales $c(u)$ being the same as in Figure 6.21. The dotted line is to θ / $c(u)$ = R / F. The persistence exponents corresponding to the binomial, negative binomial and multiple immigration population models are also plotted (red, green and blue lines respectively). The same plot for $0 < R / F < 1$ and $0 < \theta / c(u) < 1$ is plotted on the right panel.

6.7 Summary

This chapter uses a non-linear filter analogue of a phase-screen model to generate a non-Gaussian process, then proceeds to analyse the level crossings. The probability density of the intensity was seen to show a wide range of behaviour, from being exponential in the limit $\lambda \to 0$, K distributed for $\lambda << 1$, to an intermediate range in which it resembles no obvious distribution. For larger values λ, the density approaches a uniform distribution.

To analyse the level crossing distributions, nine points in the λ,u phase space were chosen: three crossing levels, and three values of the filter width λ. For all of the chosen test cases, the binomial and negative binomial distributions provided exemplary fits to the crossing distributions, even for extremes of the mean crossing rate or Fano factor. This result is significant as it extends the results of Smith et al. [83] (who considered the *zero* crossings of differentiable Gaussian processes) to *level* crossings of a *non*-Gaussian process, and implies a universality of the binomial and negative binomial distributions to point processes derived from continuous processes.

It was seen that the Fano factor of the crossing distributions has a lower bound which is a function of the crossing rate. A consequence of this is that when comparing the crossing distributions to binomial distributions – there are *no* binomially distributed crossings for which the crossing rate is very small.

The asymptotic behaviour of the distribution of times between level crossings was found to be approximated in a simple form (6.14, 6.17) which depends only on the Fano factor and the mean crossing rate. This has a wider currency since it permits assumptions about the inter-event times of the level crossing process to be made knowing only the crossing distributions.

7. Conclusion

In the introduction, the relationship between the classes of the *continuous* and *discrete*-stable distributions was considered. This thesis addresses this point using the Poisson transform, a novel result which is key to this thesis. Indeed, the recurrent motif in this thesis is the interplay between the continuous and discrete properties of random, stochastic processes. The structure of the thesis is schematically shown in Figure 7.1, which highlights the key results of each chapter separately.

The continuous and discrete stable distributions, which in the literature have had a very inconsistent system of notation were introduced in Chapter 2. One notation was chosen for its simplicity, and given the importance of the stable distributions, the known closed-form expressions were presented. The Death, Multiple-Immigration (DMI) population model was also introduced as a discrete process for which discrete-stable distributions can be found both in its stationary solution and counting statistics.

Chapter 3 served to bridge the gap between the discrete and continuous stable distributions. The 'multiply stochastic' concept of smearing the scale parameter of one distribution by another was introduced via the Gaussian and Poisson transforms. A new proof is introduced which shows that the *one-sided* continuous-stable distributions are linked to the *discrete*-stable distributions via a Poisson transform interrelationship. This proof also shows that modifying the scale parameter of *any* one-sided or symmetric stable distribution by a *one-sided* continuous-stable

distribution results in another stable distribution of the same type but with reduced power-law index.

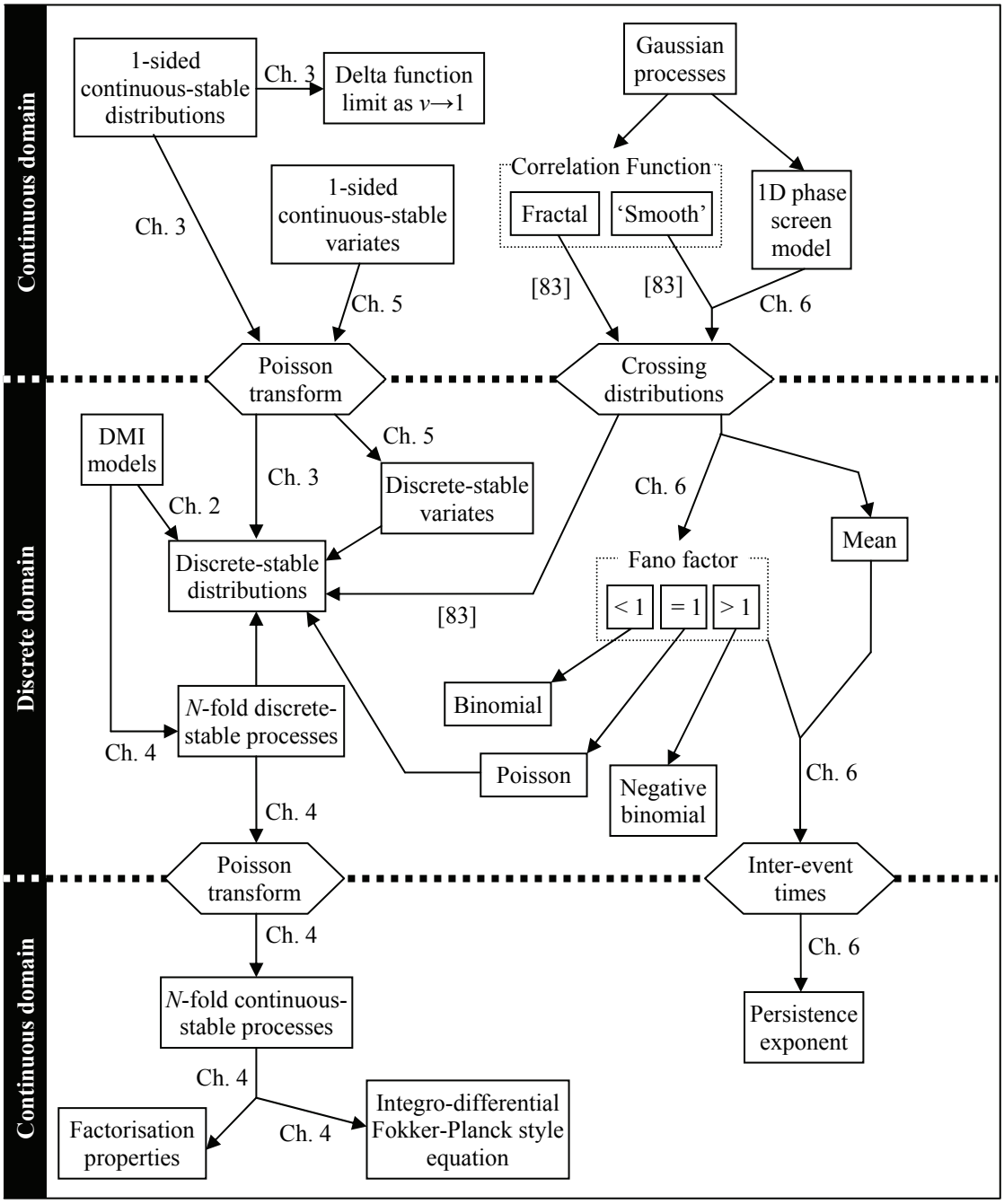

Figure 7.1

Showing the connection between the key results of the thesis. Hexagons represent the mechanism for transferring between continuous and discrete properties. Chapter or reference numbers are also given.

The Poisson transform interrelationship is exploited in Chapter 4 to generate a one-sided continuous-stable *process* using the (discrete-stable) DMI model as a basis. Properties of this continuous process were found, including the transient solution and the r-fold statistics, which give the probability that the process has values $x_1, x_2, ..., x_r$ following separation times $t_1, t_2, ..., t_{r-1}$. The factorisation of the latter is enormously significant, as it shows that the continuous-stable process is a well-defined Markov process. A integro-differential Fokker-Planck style equation governing the time evolution of the probability density function was found, and shown to have a non-local kernel, such that $p(x,t)$ has a dependence on all $p(x',t)$ for which $0 < x' < x$. This contrasts to a Fokker-Planck equation suggested in the literature for *symmetric*-stable processes, but which is readily seen to be unphysical. The results in Chapter 4 therefore permit the analysis and simulation of one-sided continuous-stable processes, or more importantly, to fit such processes to empirical data.

Chapter 5 considers the Poisson transform interrelationship in the opposite direction, firstly using an algorithm to generate negative binomially distributed variates from gamma distributed variates, since the two distributions form a Poisson transform pair. The algorithm was then applied to generate discrete-stable variates from one-sided *continuous*-stable variates. For each class of distribution, a large number of variates were collected to create an ensemble. In every case, the distribution of the ensembles were found to be an excellent match to the theoretical distributions upon comparison via the χ^2 statistic. This novel method of generating discrete-stable variates is

significant as it is vastly less computationally expensive than methods such as 'lookup tables' (which necessarily introduce inaccuracies), or approximations based on the power-law tails of the discrete-stable distributions, and is an 'exact' method.

Hopcraft, Ingrey and Jakeman [84] discovered a relationship between continuous processes which have fractal properties in their correlation functions, and the distributions of the number of crossings (which have power-laws and are asymptotically stable) of these processes which occur in intervals of arbitrary length. Smith, Hopcraft and Jakeman [83] consider Gaussian processes whose correlation functions do *not* have fractal properties. Though it may be expected that for large intervals, the central limit theorem would apply and the distribution of level crossings would be Poisson, this is not the case; instead the distribution of crossings *always* belong to the class of binomial, negative binomial or (exceptionally) Poisson distributions. Chapter 6 considers a signal processing analog of a phase-screen model as a non-Gaussian process without fractal properties in the correlation function. Over a very long integration time and depending on their Fano factors, it was found that the level crossing distributions are either binomial or negative binomial, implying a universality of these distributions when considering counting statistics over asymptotically long times. The 'persistence exponent' of the continuous process (which is a measure of the length of time the process stays above or below a prescribed level), was found to be very accurately approximated by simple functions of the mean and Fano factor of the crossing distribution. This result is noteworthy because it connects the crossing distribution (which is discrete and ostensibly has *no*

information about the interval statistics of the process) to its persistence exponent, a continuous property.

This thesis has shown that many discrete and continuous properties of stochastic processes, which are often dealt with as separate entities, have a deep relationship which connects them. For instance, the Poisson transform interrelationship found in Chapter 3 implies that if a one-sided continuous-stable process modulated the mean of an independent Poisson process, the result is a discrete-stable process – the reverse of this relationship being the basis of Chapter 4.

7.1 Further Work

This thesis has addressed many questions, for instance, whether or not the discrete-stable and the one-sided continuous-stable distributions are only superficially similar by discovering their Poisson transform interrelationship. Many further avenues of possible research have been outlined, however. One such obvious avenue is to consider the continuous-stable process developed in Chapter 4 to model *real-world* processes, in order to obtain salient results such as prediction of future events through such properties as the *inter*-event times.

It was shown that symmetric-stable distributions of index 2ν can be formed by modulating the scale parameter of a Gaussian distribution by a one-sided continuous-stable distribution of index ν. Following the discovery of a one-sided continuous-stable process in Chapter 4, it would be very enlightening to 'Gaussian transform'

that process to form a *symmetric*-stable process, and investigate the appropriate properties.

When studying the level crossing statistics of the non-Gaussian process in Chapter 6, it was necessary to fix most of the parameters (such as the properties of the Gaussian phase), and consider only varying the filter width and the crossing level. Smith, Hopcraft and Jakeman [83] considered the zero crossing distributions of Gaussian processes upon varying the correlation function. It would be extremely enlightening to study the level crossing properties of the Gaussian processes with different correlation functions, or indeed different processes entirely.

The crossing statistics in Chapter 6 was seen to exhibit very strong odd-even effects, much like the 'pairs' population model [61]. The Fano factor of the population model, however, is limited to $1 < F < 2$ which is rather restrictive when considering fitting the results to crossing distributions. Finding a process for which analytical results can be found and the Fano factor may take *any* value would therefore be very beneficial.

Deeper connections between discrete and continuous properties may yet be found, particularly in the field of zero and level crossings, which would both be enlightening and could be of enormous benefit not only to the mathematical community, but to those interested in condensed-matter physics, risk analysis, finance and indeed the physical and social sciences in general.

Appendices

Appendix A – Effect of envelopes on odd-even distributions

Recall that the generating function of an arbitrary discrete distribution $P(N)$ is (e.g. 2.7)

$$Q(s) = \sum_{N=0}^{\infty} (1-s)^N P(N).$$

It then follows that

$$\begin{aligned}(1-s)Q(s) &= \sum_{N=0}^{\infty} (1-s)^{N+1} P(N) \\ &= \sum_{N=1}^{\infty} (1-s)^N P(N-1) \\ &= \sum_{N=0}^{\infty} (1-s)^N P(N-1)\end{aligned}$$

since $P(-1) = 0$ (this can be verified by setting $s = 0$ in the left hand side). We define the envelope $P_e(N)$ of $P(N)$:

$$P_e(N) = \begin{cases} \dfrac{P(0)}{2} & N = 0 \\ \dfrac{P(N) + P(N-1)}{2} & N > 0 \end{cases}$$

for which the generating function is:

$$\begin{aligned}Q_e(s) &= \sum_{N=0}^{\infty} (1-s)^N \left[\frac{P(N) + P(N-1)}{2} \right] \\ &= \frac{2-s}{2} \cdot Q(s).\end{aligned}$$

The mean, variance and Fano factor can be recovered using (2.11) on $Q_e(s)$ in the usual fashion:

$$\begin{aligned} < N >_e &= -\frac{d}{ds}\left(\frac{2-s}{2}\cdot Q(s)\right)\Big|_{s=0} \\ &= < N > + \frac{1}{2} \end{aligned}$$

so

$$\begin{aligned} < N(N-1) >_e &= \frac{d^2}{ds^2}\left(\frac{2-s}{2}\cdot Q(s)\right)\Big|_{s=0} \\ &= < N(N-1) > + < N > \end{aligned}$$

then

$$\begin{aligned} F_e &= \frac{< N(N-1) >_e + < N >_e - < N >_e^2}{< N >_e} \\ &= \frac{< N(N-1) > + < N > - < N >^2 + (1/4)}{< N > + (1/2)} \end{aligned}$$

which shows that the mean, variance and hence the Fano factor remain relatively unchanged by taking the envelope. From the form of the Fano factor of the envelope distribution, it is expected that the $F_e \approx F$ except when the mean $< N >$ is very small.

Appendix B – Persistence Exponents

Recall that the generating function of a population process and its emigrants is given in (2.38). If the process to be considered has an exponentially distributed inter-event times for $\tau >> 1$, then it simply suffices to extract the asymptotic form of the generating function to extract the persistence exponent. The generating function of the emigrants alone is then $Q_e(z;T) = Q_c(0,z;T)$, and the inter-event density is found by [e.g. 2]:

$$P(\tau) = \frac{1}{\bar{r}} \frac{\delta^2}{\delta \tau^2} Q_e(z=1;\tau); \qquad \bar{r} = -\frac{\delta}{\delta z} Q_e(z;T)\Big|_{z=0, T=1}$$

where $\bar{r}$ is the rate at which emigrants leave the population.

Binomial model

For this model [135],

$$Q_e(z=1,\tau) = \exp(-N\gamma)\left(\cosh(y) + \frac{1}{2}\left(\frac{y}{\gamma} + \frac{\gamma}{y}\right)\sinh(y)\right)^N$$

where

$$\gamma = \frac{\bar{\mu}\tau}{2}$$

$$y^2 = \gamma^2 - \eta\lambda\tau^2 .$$

The mean and second factorial moments of the population of emigrants are:

$$< n >= \frac{\lambda\eta}{\bar{\mu}} N\tau = \bar{r}\tau$$

$$< n(n-1) >=< n >^2 \left(1 - \frac{1}{N\gamma} + \frac{1-\exp(-2\gamma)}{2N\gamma^2}\right)$$

and so the Fano factor is

$$F = 1 - \frac{< n >}{N\gamma}\left(1 - \frac{1-\exp(-2\gamma)}{2\gamma}\right).$$

For asymptotically large τ, $\gamma \to \infty$ so

$$\lim_{\tau\to\infty} 1 - F = \frac{< n >}{N\gamma} = \frac{2\bar{r}}{N\bar{\mu}}$$

and

$$y^2 = \gamma^2\left(1 - \frac{4\bar{r}}{N\bar{\mu}}\right) = \gamma^2(2F-1).$$

Then, for $\tau >> 1$,

$$Q_e(z=1,\tau) \sim \exp\left(-\frac{\bar{r}\tau}{1-F}\right)\left(\frac{1}{2} + \frac{1}{4}\left((2F-1)^{1/2} + \frac{1}{(2F-1)^{1/2}}\right)\right)^N$$
$$\times \exp\left(\frac{\bar{r}\tau}{1-F}(2F-1)^{1/2}\right)$$

so

$$\lim_{\tau\to\infty} Q_e(z=1,\tau) \sim \exp\left(-\frac{\bar{r}\tau}{1-F}\left(1-(2F-1)^{1/2}\right)\right)$$

therefore for the binomial model,

$$\theta = \frac{\bar{r}}{1-F}\left(1-(2F-1)^{1/2}\right), \qquad \frac{1}{2} < F < 1$$

Birth-Death-Immigration model

The Birth-Death-Immigration model [e.g. 53] produces negative binomial distributions as its equilibrium state, and the distribution of emigrants satisfies:

$$Q_e(z=1,\tau)=\exp(\beta\gamma)\left(\cosh(y)+\frac{1}{2}\left(\frac{y}{\gamma}+\frac{\gamma}{y}\right)\sinh(y)\right)^{-\beta}$$

where

$$\gamma=\frac{\bar{\mu}\tau}{2},\qquad y^2=\gamma^2+\frac{2<n>\gamma}{\beta}.$$

The mean and second factorial moments of the population of emigrants are:

$$<n>=\frac{\nu\eta}{\bar{\mu}}\tau=\bar{r}\tau$$

$$<n(n-1)>=<n>^2\left(1+\frac{1}{2\beta\gamma^2}(2\gamma+\exp(-2\gamma)-1)\right)$$

and so the Fano factor when $\tau>>1$ is

$$F-1\approx\frac{<n>}{\beta\gamma}=\frac{2\bar{r}}{\beta\bar{\mu}}.$$

As before,

$$y^2=\gamma^2(2F-1)$$

and

$$Q_e(z=1,\tau)=\exp(\beta\gamma)\left(\frac{1}{2}+\frac{1}{4}\left((2F-1)^{1/2}+\frac{1}{(2F-1)^{1/2}}\right)\right)^{-\beta}$$
$$\times\exp\left(-\beta\gamma(2F-1)^{1/2}\right)$$

so

$$\lim_{\tau\to\infty}Q_e(z=1,\tau)=\exp\left(-\frac{\bar{r}\tau}{F-1}\left((2F-1)^{1/2}-1\right)\right)$$

so, for the negative binomial model,

$$\theta = \frac{\bar{r}}{F-1}\left((2F-1)^{1/2}-1\right), \qquad F > 1$$

which is identical to that for the binomial model, save for the different range of F.

Multiple-Immigration model

When the distribution of the number of immigrants entering a population is geometric, the multiple-immigration population process reaches a negative binomial equilibrium distribution, however the parameterisation of the generating function and the derived statistics are different:

$$Q(z=1,\tau) = \left(\frac{1-\alpha}{\exp(2\gamma)-\alpha}\right)^{\alpha\beta}$$

where

$$\gamma = \frac{\mu\tau}{2}, \qquad \alpha = \frac{1}{1+2\beta\gamma/<n>}$$

and the moments of the distribution of emigrants are

$$<n> = \bar{r}\tau$$

$$<n(n-1)> = <n>^2\left(1+\frac{1}{2\beta\gamma^2}\left(2\gamma+\exp(-2\gamma)-1\right)\right)$$

which is identical to that of the BDI model, hence

$$F-1 \approx \frac{<n>}{\beta\gamma} = \frac{2\bar{r}}{\beta\bar{\mu}}$$

so

$$\alpha = \frac{F-1}{F+1}$$

hence as $\tau >> 1$,

$$Q_e(z=1,\tau) \approx (1-\alpha)^{\alpha\beta} \exp\left(-\frac{2\bar{r}\tau}{1-F}\right)$$

so, for the multiple-immigration model,

$$\theta = \frac{2\bar{r}}{F+1}, \qquad F > 1$$

The range of Fano factors and persistence exponents for the three models are then summarised in table form as:

Model	Fano Factor	Persistence Exponent (θ)
Binomial	$\frac{1}{2} < F < 1$	$\frac{\bar{r}}{1-F}\left(1-(2F-1)^{1/2}\right)$
Negative Binomial	$F > 1$	$\frac{\bar{r}}{F-1}\left((2F-1)^{1/2}-1\right)$
Multiple Immigration	$F > 1$	$\frac{2\bar{r}}{F+1}$

Table B.1

The Fano factor of the population of emigrants and the persistence exponent of the inter-event times for the three population models considered.

References

[1] M. Buchanan, "Ubiquity" - Weidenfeld & Nicolson, London (2000)

[2] J. O. Matthews, "Theory and application of multiple immigrant population models", Doctoral Thesis (The University of Nottingham), (2003)

[3] C. W. Gardiner, "Handbook of Stochastic Methods (3rd ed.)" - Springer-Verlag, Berlin (2004)

[4] N. G. Van Kampen, "Stochastic Processes in Physics and Chemistry" - Elsevier, Amsterdam (2006)

[5] K. I. Hopcraft, E. Jakeman, J. O. Matthews, "Generation and monitoring of a discrete stable random process", Journal of Physics A: Mathematical and General **35**, L745-L751 (2002)

[6] J. O. Matthews, K. I. Hopcraft, E. Jakeman, "Generation and monitoring of discrete stable random processes using multiple immigration population models", Journal of Physics A: Mathematical and General **36**, 11585-11603 (2003)

[7] B. Mandelbrot, "New Methods in Statistical Economics", The Journal of Political Economy **71** #5, 421-440 (1963)

[8] W. H. Press, "Flicker noises in astronomy and elsewhere", Comments on Modern Physics, Part C - Comments on Astrophysics **7** #4, 103-119 (1978)

[9] P. Lévy, "Théorie de l'Addition des Variables Aléatoires" - Gaulthier-Villars, Paris (1937)

[10] B. V. Gnedenko, A. N. Kolmogorov, "Limit Distributions for Sums of Independent Random Variables" - Addison-Wesley, Massachusetts (1954)

[11] F. W. Steutel, K. van Harn, "Discrete Analogues of Self-Decomposability and Stability", The Annals of Probability **7** #5, 893-899 (1979)

[12] P. Bak, C. Tang, K. Wiesenfeld, "Self-Organized Criticality - An explanation of 1/f noise", Physical Review Letters **59** #4, 381-384 (1987)

REFERENCES

[13] R. Albert, A. L. Barabási, "Statistical mechanics of complex networks", Reviews Of Modern Physics **74** #1, 47-97 (2002)

[14] R. Brown, Philosophical Magazine **4** 161-173 (1828); R. Brown, Ann. Phys. Chem. **14** 294 (1828).

[15] A. Einstein, "Über die von der molekularkinetischen Theorie der Wärme geforderte Bewegung von in ruhenden Flüssigkeiten suspendierten Teilchen", Annalen der Physik **17**, 549-560 (1905)

[16] A. D. Fokker, Ann. Physsik **43**, 810, (1914); M. Planck, Sitzber. Preuß. Akad. Wiss. 324 (1917)

[17] S. O. Rice, "Mathematical Analysis of Random Noise - and Appendices" - Bell Telephone Labs, New York (1952)

[18] M. Kac, "On the average number of real roots of a random algebraic equation", Bulletin of the American Mathematical Society **49**, 314-320 (1943)

[19] J. H. van Vleck, D. Middleton, "The Spectrum of Clipped Noise", Proceedings Of The IEEE **54** #1, 2-19 (1966)

[20] E. Jakeman, P. Pusey, "A model for non-Rayleigh sea echo", IEEE Transactions on Antennas and Propagation **24** #6, 806-814 (1976)

[21] P. Bak, C. Tang, K. Wiesenfeld, "Self-Organized Criticality", Physical Review A **38** #1, 364-375 (1988)

[22] R.P. Taylor, R. Guzman, T.P. Martin, G.D.R. Hall, A.P. Micolich, D. Jonas, B.C. Scannell, M.S. Fairbanks, C.A. Marlow, "Authenticating Pollock paintings using fractal geometry", Pattern Recognition Letters **28** #6, 695-702 (2007)

[23] B. B. Mandelbrot, "Fractals and an Art for the Sake of Science", Leonardo **2**, 21-24 (1989)

[24] A. E. Jacquin, "Fractal image coding: a review", Proceedings of the IEEE **81** #10, 1451-1465 (1993)

[25] G. P. Cherepanov, A. S. Balankin, V. S. Ivanova, "Fractal fracture mechanics - A review", Engineering Fracture Mechanics **51** #6, 997-1033 (1995)

REFERENCES

[26] A. Rinaldo, I. Rodriguez-Iturbe, R. Rigon, E. Ijjasz-Vasquez, R. L. Bras, "Self-organized fractal river networks", Physical Review Letters **70** #6, 822-825 (1993)

[27] E. F. Fama, "The Behavior of Stock-Market Prices", The Journal of Business **38** #1, 34-105 (1965)

[28] T. Wilhelma, P. Hänggi, "Power-law distributions resulting from finite resources", Physica A **329**, 499-508 (2003)

[29] P. Hänggi, P. Jung, "Colored Noise in Dynamical Systems", Advances in Chemical Physics **89**, 239-326 (1995)

[30] D. L. Turcotte, "Self-organized criticality", Reports on Progress in Physics **62** #10, 1377–1429 (1999)

[31] J. Aguirre, R. L. Viana, M. A. F. Sanjuán, "Fractal structures in nonlinear dynamics", Reviews Of Modern Physics **81** #1, 333- (2009)

[32] C. Tsallis, S. V. F. Levy, A. M. C. Souza, R. Maynard, "Statistical-Mechanical Foundation of the Ubiquity of Lévy Distributions in Nature", Physical Review Letters **75** #20, 3589-3593 (1995)

[33] M. E. J. Newman, "Power laws, Pareto distributions and Zipf's law", Contemporary Physics **46** #5, 323-351 (2005)

[34] C. C. Lo, L. A. N. Amaral, S. Havlin, P. C. Ivanov, T. Penzel, J. H. Peter, H. E. Stanley, "Dynamics of sleep-wake transitions during sleep", Europhysics Letters **57** #5, 625-632 (2002)

[35] P. Bak, K. Christensen, L. Danon, T. Scanlon, "Unified Scaling Law for Earthquakes", Physical Review Letters **88** #17, 178501-1-4 (2002)

[36] Y. Huang, H. Saleur, C. Sammis, D. Sornette, "Precursors, aftershocks, criticality and self-organized criticality", Europhysics Letters **41** #1, 43-48 (1998)

[37] O. Peters, C. Hertlein, K. Christensen, "A Complexity View of Rainfall", Physical Review Letters **88** #1, 018701-1-4 (2002)

REFERENCES

[38] A. B. Chhabra, M. J. Feigenbaum, L P. Kadanoff, A. J. Kolan, I. Procaccia, "Sandpiles, avalanches, and the statistical mechanics of nonequilibrium stationary states", Physical Review E **47** #5, 3099-3121 (1993)

[39] G. Samorodnitsky, M. S. Taqqu, "Stable Non-Gaussian Random Processes" - Chapman & Hall, London (1994)

[40] V. M. Zolotarev, "One-Dimensional Stable Distributions" - American Mathematical Society, Rhode Island (1986)

[41] W. Feller, "An introduction to probability theory and its applications (3rd ed.)" - Wiley-Interscience, New York (1968)

[42] E. Lukacs, "Characteristic functions (2nd ed.)" - Griffin, London (1970)

[43] F. W. Steutel, "Some recent results in infinite divisibility", Stochastic Processes and their Applications **1** #2, 125-143 (1973)

[44] M. Fisk, "Infinitely Divisible Distributions: Recent Results and Applications", The Annals of Mathematical Statistics **33** #1, 68-84 (1962)

[45] K. I. Hopcraft, E. Jakeman, J. O. Matthews, "Discrete scale-free distributions and associated limit theorems", Journal of Physics A: Mathematical and General **37** #48, L635–L642 (2004)

[46] M. Steyvers, J. B. Tenenbaum, "The Large-Scale Structure of Semantic Networks: Statistical Analyses and a Model of Semantic Growth", Cognitive Science: A Multidisciplinary Journal **29** #1, 41-78 (2005)

[47] R. Albert, A. L. Barabási, "Topology of Evolving Networks: Local Events and Universality", Physical Review Letters **85** #24, 5234-5237 (2000)

[48] S. Redner, "How popular is your paper? An empirical study of the citation distribution", The European Physical Journal B - Condensed Matter and Complex Systems **4**, 131-134 (1998)

[49] V. M. Eguíluz, D. R. Chialvo, G. A. Cecchi, M. Baliki, A. V. Apkarian, "Scale-Free Brain Functional Networks", Physical Review Letters **94**, 018102-1-4 (2005)

REFERENCES

[50] A. Vázquez, J. G. Oliveira, Z. Dezsö, K. I. Goh, I. Kondor, A. L. Barabási, "Modeling bursts and heavy tails in human dynamics", Physical Review E **73** #3, 036127-1-19 (2006)

[51] Z. Dezső, A. L. Barabási, "Halting viruses in scale-free networks", Physical Review E **65** #5, 055103-1-4 (2002)

[52] D. McGuire: "'DDoS' Attacks Still Pose Threat to Internet" The Washington Post (4 Nov. 2003)

[53] E. Jakeman, K. I. Hopcraft, J. O. Matthews, "Distinguishing population processes by external monitoring", Proceedings of the Royal Society of London A **459**, 623-639 (2003)

[54] D. L. Snyder: "Random Point Processes" – Wiley-Interscience Publications, New York (1975)

[55] E. Parzen, "Stochastic Processes" - Holden-Day, San Francisco (1962)

[56] S. B. Lowen, M. C. Teich, "Fractal-Based Point Processes" - Wiley-Interscience, New Jersey (2005)

[57] D. Stirzaker, "Advice to Hedgehogs, or, Constants Can Vary", The Mathematical Gazette **84** #500, 197-210 (2000)

[58] D. R. Cox, "Some Statistical Methods Connected with Series of Events", Journal of the Royal Statistical Society Series B (Methodological) **17** #2, 129-164 (1955)

[59] L. Mandel, E. Wolf, "Optical Coherence and Quantum Optics" - Cambridge University Press, Cambridge

[60] U. Fano, "Ionization Yield of Radiations. II. The Fluctuations of the Number of Ions", Physical Review **72** #1, 26-29 (1947)

[61] E. Jakeman, S. Phayre, E. Renshaw, "Evolution and Measurement of a Population of Pairs", Journal of Applied Probability **32**, 1048-1062 (1995)

[62] D. Chowdhury, "100 years of Einstein's Theory of Brownian Motion: from Pollen Grains to Protein Trains", arXiv: Condensed Matter / Statistical Mechanics , 0504610v1 (2005)

REFERENCES

[63] J. W. Essam, "Percolation theory", Reports on Progress in Physics **43** #7, 833-912 (1980)

[64] R. Metzler, J. Klafter, "The random walk's guide to anomalous diffusion - a fractional dynamics approach", Physics Reports **339**, 1-77 (2000)

[65] R. Metzler, J. Klafter, "The restaurant at the end of the random walk - recent developments in the description of anomalous transport by fractional dynamics", Journal of Physics A: Mathematical and General **37**, R161–R208 (2004)

[66] S. Chandrasekhar, "Stochastic Problems in Physics and Astronomy", Reviews Of Modern Physics **15**, 1-89 (1943)

[67] H. Fogedby, "Langevin Equations for Continuous time Lévy flights", Physical Review E **50** #2, 1657-1660 (1994)

[68] M. F. Shlesinger, B. J. West, J. Klafter, "Lévy dynamics of enhanced diffusion: Application to turbulence", Physical Review Letters **58** #11, 1100-1103 (1987)

[69] V. V. Yanovsky, A. V. Chechkin, D. Schertzer, A. V. Tur, "Lévy anomalous diffusion and fractional Fokker–Planck equation", Physica A **282** #1, 13-34 (2000)

[70] T. Rhodes, M. T. Turvey, "Human memory retrieval as Lévy foraging", Physica A **385** #1, 255-260 (2007)

[71] G. M. Viswanathan, V. Afanasyev, S. V. Buldyrev, S. Havlin, M. G. E. da Luz, E. P. Raposo, H. E. Stanley, "Lévy flights in random searches", Physica A **282** #1, 1-12 (2000)

[72] E. Jakeman, R. J. A. Tough, "Non-Gaussian models for the statistics of scattered waves", Advances in Physics **37** #5, 471-529 (1988)

[73] H. Risken, "The Fokker-Planck Equation (2nd ed.)" - Springer-Verlag, Berlin (1996)

[74] H. Haken, "Cooperative phenomena in systems far from thermal equilibrium and in nonphysical systems", Reviews Of Modern Physics **47** #1, 67-121 (1975)

[75] G. E. Uhlenbeck, L. S. Ornstein, "On the Theory of Brownian Motion", Physical Review **36**, 823-841 (1930); M. C. Wang, G. E. Uhlenbeck, "On the Theory of the Brownian Motion II", Reviews Of Modern Physics **17** #2, 323-342 (1945)

REFERENCES

[76] J. L. Doob, "The Elementary Gaussian Processes", The Annals of Mathematical Statistics **15** #3, 229-282 (1944)

[77] D. Middleton, "S. O. Rice and the Theory of Random Noise: Some Personal Recollections", IEEE Transactions on Information Theory **34** #6, 1367-1373 (1988)

[78] M. I. Skolnik, "Radar handbook (3rd ed.)" - McGraw-Hill, New York (2008)

[79] H. Steinberg, P. M. Schultheiss, C. A. Wogrin, F. Zweig , "Short-Time Frequency Measurement of Narrow-Band Random Signals by Means of a Zero Counting Process", Journal of Applied Physics **26** #2, 195-201 (1955)

[80] M. R. Leadbetter, J. D. Cryer, "The variance of the number of zeros of a stationary normal process", Bulletin of the American Mathematical Society **71** #3, 561-563 (1965)

[81] I. F. Blake, W. F. Lindsey, "Level-Crossing Problems for Random Processes", IEEE Transactions on Information Theory **19** #3, 295-315 (1973)

[82] B. Kedem, "Spectral analysis and discrimination by zero-crossings", Proceedings of the IEEE **74** #11, 1477-1493 (1986)

[83] J. M. Smith, K. I. Hopcraft, E. Jakeman, "Fluctuations in the zeros of differentiable Gaussian processes", Physical Review E **77** #03, 031112-1-13 (2008)

[84] K. I. Hopcraft, P. C. Ingrey, E. Jakeman, "Power-law-distributed level crossings define fractal behavior", Physical Review E **76** #3, 031134-1-11 (2007)

[85] J. O. Matthews, K. I. Hopcraft, E. Jakeman, G. B. Siviour, "Accuracy analysis of measurements on a stable power-law distributed series of events", Journal of Physics A: Mathematical and General **39**, 13967–13982 (2006)

[86] J. P. Nolan, "Parameterizations and modes of stable distributions", Statistics & Probability Letters **38**, 187-195 (1998)

[87] M. Yamazato, "Unimodality of Infinitely Divisible Distribution Functions of Class L", The Annals of Probability **6** #4, 523-531 (1978)

[88] V. M. Zolotarev, "On Representation of Densities of Stable Laws by Special Functions", Theory of Probability and its Applications **39** #2, 354-362 (1994)

REFERENCES

[89] C. Fox, "The G and H Functions as Symmetrical Fourier Kernels", Transactions of the American Mathematical Society **98** #3, 395-429 (1961)

[90] J. Hoffmann–Jørgensen, "Stable Densities", Theory of Probability and its Applications **38** #2, 350-355 (1993)

[91] H. Bergström, "On some expansions of stable distribution functions", Arkiv för Matematik **2** #4, 375-378 (1952)

[92] A. Erdélyi, "Asymptotic Expansions" - Dover Publications, New York (1956)

[93] M. Abramowitz, I. A. Stegun: “Handbook of Mathematical Functions” – Dover Publications, New York (1970)

[94] J. P. Nolan, "Numerical calculation of stable densities and distribution functions", Stochastic Models **13** #4, 759-774 (1997)

[95] J. P. Nolan, "stable.exe", available online at http://academic2.american.edu/~jpnolan/stable/stable.html

[96] T. M. Garoni, N. E. Frankel, "Lévy flights: Exact results and asymptotics beyond all orders", Journal of Mathematical Physics **43** #5, 2670-2689 (2002)

[97] K. I. Hopcraft, E. Jakeman, R. M. J. Tanner, "Lévy random walks with fluctuating step number and multiscale behavior", Physical Review E **60** #5, 5327-5343 (1999)

[98] E. T. Whittaker, G. N. Watson, "A Course of Modern Analysis (4th ed.)" - Cambridge University Press, Cambridge (1965)

[99] V. V. Uchaikin, V. M. Zolotarev, "Chance And Stability - Stable Distributions And Their Applications" - VSP, Utrecht, Netherlands (1999)

[100] V. M. Zolotarev, "Expression of the density of a stable distribution with exponent alpha greater than one by means of a frequency with exponent 1/alpha", In Selected Translations in Mathematical Statistics and Probability **1**, 163-167 (1961). Translated from the Russian article: Dokl. Akad. Nauk SSSR. **98**, 735-738 (1954)

[101] I. V. Zaliapin, Y. Y. Kagan, F. P. Schoenberg, "Approximating the Distribution of Pareto Sums", Pure and Applied Geophysics 162 #6, 1187-1228 (2005)

REFERENCES

[102] E. Lommel, "Ueber eine mit den Bessel'schen Functionen verwandte Function", Mathematische Annalen **9** #3, 425-444 (1875)

[103] J. Steinig, "The Sign of Lommel's Function", Transactions of the American Mathematical Society **163**, 123-129 (1972)

[104] E. Jakeman, K. I. Hopcraft, J. O. Matthews, "Fluctuations in a coupled population model", Journal of Physics A: Mathematical and General **38**, 6447-6461 (2005)

[105] K. Shimoda, H. Takahasi, C. H. Townes, "Fluctuations in Amplification of Quanta with Application to Maser Amplifiers", Journal of the Physical Society of Japan **12**, 686-700 (1957)

[106] D. C. Burnham, D. L. Weinberg, "Observation of Simultaneity in Parametric Production of Optical Photon Pairs", Physical Review Letters **25** #2, 84-87 (1970)

[107] M. C. Teich, P. Diament, "Multiply stochastic representations for K distributions and their Poisson transforms", Journal of the Optical Society of America A **6** #1, 80-91 (1989)

[108] L. Mandel, E. C. G. Sudarshan, E. Wolf, "Theory of Photoelectric detection of light fluctuations", Proceedings of the Physical Society **84**, 435-444 (1964)

[109] W. H. Lee, K. I. Hopcraft, E. Jakeman, "Continuous and discrete stable processes", Physical Review E **77** #1, 011109-1-4 (2008)

[110] I. S. Gradshteyn, I. M. Ryzhik: “Tables of Integrals, Series and Products (6th ed.)” – Academic Press, London (2000)

[111] B. West, M. Bologna, P. Grigolini, "Physics of Fractal Operators" - Springer-Verlag, New York (2003)

[112] B. J. West, V. Seshadri, "Linear systems with Lévy fluctuations", Physica A **113**, 203-216 (1982)

[113] L. Devroye, "Non-Uniform Random Variate Generation" - Springer-Verlag, New York (1986)

[114] D. E. Knuth, "The Art of Computer Programming, Volume 2: Seminumerical Algorithms" - Addison-Wesley, Massachusetts (1969)

REFERENCES

[115] G. E. P. Box, M. E. Muller, "A Note on the Generation of Random Normal Deviates", The Annals of Mathematical Statistics **29** #2, 610-611 (1958)

[116] M. Kanter, "Stable Densities Under Change of Scale and Total Variation Inequalities", The Annals of Probability **3** #4, 697-707 (1975)

[117] I. A. Ibragimov, K. E. Chernin, "On the Unimodality of Stable Laws", Theory of Probability and its Applications **4** #4, 417-419 (1959)

[118] J. M. Chambers, C. L. Mallows, B. W. Stuck, "A Method for Simulating Stable Random Variables", Journal of the American Statistical Association **71** #354, 340-344 (1976)

[119] V. M. Zolotarev, "On the representation of stable laws by integrals", Selected translations in mathematical statistics and probability **6**, 84-88 (1966)

[120] A. Janicki, A. Weron, "Simulation and Chaotic Behavior of α-stable Stochastic Processes" - CRC Press, London (1994)

[121] R. Weron, "On the Chambers-Mallows-Stuck method for simulating skewed stable random variables", Statistics & Probability Letters **28** #2, 165-171 (1996); R. Weron, "Correction to: On the Chambers-Mallows-Stuck method for simulating skewed stable random variables", Wroclaw University of Technology Research Report HSC/96/1 (1996)

[122] A. Janicki, A. Weron, "Can One See α-Stable Variables and Processes?", Statistical Science **9** #1, 109-126 (1994)

[123] C. Lemieux, "Monte Carlo and Quasi-Monte Carlo Sampling" - Springer, New York (2009)

[124] E. Jakeman, K. D. Ridley, "Signal processing analog of phase screen scattering", Journal of the Optical Society of America A **15** #5, 1149-1159 (1998)

[125] E. Jakeman, K. Ridley, "Modeling Fluctuations in scattered waves" - CRC Press, Florida (2006)

[126] O. E. French, "From doubly stochastic representations of K distributions to random walks and back again: an optics tale", Journal of Physics A: Mathematical and Theoretical **42** #22, 225007-1-13 (2009)

REFERENCES

[127] E. Jakeman, "On the statistics of K-distributed noise", Journal of Physics A: Mathematical and General **13** #1, 31-48 (1980)

[128] N. Yasuda, "The random walk model of human migration", Theoretical Population Biology **7** #2, 156-167 (1975)

[129] A. P. Doulgeris, S. N. Anfinsen, T. Eltoft, "Classification With a Non-Gaussian Model for PolSAR Data", IEEE Transactions on Geoscience and Remote Sensing **46** #10, 2999-3009 (2008)

[130] B. Liu, D. C. Munson, "Generation of a Random Sequence Having a Jointly Specified Marginal Distribution and Autocovariance", IEEE Transactions on Acoustics, Speech, and Signal Processing **30** #6, 973-983 (1982)

[131] J. M. Smith, "Discrete Properties of Continuous, non-Gaussian Random Processes", Doctoral Thesis, University of Nottingham (2007)

[132] E. Jakeman, J. G. McWhirter, "Correlation function dependence of the scintillation behind a deep random phase screen", Journal of Physics A: Mathematical and General **10** #9, 1599-1643 (1977)

[133] S. N. Majumdar, "Persistence in nonequilibrium systems", Current Science **77** #3, 370-375 (1999)

[134] K. I. Hopcraft, "Tails of the inter-event distributions and persistence exponents", Unpublished memo, 2007

[135] E. Jakeman, "Statistics of binomial number fluctuations", Journal of Physics A: Mathematical and General **23**, 2815-2825 (1990)

Publications

W. H. Lee, K. I. Hopcraft, E. Jakeman, "Continuous and discrete stable processes", Physical Review E **77** #1, 011109-1-4 (2008); DOI: 10.1103/PhysRevE.77.011109 – based on the results of Chapter 3.

W. H. Lee, "Simulation of Discrete-Stable Random Variables" – Manuscript in progress based on Chapter 5, to be submitted to The Journal of the American Statistical Association.

W. H. Lee, K. I. Hopcraft, E. Jakeman, "Level-crossing statistics of non-Gaussian processes" – Manuscript in progress based on Chapter 6, to be submitted to Physical Review E.